ISSN 0280-5316
ISRN LUTFD2/TFRT--5882--SE

Design of an Energy-Efficient Climate Control Algorithm for Electric Cars

Matthias Busl

Department of Automatic Control
Lund University
June 2011

Lund University **Department of Automatic Control** **Box 118** **SE-221 00 Lund Sweden**	*Document name* MASTER THESIS *Date of issue* June 2011 *Document Number* ISRN LUTFD2/TFRT--5882--SE
Author(s) Matthias Busl	*Supervisor* Manuel Lorents Technische Universität München, Germany. Tore Hägglund Automatic Control Lund, Sweden (Examiner) *Sponsoring organization*

Title and subtitle

Design of an Energy-Efficient Climate Control Algorithm for Electric Cars (Design av en energieffektiv klimatregleringsmetod för elektriska bilar)

Abstract

A climatisation controller for a car with multiple objectives is developed, implemented and tested in simulations. The design focuses on electric cars and their specific characteristics. In this context the goal has been to fulfil common comfort and safety standards while having a low energy consumption. The main idea of the control in order to achieve this is to use a simplified model predictive control scheme to find the best compromise between those objectives. A special evolutionary algorithm and a simplified system model are developed for this purpose. Another feature of the control design is adaption of disturbance terms in this model based on their estimation. As interface to the hardware a second controller is introduced. The approach has been implemented for the electric car MUTE which is currently developed at the TU München. This implementation was verified to work with the available hardware and tested using a thermal car interior simulation model.

Keywords

Classification system and/or index terms (if any)

Supplementary bibliographical information

ISSN and key title 0280-5316		*ISBN*
Language English	*Number of pages* 184	*Recipient's notes*
Security classification		

http://www.control.lth.se/publications/

Diploma thesis subject

Problem statement:

The more efficient car engines become, the more important the consumption of other power train elements gets. This becomes visible in the case of the electric car, where the power necessary for heating and cooling can exceed the drive power. Because there is no sufficient source of waste heat available, especially for the heating, the range of the car can be drastically reduced with an electrically powered heater. Therefore, countermeasures have to be taken in order to reduce the energy need and use as little electric energy as possible. Amongst others, these goals raise new questions in (automatic) control.

Task:

In the diploma thesis a control and an automatic control for the heating system of the car developed in the *MUTE* project should be designed. This system contains a liquid fuel heater and a heating, ventilating and air conditioning (HVAC) unit for air distribution. Control and automatic control should provide the following functionality through automatic programs and options chosen by hand:

- Heating (Automatic and manual mode)
- Preconditioning of the passenger compartment and of the battery
- Recirculating air control
- Defrost mode

The energy demand can be considerably reduced through an increased percentage of recirculated air in the passenger compartment. The tendency of window fogging, which is measured with humidity and temperature sensors, should be added as control variable. The functionality, the control and the activation of the actuators should be tested with a test carrier. Sensors, actors and the developed control algorithm should then be implemented in the *MUTE* prototype. This has to be done in coordination with the institute for automotive engineering at the TUM, due to interfaces that have to be defined accurately. In a further step the integration of a heat pump as heat source/sink for the climatisation should be investigated on a simulation basis. The developed control algorithm should on the one hand take the dynamics and output limits of the heat pump into account and on the other drive the heating/cooling system towards its energetic optimal working point.

Abstract

A climatisation controller for a car with multiple objectives is developed, implemented and tested in simulations. The design focuses on electric cars and their specific characteristics. In this context the goal has been to fulfil common comfort and safety standards while having a low energy consumption. The main idea of the control in order to achieve this is to use a simplified model predictive control scheme to find the best compromise between those objectives. A special evolutionary algorithm and a simplified system model are developed for this purpose. Another feature of the control design is adaption of disturbance terms in this model based on their estimation. As interface to the hardware a second controller is introduced. The approach has been implemented for the electric car *MUTE* which is currently developed at the TU München. This implementation was verified to work with the available hardware and tested using a thermal car interior simulation model.

Kurzfassung

Ein Regelalgorithmus für eine Fahrzeugklimatisierung mit mehreren Zielvorgaben ist entwickelt, umgesetzt und durch Simulation getestet worden. Das Hauptaugenmerk lag dabei auf elektrisch angetriebenen Autos und ihren speziellen Eigenschaften. In diesem Kontext war das Ziel, allgemeine Anforderungen an Komfort und Sicherheit zu erfüllen und dabei möglichst wenig Energie zu verbrauchen. Die Hauptidee, um dies mit einer Regelung zu erreichen, ist der Einsatz einer vereinfachten Form der *model predictive control*, um den besten Kompromiss zwischen den Regelungszielen zu finden. Dafür ist ein spezieller evolutionärer Algorithmus und ein vereinfachtes Model des zu regelnden Systems entwickelt worden. Ein weiterer Bestandteil des Reglerdesigns ist die Anpassung der Modellabweichungen durch eine Abschätzung. Als Schnittstelle zur Hardware wird ein weiterer Regler benutzt. Der Regelungsansatz ist für das Elektro-Auto *MUTE*, das zur Zeit an der TU München entwickelt wird, umgesetzt worden. Das Programm arbeitet in einem Teststand bereits mit der Hardware zusammen und ist mit einer Simulation des Fahrzeug-Innenraums getestet worden.

Acknowledgements

I would like to thank my supervisors, Manuel Lorenz and Leonhardt Hörth, for giving me the chance to work on this interesting and interdisciplinary topic and for their support. I am also very grateful to Tore Häggelund, who was willing to be my "examinator" without having had much information about the subject of this thesis.
Many thanks as well to the creators and contributors of the open source community, especially Arch Linux, Gnome, LaTex, JLaTexEditor and gnuplot. Without this software this thesis would not be the same.
I want to thank my parents for their love and their concerns and my sisters for the joyful time spent so far.
In addition, I like to thank my friends, especially Desiderius for trying to fix my English and Zoe for calling if I did not. Special thanks to Regina for listening to my car climate control explanations and the support (not only the cooking). mpfh.

Contents

Nomenclature

Symbols

Symbol	Unit	Description
A	[m^2]	Area
Bi	[-]	Biot number
c_p, c_V, c	[$\frac{\mathrm{J}}{\mathrm{kg}\cdot\mathrm{K}}$]	Heat capacity
C	[-]	Pressure coefficient, constant
d	[m]	Distance, thickness
D	[m]	Diameter
e	[-]	Euler's number
E	[J]	Internal energy
f	[-]	Ratio
h	[$\frac{\mathrm{W}}{\mathrm{m}^2\cdot\mathrm{K}}$]	Convective heat transfer coefficient
h	[$\frac{\mathrm{kJ}}{\mathrm{kg}}$]	Specific enthalpy
k	[$\frac{\mathrm{W}}{\mathrm{m}\cdot\mathrm{K}}$]	Thermal conductivity
K	[-]	Gain
l, L	[m]	Length
m	[kg]	Mass
$\dot{m}$	[$\frac{\mathrm{kg}}{\mathrm{s}}$]	Mass flow
M	[met][1]	Metabolism
p	[Pa]	Pressure
P	[W]	Power
$\dot{q}$	[$\frac{\mathrm{W}}{\mathrm{m}^2}$]	Heat flux
Q	[J]	Heat energy
$\dot{Q}$	[W]	Heat transfer rate
$r_c l$	[clo][2]	Clothes insulation, thermal resistance per area
R	[$\frac{\mathrm{m}^2\cdot\mathrm{K}}{\mathrm{W}}$]	Thermal resistance

Continued on the next page

[1] $1\,\mathrm{met} = 58,15\,\frac{\mathrm{W}}{\mathrm{m}^2}$, sitting calm [1]

[2] $1\,\mathrm{clo} = 0.155\,\frac{\mathrm{m}^2\cdot\mathrm{K}}{\mathrm{W}}$, business clothes [1]

Symbol	**Unit**	**Description**
t	[s]	Time
T	[°C]	Temperature
v	$[\frac{\mathrm{m}}{\mathrm{s}}]$	Speed
V	$[\mathrm{m}^3]$	Volume
w	[-]	Weight
W	[met][1]	External work
W	[J]	Energy
x	[m]	Variable distance
x, y	[-]	Variables
x_w	$[\frac{\mathrm{g}_{\mathrm{water}}}{\mathrm{kg}_{\mathrm{air}}}]$	Absolute humidity
x_{CO_2}	$[\frac{\mathrm{mg}_{\mathrm{CO_2}}}{\mathrm{kg}_{\mathrm{air}}}]$	Absolute carbon dioxide concentration

Greek symbols

Symbol	**Unit**	**Description**
α	[°]	Angle
γ	[-]	Transmittance
κ	[°C]	Distance to water vapour saturation
μ	[-]	Air fraction passing a flap
τ	[s]	Time constant, time
φ	[%]	Relative humidity

Other symbols

Symbol	**Description**
$\boldsymbol{a}$	Objective values of an individual a
$\boldsymbol{b}$	Objective values of an individual b
f	Function
fit, $\boldsymbol{fit}$	Fitness, here: weighted sum
g	Constraint function
l, $\boldsymbol{l}$	Limits for the objectives
L	Trajectory cost
lb, $\boldsymbol{lb}$	Vector with lower bounds for the design variables
n	Number
o, $\boldsymbol{o}$	(Panic) ordering
p, $\boldsymbol{p}$	Priorities for the objectives
$prob$	Selection probability
r	Random value
s_x	Exploration factor
u, $\boldsymbol{u}$	Control output
$\mathbb{U}$	Set of allowed control outputs
ub, $\boldsymbol{ub}$	Vector with upper bounds for the design variables
w, $\boldsymbol{w}$	Weights for the objectives
x, $\boldsymbol{x}$	System state
$\mathbb{X}$	Set of allowed system states
δ_{s_x}	Exploration factor in-/decrement
δt	Sample time
ϵ_{thr}	Elite selection threshold percentage
$\boldsymbol{\lambda_{change}}$	Maximum allowed distances from the old control value
σ, $\boldsymbol{\sigma}$	Standard deviation
ϕ, $\boldsymbol{\phi}$	Final cost, objective (function)

Bold symbols indicate vectors.

Subscripts

Subscript	**Description**
act	Actual, measured
air	Air
amb	Ambient, the air outside the car
base	Base individuals
c	Child/children
cab	Car cabin
cl	Clothes
defrost	Defrost air outlets
elite	Elite individuals
eval	Evaluations
face	Face air outlets
foot	Foot air outlets
gen	Generation
h	Height
horizon	Prediction time, horizon
in	In or into the car cabin
i, j, k ,n	Numbering
max	Maximum
min	Minimum
obj	Objective(s)
out	Outside or out of the car cabin
pas	Passenger
par	Parent
pop	Population
pow	Power
r	(Solar) radiation
random	Random immigrants

Continued on the next page

Subscript	**Description**
recirc	Recirculation
sat	Saturated
sun	Sun
tot	Total
v	(Water) vapour
w	Water
ws	Windscreen

Abbreviations

Abbreviation	Description
BIBO	Bounded-Input Bounded-Output
CAD	Computer Aided Design
CAN	Controller-Area-Network
CFRP	Carbon Fiber Reinforced Plastic
CO_2	Carbon dioxide
COP	Coefficient Of Performance
EA	Evolutionary Algorithm
GAME	Genetic Algorithm for Multicriteria Engineering
HVAC	Heating, Ventilating, and Air Conditioning
IMEA	Incremental Multi-objective Evolutionary Algorithm
ISO	International Organisation for Standardisation
LTI	Linear Time Invariant (system)
MPC	Model Predictive Control
NSGA-II	Non-dominated Sorting Genetic Algorithm II
OEL	Occupational Exposure Limits
PID	Proportional–Integral–Derivative (controller)
PMV	Predicted Mean Vote
PPD	Predicted Percentage of Dissatisfied
PTC	Positive temperature coefficient; materials used for electric heating
PWM	Pulse Width Modulation
rH	Relative Humidity
SoC	System-On-a-Chip
SQP	Sequential Quadratic Programming
TCO	Total Cost of Ownership

1 Introduction

Energy consumption takes a growing importance in industry and consumer products, as a risk for the world climate, but also as a cost factor and selling point. The car industry is on the run for the “green” car, driven by growing international standards and restrictions for emissions and consumers demands. On the horizon a new type, the electric car, can be seen.

The climatisation of these vehicles becomes a difficult task. On the one hand the power consumption should decrease, on the other hand a replacement for the lower “waste-heat” of motors (especially when using electric ones) needs to be available. In order to solve this dilemma, car climatisation becomes a field of innovative concepts offering new possibilities of (automatic) climate control.

1.1 A brief history of car climate control

When the first cars got faster they needed a closed car body. This enclosed space had to be ventilated in order to provide the passengers with fresh air. The first ventilation systems - windows that could be opened - were controlled by hand. The heaters that became standard in the fifties [1] were operated by the driver as well via a turning knob or other elements.

This did not change even when the first air conditioning providing cooling and dehumidification (without the option of air humidification) was introduced into the mass market (first 1954). The mechanics behind the knobs were changed to potentiometers and motors from the 1970s onward (seen in Figure 1.1), but today the “thermal control loop” is still often closed by the human in the car: The driver adjusts the inlet-air settings in order to achieve a comfortable climate.

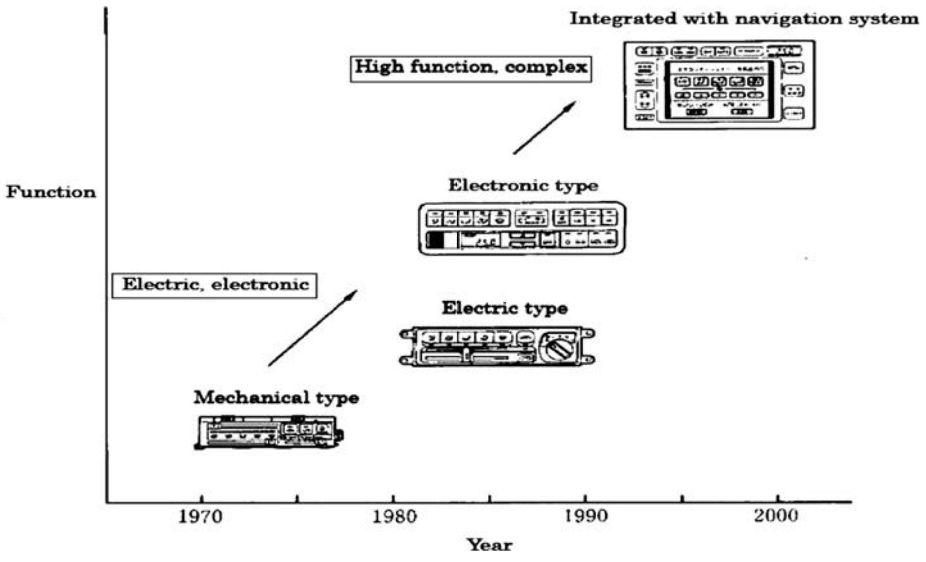

Figure 1.1: The development of climate control units. [2]

In 1964 the first system for an automatic controlled cabin temperature was brought onto the market by Cadillac. Having been an optional feature for upper class cars regarded as a luxury in the beginning, an automatic "climate control" can now be ordered for almost every car. This is easily possible through the electrification mentioned before and the introduction of digital control (first 1975 by Rolls-Royce). Still what is called automatic climate control is in most cases only automatic temperature control.

A *climate* control should also include humidity control if not other factors like the carbon dioxide concentration [3] and the air outlet distribution. Basic approaches are found for example in air quality sensors for automatically enabling air recirculation in order to prevent odours and exhaust gases from entering the cabin. However, increased passenger comfort still is the main reason for these systems being integrated into cars.

1.2 Trends in car climate control

There are two trends that can be seen in automatic climate control in cars.

First there is a trend towards more complexity in the equipment. New sensors allow better automatic control, for example an improved solar sensor [4] and the already mentioned CO_2 sensor. The use of decoupled electronic operated compressors (as in the Toyota Prius [5]) and humidity sensors allows better use of recirculation and better adjustment of the compressors working point. These new “tools” make it possible to increase safety through fogging-prevention and providing better thermal comfort while using less electricity.

The second trend is a constant pricing pressure. This is nothing in car industry, but leads to the result that only such features are integrated into a new model which give a benefit to the customer that she or he is willing to pay for or are cheaper. Therefore, the possibilities described in the paragraph above will mostly be offered as an expensive option or not used at all in combustion cars.

In an electric car, however, these new developments give a benefit that is very valuable: extended range. Their integration into hybrid cars has prove that they are worth the price.

1.3 Overview of this work

In Chapter 2 the objectives for a car climate control will be shown in detail. Chapter 3 presents the subject of the control, the car cabin system and the HVAC-hardware, with simple system equations. Then, an automatic climate control strategy is presented in Chapter 4. Its components and the applied algorithms are described in Chapters 5, 6 and 7. How the control objectives, the system and the required functionality are integrated into this control concept is shown in Chapter 8.

The designed algorithm is implemented in Matlab for the use in the electric car *MUTE*. The concept of *MUTE* and and its climatisation strategy are found in Chapter 9. The car's material, actors, sensors and processing hardware are explained in the following Chapter 10. Chapter 11 covers the implementation of the presented solution in Matlab and Simulink. Results of this working control program are presented in Chapter 12, as far as they could be obtained without an existing car in the hardware-in-the-loop test rig and in simulations. The thesis concludes with a summary and an outlook at possible improvements.

2 Control objectives

For an electric car energy saving is especially important. Accordingly, the *power consumption* should be minimised by the controller. However, other objectives have to be taken into account, too.

The cooling/heating system may also be used for tempering car components as power electronics and the motor. Their *thermal working point* has then to be taken care of, too. The main reason, however, for advanced climate control in cars still is *comfort* - as stated in the last chapter. More fundamentally, it has to provide *safety*.

A closer look will be taken in this chapter at the following four general objectives:

- maximising *safety*
- maximising *comfort*
- minimising *power consumption*
- optimising the *(thermal) working point of components*

The reduced power consumption is often opposed to the other objectives although it may match comfort wishes like low noise. For example, recirculating air reduces the required heating (or cooling) power, but it leads to faster fogging and impairs the air quality.

This is only accepted to a certain degree by the passengers. Of course, a high thermal comfort is an important sales argument for a car, but it is also connected to safety. A good automatic operation with little need to adjust leads to less distraction, and a driver who is in a comfortable (thermal) environment can focus better on the traffic [1]. However, the most important safety aspect is free view trough the windscreen (i.e. no fogging or icing).

2.1 Windscreen defogging

Fogging occurs when the air at the windscreen is saturated with water. Water precipitates on the glass and limits the view. The amount of water in the air leading to condensation is dependent on the air temperature. The saturation vapour pressure (maximum partial vapour pressure) can be well approximated within the relevant limits for a car by the following equation taken from DIN 4108-5 [6]. The resulting curve is shown in Figure 2.1.

$$p_{sat}(T) = C_1 \cdot \left(C_2 + \frac{T}{100\text{°C}} \right)^{C_3} \tag{2.1}$$

p_{sat}	Water vapour saturation pressure [Pa]
T	Water vapour temperature [°C]
C_1, C_2, C_3	Constants

Table 2.1: Constants used in equation 2.1 for the different temperature ranges. [6]

Phase	Temperature range	C_1 [Pa]	C_2	C_3
Ice		4.689	1.486	12.30
Water	0 °C - 30 °C	288.68	1.098	8.02

There exist several solutions to detect fogging. Some are based on optic effects (infrared or a camera). The majority of implementations use a humidity sensor coupled with temperature measurements on the (glass) surface. The following will focus on a system where the absolute humidity in the cabin as well as the windscreen temperature is known (i.e. measured) . With this data the position in Figure 2.1 can be determined and a “fogging risk” can be calculated. In this way an impairment of the driver’s vision can be avoided.

Relative humidity is not a good indicator to determine how close to fogging the conditions are since it depends a lot on the temperature. In the paper *Prediction of Water Vapor Condensation on Automobile Windscreens* [6] C. Gühmann defines an absolute distance of a point to the saturation curve in the temperature-water vapour pressure diagram. To compensate for the different units of both axes in the graph a factor is

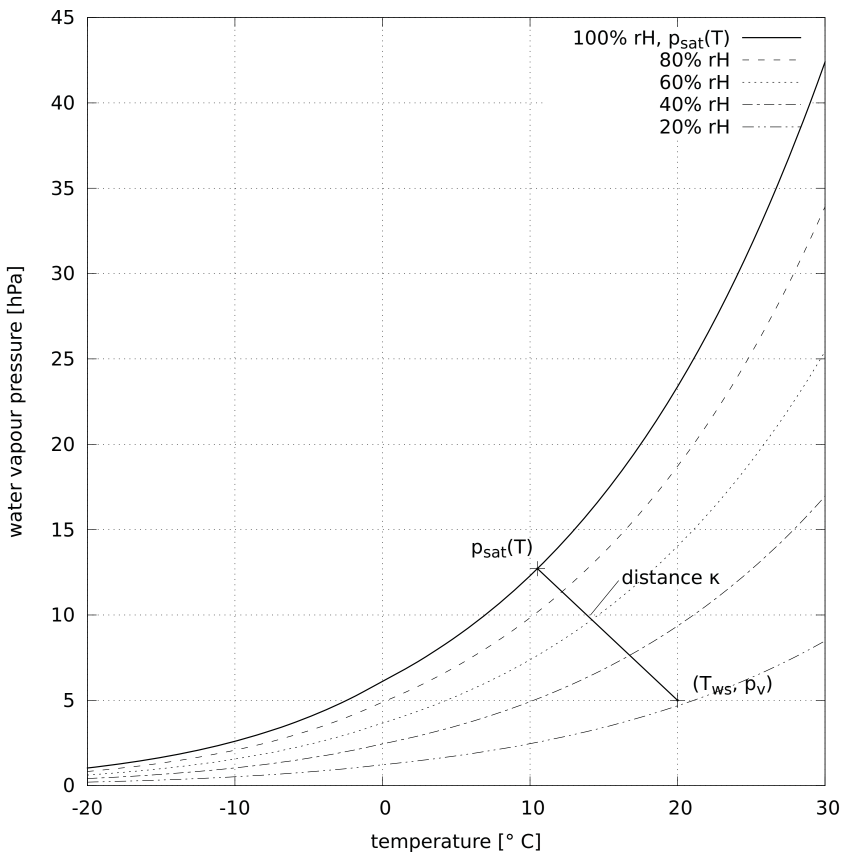

Figure 2.1: Saturation vapour pressure curve and the fogging affinity κ.

required. This is achieved by taking the average slope of the saturation curve in the range from -20 to 30 ℃.

$$a_{p_{sat}} = \frac{\Delta p_{sat}}{\Delta T} = \frac{p_{sat}(-20℃ - p_{sat}(30℃)}{-20℃ - 30℃} = 83\,\frac{\mathrm{Pa}}{\mathrm{K}} \tag{2.2}$$

The distance κ represents the affinity to condensate of a partial water vapour pressure p_v on a windscreen with the temperature T_{ws} and is then calculated by [6]

$$\kappa = \min\left(\sqrt{\left(\frac{p_{sat} - p_v}{a_{p_{sat}}}\right)^2 + (T_{sat} - T_{ws})^2}\right) \tag{2.3}$$

An example can be seen in Figure 2.1.

2.2 Comfort

General influences on comfort by P.O. Fanger can be seen in Figure 2.2. The *environmental* factors are those of highest interest here since they can be influenced by the climatisation. The *human* and *other factors* differ between passengers. They need to be estimated the best possible or adjustable. Among the *psychological factors*, noise will not be taken into

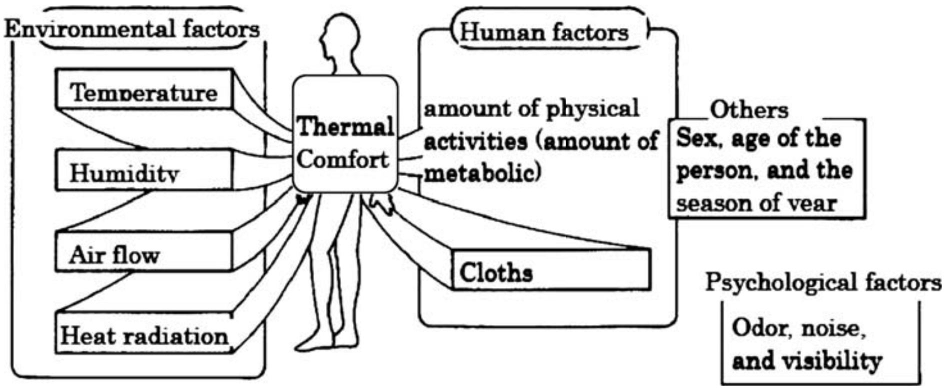
Environmental factors
Temperature
Humidity
Air flow
Heat radiation
Thermal Comfort
Human factors
amount of physical activities (amount of metabolic)
Cloths
Others
Sex, age of the person, and the season of year
Psychological factors
Odor, noise, and visibility

Figure 2.2: Influences on comfort as found by P. O. Fanger. [2]

account since it can hardly be influenced by the climate control. Its main source in the HVAC-unit is the fan. This topic will mostly be addressed in the hardware development. The fan speed will also be regarded through the energy consumption objective. A quite important factor is odour in the sense of air quality since fresh air supply is the main reason for having a ventilation system in a car.

2.2.1 Thermal comfort

A well established calculation of thermal comfort is the one found by Fanger in the 1970s. It is also included in the ISO standard 7730 [7].

The method is based on a body's heat balance equation:

$$\dot{q}_H - \dot{q}_d - \dot{q}_{sw} - \dot{q}_{re} - \dot{q}_L = \dot{q}_R + \dot{q}_C \qquad (2.4)$$

$\dot{q}_H$	Internal heat production
$\dot{q}_d$	Heat loss due to water vapour diffusion through the skin
$\dot{q}_{sw}$	Heat loss due to sweating
$\dot{q}_{res}$	Latent heat loss due to respiration
$\dot{q}_L$	Dry respiration heat loss
$\dot{q}_R$	Heat loss by radiation from the surface of the clothed body
$\dot{q}_C$	Heat loss by convection from the surface of the clothed body

By combining this equation with experimental data a comfort index reaching from -3 (too cold) to +3 (too hot) has been found. The resulting figure is called *Predicted Mean Vote* (PMV).

$$PMV = (0.303e^{-0.036M} + 0.028) \cdot \{\dot{q}_H - \dot{q}_d - \dot{q}_{sw} - \dot{q}_{re} - \dot{q}_L - \dot{q}_R - \dot{q}_C\} \tag{2.5}$$

The expressions used in equation 2.5 can be stated as follows [8]:

$$\begin{aligned}
\dot{q}_H &= M - W \\
\dot{q}_d &= 3.05 \cdot 10^{-3}\, [5733 - 6.99\, (M - W) - p_v] \\
\dot{q}_{sw} &= 0.42\, [(M - W) - 58.15] \\
\dot{q}_{res} &= 1.7 \cdot 10^{-5}\, (5867 - p_v) \\
\dot{q}_L &= 0.0014\, M\, (34 - T_{air}) \\
\dot{q}_R &= 3.96 \cdot 10^{-8}\, f_{cl}\, [(T_{cl} + 273)^4 - (T_r + 273)^4] \\
\dot{q}_C &= f_{cl}\, h_{cl}\, (T_{cl} - T_{air})
\end{aligned} \tag{2.6}$$

$$\begin{aligned}
T_{cl} &= 35.7 - 0.028\, (M - W) - 0.155\, r_{cl}\, [\dot{q}_R + \dot{q}_C] \\
h_{cl} &= \begin{cases} 2.38\, (T_{cl} - T_{air})^{0.25} & \text{for } 2.38\, (T_{cl} - T_{air})^{0.25} > 12.1\sqrt{v_{air}} \\ 12.1\sqrt{v_{air}} & \text{for } 2.38\, (T_{cl} - T_{air})^{0.25} < 12.1\sqrt{v_{air}} \end{cases} \\
f_{cl} &= \begin{cases} 1.00 + 0.2\, r_{cl} & \text{for } r_{cl} < 0.5\,\text{clo} \\ 1.05 + 0.1\, r_{cl} & \text{for } r_{cl} > 0.5\,\text{clo} \end{cases}
\end{aligned} \tag{2.7}$$

M	Metabolism [met] ($1\,\text{met} = 58,15\,\frac{\text{W}}{\text{m}^2}$, sitting calm)
W	External work [met]
p_v	Water vapour pressure [Pa]
T_{air}	Air temperature [°C]
f_{cl}	Ratio of the surface area of the clothed body to the surface area of the nude body [-]
T_{cl}	Surface temperature of the clothing [°C]
T_r	Mean radiant temperature [°C]
h_{cl}	Convective heat transfer coefficient [$\frac{\text{W}}{\text{m}^2\cdot\text{K}}$]
r_{cl}	Thermal resistance of clothing [clo] ($1\,\text{clo} = 0.155\,\frac{\text{m}^2\cdot\text{K}}{\text{W}}$)
v_{air}	Relative air velocity [$\frac{\text{m}}{\text{s}}$]

2.2.2 Inhomogeneous climate

The model by Fanger was developed for stationary environmental conditions. It gives no means of including the influence of different temperatures and air flows on the body.

A more complex approach is used in the ISO standard 14505-2 [9] by measuring temperatures of body parts. A comfort function chart found in these experiments is given for a winter and a summer case. It is found that a cooler temperature in the head area is desired, while warm feet lead to maximum comfort, especially with cooler ambient temperatures. This is opposed to the natural air layering where the warmer and lighter air is on top.

Controlling this online would require a lot of sensors and actors. Therefore, this is usually implemented in hardware in a car HVAC-system. The air flow is optimised in such way that warm air is output through the foot and defrost outlets, while cooler air is going directly to the passenger. Manual adaption of the direct air flow temperature is sometimes implemented. Since this is related to the hardware, the temperature layering will not be regarded further in this work.

The air flow itself can also cause discomfort. Higher air speed on the body leads to higher heat transfer coefficients and consequently to an intensified temperature sensation. The effect of moving air with ambient temperature is included in the comfort calculation in equation 2.6. Local air jets with a different temperature, however, as they occur in a car, are not considered. They can be comfortable when the air from the outlet is warm but should be avoided when it is cold. A more detailed temperature dependent sensation chart by Teerhag (1986) [10] is shown in Figure 2.3. A formula to calculate the percentage

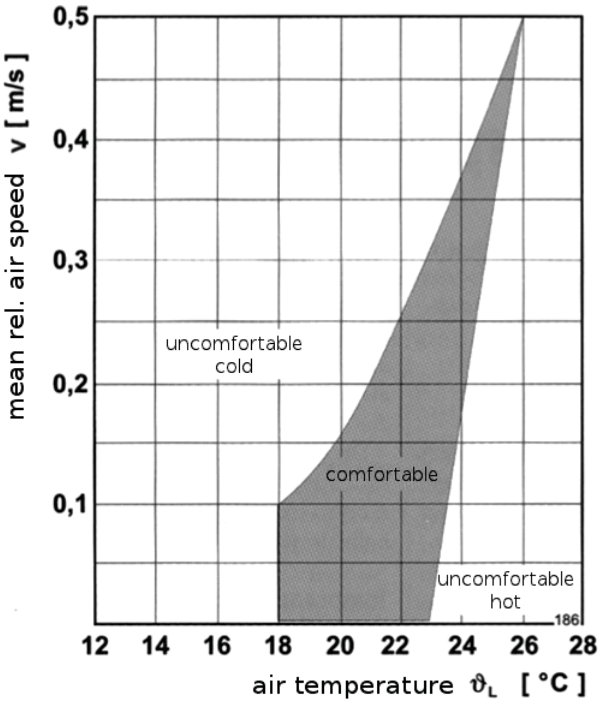

Figure 2.3: Comfort in relation to air speed and its temperature as found by Teerhag (1986). [10]

of dissatisfied persons by air flow is given in ISO 7730 [7] and illustrated in Figure 2.4. It is also noted that air speeds above 0.82 $\frac{\text{m}}{\text{s}}$ should be avoided. However, no other influences (like radiation) which could lead to a comfortable feeling even at cooler or higher air flows are included in both charts .

2.2.3 Air humidity

Not only (felt) air temperature is influencing comfort. High humidity can lead to oppressive climate even if one is not feeling hot [1].Moisture is undesired since it supports the development of microorganisms. On the other hand very dry air can irritate the mucous membranes and the skin. In 1951, Leudsen and Freymark found a correlation for buildings shown in Figure 2.5. The recommendations made in DIN 1946-3 [11] to keep the relative humidity between 30% and 60% for comfort temperatures are also shown in this figure.

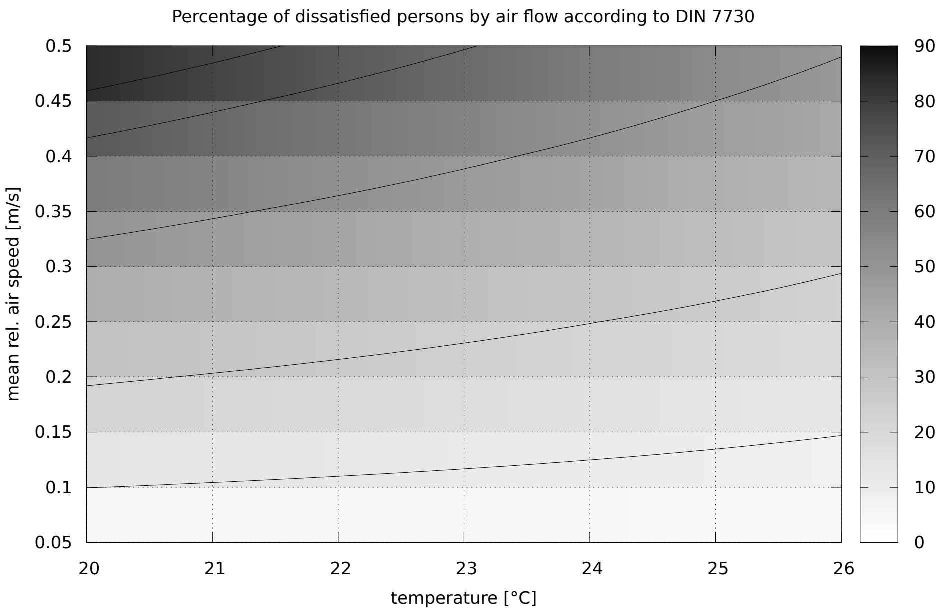

Figure 2.4: The percentage of dissatisfied people by air flow according to ISO 7730 [7] (turbulence = 40%).

Another general proposed rule of thumb is to keep the absolute humidity below 13 $\frac{\mathrm{g}}{\mathrm{kg}}$ [1].

It can be seen that a large range of air humidity is acceptable. Influences on the felt temperature are already implemented in the equations 2.6.

2.2.4 Air quality

Apart from humidity the air in a car contains many other substances. In too high concentrations most of them lead to unpleasant side effects. Particles like pollen can irritate the eyes and the mucous membranes. They are mostly filtered in the HVAC-system and will therefore not be taken into account. Gases in differing concentrations can lead to odour and - very undesirable in a car - impair concentrativeness [13].

The most important of these gases is carbon dioxide which is often used as an indicator for air quality and emitted by humans. A maximum concentration in a working environment or occupational exposure limit (OEL) is given by a value of 0.5 Vol% (which equals 5000 ppm or 9000 $\frac{\mathrm{mg}}{\mathrm{m}^3}$) [1]. This level can be reached after 8 minutes in a standard

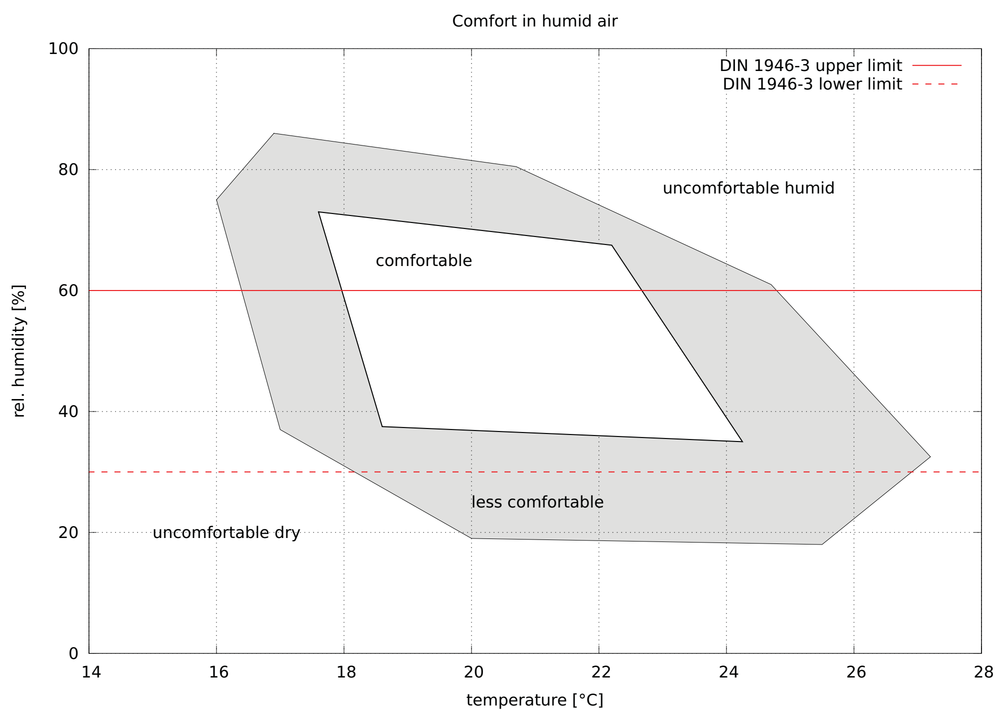

Figure 2.5: Comfort in humid air as found in Leudsen and Freymark (1951) [12] and DIN 1946-3 [11].

car with four persons and without fresh air supply (e.g. in recirculation mode) [1].

Most of the other sources give a lower concentration as guideline value. A relation between the percentage of dissatisfied people and the CO_2 level [14] is shown in Figure 2.6.

It is seen that at a level of 650 ppm above the outdoor carbon dioxide concentration (of around 350 ppm-400 ppm) nearly 20% percent of the people are dissatisfied.

This causes no problem as long as only fresh air ventilation is used. With an increased use of recirculation though, the concentration can increase quite fast. Hence pure recirculation should be avoided. A minimum fresh air supply rate of $22\,\frac{\mathrm{m}^3}{\mathrm{h\ Person}}$ is advised to obtain an acceptable air quality [13].

2.3 Power consumption

An HVAC-system has three main power consumers: the cooling unit, the heating unit and the ventilation. The remaining electric components, like motors for the flaps or sensors,

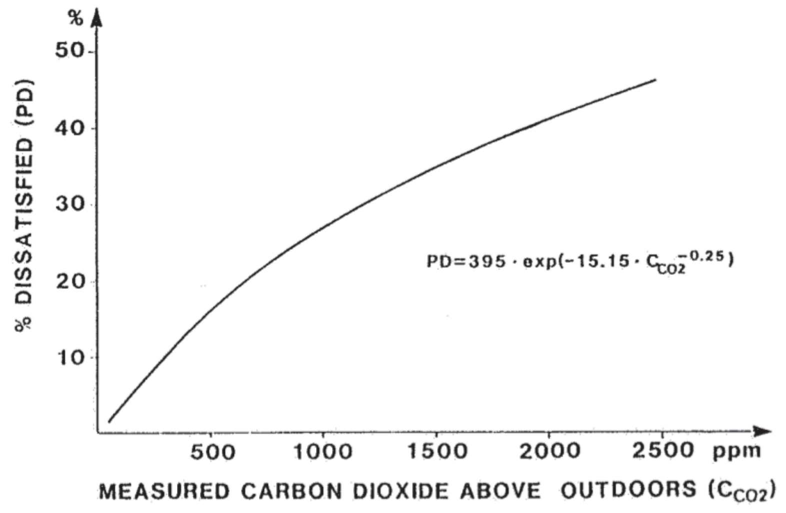

Figure 2.6: The perceived air quality (% dissatisfied) as a function of the carbon dioxide concentration. [14]

do not take much power.

The fan is spinning nearly all the time to provide the passengers with fresh air. This is necessary as seen in Section 2.2.4. Depending on the model its power consumption can be as high as 250 W [1]. Although this will be needed rarely. An average consumption below 100 W is realistic for normal car.

A typical cooling power in a car is around 5 kW [2]. The installed and maximum power may be higher. In the refrigeration circuit the only powered unit is the compressor. The refrigerant is compressed and enters the condenser to transfer heat to the ambient air. It is then liquefied and expanded into the evaporator cooling the inlet-air. The vaporised gas returns to the compressor and the cycle starts again. In this way heat is transferred from the interior to the outside and the car is cooled. The compressor only consumes the electric power to compress the gas. This corresponds to around 33%-50% of the cooling power. The energy is mostly taken mechanically from the (fuel-)engine and is replaced by a separate motor in an electric car.

A typical heating power for a car is around 4 kW and thus of the same magnitude as the cooling power [2]. In today's fuel-run cars most of this is provided by the engines' waste heat. Only if this it not sufficient, electrically heated PTC-elements are used. Taking away the combustion process as main heat source other solutions have to be found for the electric car. Using electricity directly with PTC-elements is not economical. Heat pumps or fuel heaters are more efficient options when it comes to power consumption.

A fuel heater only needs electric power for the ignition process and for its fan. During the ignition around 100 W can be drawn from the power supply. Once started the consumption is quite low. The fuel consumption for such small heaters are around $0.14\,\frac{\mathrm{l}}{\mathrm{h \cdot kW}}$. However, a reservoir for the fuel has to be provided.

A heat pump is basically working like a refrigeration circuit, but with the possibility to heat the passenger compartment as well. As heat sources not only the ambient air can be used, but also internal components like the battery pack or the electric motor. A detailed description of the functioning is found in section 3.3. The advantage of this solution is that it does not need a separate energy source like fuel. In addition, nowadays' standard of heating *and* cooling (and thereby dehumidification) can be combined in one system. On the other hand, the electric energy consumption will be higher than a fuel based solution. The power demand is dependent on the components (e.g. the compressor) and on the temperature level of the heat source/sink and the desired output temperature. One critical point concerning the use of a heat pump in a car is icing of the front heat exchanger (evaporator) when heating in winter. This leads to a dramatically decreased efficiency down to a point where the refrigerant circuit does not work anymore.

Typically there are no sensors measuring the power consumption of the components, but since they are directly controlled the current can be estimated. The components' consumption has to be measured once and then these values are used.

When the energy is consumed is also an important fact in an electric car. There might be situations, when it is good to consume as much as possible, for example when the battery is fully charged, but the car is recuperating. On the other hand when the car is short on electric power or the connection to the high voltage system fails, only the current absolutely necessary may be drawn. In general the power consumption should be minimised while providing a maximum comfort, but this is dependent on the cars energy overall situation.

2.4 Influence on other components

Components like the battery, the power electronics and/or the electric machine can be used as heat sources or sinks with a heat pump as mentioned before. When doing so the influences on these parts have to be taken into account.

The battery, for example, needs a certain temperature to be able to deliver high power. Above a certain temperature, though, gases will evaporate and lead to possible failure or even safety risks up to inflammation and explosion. For a prolonged lifetime, which is of interest since the battery is most expensive part of an electric car at the moment, an optimal temperature frame exists. For the electrics it might be advantageous to be as cold as possible, but below a certain level mechanics (lubricant viscosity) will oppose.

The component manufacturers specify a temperature range for an optimal functioning. The thermal management system takes the responsibility for not exceeding these limits.

3 System description

In order to understand how the involved systems are working and interacting physical models are made use of. These are kept as simple as possible to find out about the (main) influences. The use in the controller requires as well models that are fast to calculate. For this reason, 3D fluid dynamics simulations will not be treated here. The following equations will be one-dimensional and will not describe details of disturbances which are very hard to measure online (as e.g. air leakage).

3.1 The car cabin system

In the car cabin system, the air in the car and the windscreen will be considered. Four quantities or states were identified to be relevant for the objectives found in Chapter 2: Air temperature, absolute humidity, carbon dioxide concentration as well as the windscreen surface temperature for the fog detection.

3.1.1 Cabin air temperature

In a car we have first the desired and controlled air flow from the HVAC-unit. The amount of air blown into the cabin will also leave it (in a steady state). These two heat flows are denoted by $\dot{Q}_{in}$ and $\dot{Q}_{out}$. The sources not connected to air flow are the heat transfer through the car body ($\dot{Q}_{cab}$) and the solar radiation ($\dot{Q}_{r}$). These two influences can in most cases be regarded as static or slowly changing over one trip. Transient heat sources are the thermal masses in a car. For heating a car in the winter a lot of energy is used to heat-up the seats, the car body and other parts. This heat source (or sink) is named $\dot{Q}_{mass}$. Other influences on the temperature in the car are often hard to quantify and will be summed into $\dot{Q}_{other}$. This can be air leakage, the passengers in the car, electronics or heat coming from the engine. There are additional disturbances like open windows or doors which are important to the air temperature. They are also covered by “others” since they are unpredictable and hard to compensate for. Figure 3.1 shows all the heat flows and approximately where they occur in the car.

If the sum of these influence is unbalanced (i.e. $\neq 0$), a change in the thermal energy of the air in the cabin ($E_{air,cab}$) occurs, giving a $\frac{\mathrm{d}E_{air,cab}}{\mathrm{d}t}$.

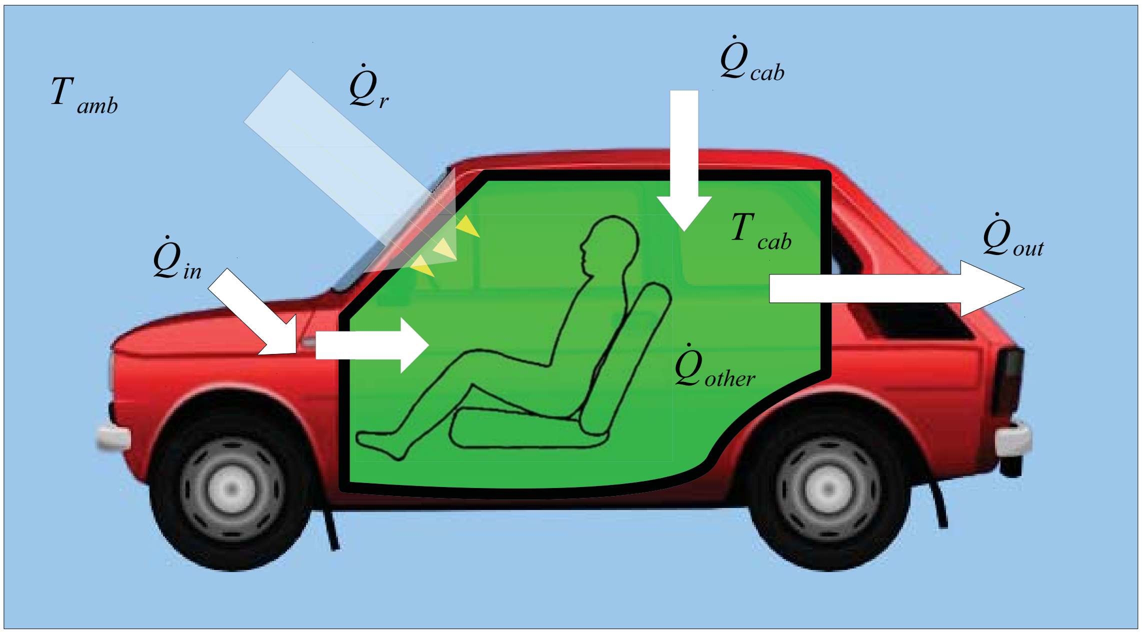

Figure 3.1: Heat balance in a car.

The resulting basic heat balance equation reads:

$$\frac{\mathrm{d}E_{air,cab}}{\mathrm{d}t} = \dot{Q}_{in} + \dot{Q}_{cab} + \dot{Q}_{out} + \dot{Q}_{mass} + \dot{Q}_r + \dot{Q}_{other} \tag{3.1}$$

H. Großmann [1] gives formulas for most of the heat flows. They are extended and a parameter for the fraction of recirculated air, μ_{recirc}, is introduced.

$$\begin{aligned}
\frac{\mathrm{d}E_{air,cab}}{\mathrm{d}t} &= m_{air,cab} \cdot c_{V,air} \cdot \frac{\partial T_{cab}}{\partial t} \\
\dot{Q}_{in} &= \dot{Q}_{heat} \\
\dot{Q}_{cab} &\approx \frac{A_{cab}}{R_{cab}} \cdot (T_{amb} - T_{cab}) \\
\dot{Q}_{out} &= (100\% - \mu_{recirc}) \cdot \dot{m}_{air,in} \cdot c_{p,air} \cdot (T_{amb} - T_{out}) \\
\dot{Q}_{mass} &= -\frac{\partial T_{cab}}{\partial t} \cdot \sum_i (m_i \cdot c_i) \\
\dot{Q}_{r} &= \sum_j \left(A_j \cdot \cos(\alpha_j) \cdot \dot{q}_{sun} \cdot \gamma_j\right)
\end{aligned} \tag{3.2}$$

$m_{air,cab}$	Air mass in the cabin [kg]
$c_{V,air}$	Specific heat capacity of the air at constant volume [$\frac{\mathrm{kJ}}{\mathrm{kg \cdot K}}$]
$\dot{m}_{air,in}$	Air mass flow through the car [$\frac{\mathrm{kg}}{\mathrm{s}}$]
μ_{recirc}	Percentage of $\dot{m}_{air,in}$ being recirculated [%]
$c_{p,air}$	Specific heat capacity of the air at constant pressure [$\frac{\mathrm{kJ}}{\mathrm{kg \cdot K}}$]
$\frac{A_{cab}}{R_{cab}}$	Heat transfer through the car body [$\frac{\mathrm{W}}{\mathrm{K}}$]
$m_i \cdot c_i$	Heat capacity of the parts of the car interior and body [$\frac{\mathrm{kJ}}{\mathrm{K}}$]
t	Time [s]
$\dot{Q}_{heat}$	Thermal power of the HVAC-system heater [W]
T_{cab}	(Mean) temperature of the air in the cabin [°C]
T_{out}	Temperature of the air leaving the cabin [°C]
A_j	Window area j [m^2]
α_j	Angle between surface normal of j and direction to the sun [°]
γ_j	Transmittance of j [-]
$\dot{q}_{sun}$	Sun intensity [$\frac{\mathrm{W}}{\mathrm{m}^2}$]

Interior parts and the air are assumed to have the same temperature here. This is not correct, however, since the sun influence heats up the interior much more than the air. If this was considered, a more complicated model will be required introducing the (surface) temperature of the interior as a new state.

The outlet temperature T_{out} will be simplified set equal to T_{cab}. Different approaches to estimate this temperature [1] are suggested but they are only valid without recirculating air and for standard car layouts. The heat transfer of the car $\frac{A_{cab}}{R_{cab}}$ can be calculated by summing up the contributions of all the cabin parts [1]:

$$\frac{A_{cab}}{R_{cab}} = \sum_{n=1}^{n_{surfaces}} \frac{A_n}{\frac{1}{h_{cab,in,n}} + \frac{d_n}{k_n} + \frac{1}{h_{cab,out,n}}} \tag{3.3}$$

While the thermal conductivity k and the material thickness d and area A are usually known and constant, the convection heat transfer coefficients on the outside, $h_{cab,out}$, and inside the cabin, $h_{cab,in}$, depend on the air speed. Großmann gives approximations for these correlations: $h_{cab,in} \propto \dot{m}_{air,in}^{0.5}$, $h_{cab,out} \propto v_{air}^{0.8}$

The temperature of the air blown into the cabin can be expressed with the following equation:

$$T_{in} = \dot{Q}_{heat} \cdot \frac{1}{\dot{m}_{air,in} \cdot c_{p,air}} + (100\% - \mu_{recirc}) \cdot T_{amb} + \mu_{recirc} \cdot T_{cab} \tag{3.4}$$

Combining equations 3.1, 3.2 and 3.4, a differential equation for an estimation of the mean cabin temperature can be given.

$$\begin{aligned}\frac{\partial T_{cab}}{\partial t} =& \frac{1}{m_{air,cab} \cdot c_{V,air} + \sum_i (m_i \cdot c_i)} \cdot \\ & \left[\dot{m}_{air,in} \cdot c_{p,air} \cdot (T_{in} - T_{cab}) + \frac{A_{cab}}{R_{cab}} \cdot (T_{amb} - T_{cab}) + \dot{Q}_r + \dot{Q}_{others}\right]\end{aligned} \tag{3.5}$$

3.1.2 Water mass in the cabin air

Water in the cabin has two sources. One is the incoming (moist) air. The other are the passengers with their respiration, sweat as well as other humidity in the clothes and shoes. Water leaves the car through the air outlet or is separated at the evaporator.

A basic water equation is found at Großmann [1]. It is however only applicable in a steady context and does not implement a recirculated air percentage μ_{recirc}. Therefore, it is modified in the following:

$$\frac{\partial m_{w,cab}}{\partial t} = \dot{m}_{w,in} - \dot{m}_{w,out} + \dot{m}_{w,pas} - \dot{m}_{w,cond} \tag{3.6}$$

$m_{w,cab}$	Water mass in the cabin air [kg]
$\dot{m}_{w,in}$	Water mass flow in the incoming air [$\frac{\text{kg}}{\text{s}}$]
$\dot{m}_{w,out}$	Water mass flow leaving the car [$\frac{\text{kg}}{\text{s}}$]
$\dot{m}_{w,pas}$	Water mass flow produced by the passengers [$\frac{\text{kg}}{\text{s}}$]
$\dot{m}_{w,cond}$	Water mass flow condensed at the evaporator [$\frac{\text{kg}}{\text{s}}$]

The water emitted by a human is dependent on many environmental and physiological factors (cf. Section 2.2.1). A value of $50 - 100\,\frac{\text{g}}{\text{h}}$ per person [1] can be assumed for an activity between 1 and 2 met [14].The amount of condensed water is regarded in Section 3.2. For the other components equations can be given:

$$\begin{aligned} m_{w,cab} =& \; m_{air,cab} \cdot x_{w,cab} \\ \dot{m}_{w,in} =& \; \dot{m}_{air,in} \cdot (100\% - \mu_{recirc}) \cdot x_{w,amb} \\ \dot{m}_{w,out} =& \; \dot{m}_{air,in} \cdot (100\% - \mu_{recirc}) \cdot x_{w,cab} \end{aligned} \tag{3.7}$$

$x_{w,cab}$	Absolute humidity of the cabin air [$\frac{\text{g}_{\text{vapour}}}{\text{kg}_{\text{dryair}}}$]
$x_{w,amb}$	Absolute humidity of the ambient air [$\frac{\text{g}_{\text{vapour}}}{\text{kg}_{\text{dryair}}}$]
$\dot{m}_{air,in}$	Dry air mass flow into the car [$\frac{\text{kg}}{\text{s}}$]

A complete differential equation for the absolute humidity in the cabin air is obtained by combining the relations found in equations 3.6 and 3.7.

$$\frac{\partial x_{w,cab}}{\partial t} = \frac{1}{m_{air,cab}} \cdot [\dot{m}_{air,in} \cdot (100\% - \mu_{recirc}) \cdot (x_{w,amb} - x_{w,cab}) + \dot{m}_{w,pas} - \dot{m}_{w,cond}] \tag{3.8}$$

3.1.3 Carbon dioxide concentration

A basic equation for concentrations of gases is given by Temming (1984) [1]. This is modified and the recirculation introduced with μ_{recirc}. As result a differential equation to quantify the CO_2 concentration is obtained.

$$\frac{\partial x_{CO_2,cab}}{\partial t} = \frac{1}{m_{air,cab}} \cdot [\dot{m}_{air,in} \cdot (100\% - \mu_{recirc}) \cdot (x_{CO_2,amb} - x_{CO_2,cab}) + \dot{m}_{CO_2,pas}] \tag{3.9}$$

$x_{CO_2,cab}$	Absolute CO_2 concentration in the cabin air $[\frac{g_{CO_2}}{kg_{air}}]$
$x_{CO_2,amb}$	Absolute CO_2 concentration in the ambient air $[\frac{g_{CO_2}}{kg_{air}}]$
$\dot{m}_{CO_2,pas}$	CO_2 production rate (by passengers) $[\frac{g}{s}]$

The carbon dioxide emission of a person is given as 45 $\frac{g}{h}$ [1]. Different values of 31.3 $\frac{g}{h}$ for an activity of 1-1.2 met and 82.4 $\frac{g}{h}$ for 3 met can also be found [14].

3.1.4 Windscreen temperature

The temperature at the inner side of the windscreen is of interest since fogging usually occurs here. Even if it is not equal on the whole surface, a mean value allows to estimate a temperature at least for the important middle part. In Figure 3.2 an overview of the

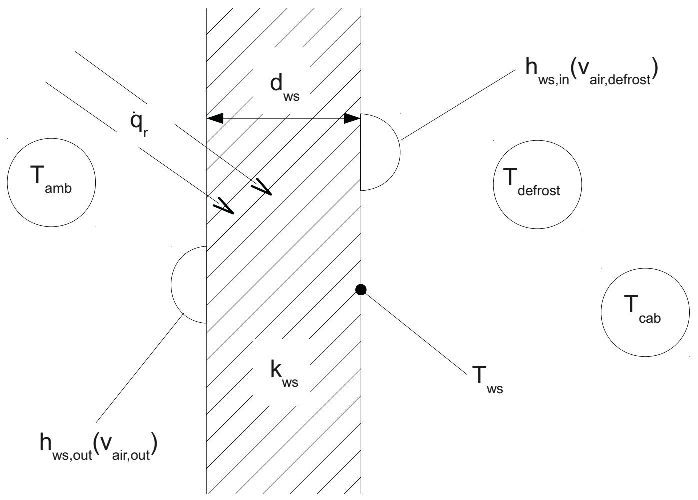

Figure 3.2: A schematic drawing of the heat transfer at the windscreen.

influences and the heat transfer is shown. On the outer side ambient air flows over the glass depending on the car speed. On the inner side temperature and air speed are governed by the air coming from the defrost outlets. Finally, other influences like sun or rain contribute to the windscreen temperature T_{ws}.

Heat transfer coefficients

The convection heat transfer coefficients $h_{ws,in}$ and $h_{ws,out}$ depend on the temperatures and the flow conditions. A forced convection is assumed in the following. This corresponds to a driving car and air blowing out of the defrost outlets.

Accurate values are hard to calculate since flow conditions change with speed, wind and weather. Therefore, a simple approximation [1] of the coefficients for a longitudinal flow on a plate will be used:

$$h \approx \begin{cases} 6.2 + 4.2 \cdot v_{air} & \text{for } v_{air} < 5\,\frac{\mathrm{m}}{\mathrm{s}} \\ 7.15 \cdot v_{air}^{0.8} & \text{for } v_{air} \geq 5\,\frac{\mathrm{m}}{\mathrm{s}} \end{cases} \tag{3.10}$$

h	Convection heat transfer coefficient $[\frac{\mathrm{W}}{\mathrm{m}^2\cdot\mathrm{K}}]$
v_{air}	Air speed $[\frac{\mathrm{m}}{\mathrm{s}}]$

To calculate the coefficient on the outside of the windscreen, $h_{ws,out}$, the car speed has to be corrected with a pressure coefficient $C_{ws,p}$ in order to obtain the air speed.

$$v_{air,out} = (1 - C_{ws,p})^{0.5} \cdot v_{car} \tag{3.11}$$

$C_{ws,p}$	Pressure coefficient [-]
v_{car}	Car speed $[\frac{\mathrm{m}}{\mathrm{s}}]$

An average $C_{ws,p}$ can be determined with experiments for a real car, but the true value cannot be given since it will be dependent on environmental influences like wind and rain. For a rough estimation it will be approximated by 0.75, a value obtained in a wind tunnel by the Modine Europe GmbH [15].

At the interior the air from the defrost outlets is blown onto the windscreen. The jet widens and the gets slower. As an estimation of the air speed the maximum velocity of a plane wall jet is taken [16]:

$$v_{air,max} = 3.5 \cdot \left(\frac{d}{x}\right)^{0.5} \cdot v_0 \tag{3.12}$$

d	Defrost nozzle size (see Figure 3.3) [m]
x	Distance from the nozzle [m]
v_0	Air speed at the outlet $[\frac{\mathrm{m}}{\mathrm{s}}]$

The defrost nozzle size ($d_{out,defrost}$) is typically around 1 cm. As distance from the

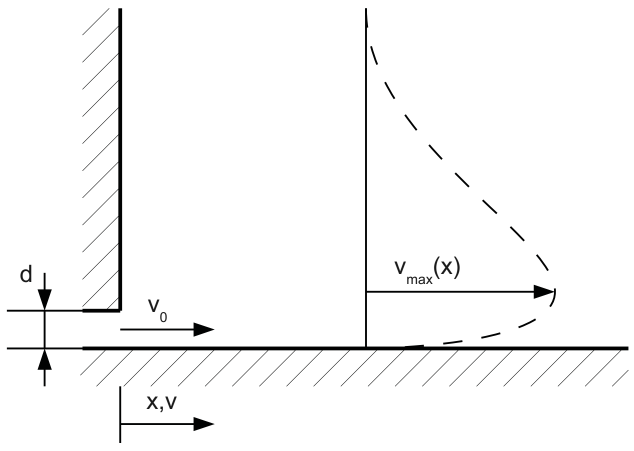

Figure 3.3: Configuration and nomenclature for the plane wall jet.

outlet half the windscreen height $l_{ws,h}$ is taken since this is the area of interest.

$$v_{air,defrost} = 3.5 \cdot \left(\frac{2 \cdot d_{out,defrost}}{l_{ws,h}} \right)^{0.5} \cdot v_{defrost,outlet} \tag{3.13}$$

$v_{defrost,outlet}$ can be estimated by dividing the air volume flow by the defrost outlet area. The air speeds obtained by this equation fit well with the magnitude of 2 $\frac{\mathrm{m}}{\mathrm{s}}$ found in an example [1].

Differential equation for the temperature

The temperature of the windscreen glass will be assumed to be approximately equal. This is permissible if the Biot number $Bi = \frac{h \cdot L}{k_{ws}} < 0.2$. A calculation with typical values gives $Bi \approx 0.02$.

The thermal conductivity of the windscreen material is assumed to be constant. A value for it is $k_{ws} = 1163 \, \frac{\mathrm{W}}{\mathrm{m \cdot K}}$ (window glass, [17]). As a typical height for a windscreen being one meter is taken. The convection heat transfer coefficient for a car with a speed of 50 $\frac{\mathrm{km}}{\mathrm{h}}$ and a pressure coefficient of 0.75 can be estimated with equations 3.10 and 3.11 to be 33.7 $\frac{\mathrm{W}}{\mathrm{m^2 \cdot K}}$.

This reasoning, however, has to be reconsidered if the windscreen is made out of different, poorly heat conducting materials like plastic.

With the assumption of an equal temperature made, an energy balance can be given based on Figure 3.2.

$$\frac{\mathrm{d}E_{ws}}{\mathrm{d}t} = \dot{Q}_{ws,in} + \dot{Q}_{ws,out} + \dot{Q}_{ws,weather} \tag{3.14}$$

$\frac{\mathrm{d}E_{ws}}{\mathrm{d}t}$	Thermal energy change of the windscreen glass [W]
$\dot{Q}_{ws,in}$	Heat transfer rate between the cabin and the windscreen [W]
$\dot{Q}_{ws,out}$	Heat transfer rate between the ambient air and the windscreen [W]
$\dot{Q}_{ws,weather}$	Heat transfer caused by other influences like rain or sun [W]

$$\begin{aligned} \frac{\mathrm{d}E_{ws}}{\mathrm{d}t} &= \rho_{glass} \cdot A_{ws} \cdot d_{ws} \cdot c_{glass} \cdot \frac{\partial T_{ws}}{\partial t} \\ \dot{Q}_{ws,in} &= h_{ws,in} \cdot A_{ws} \cdot (T_{defrost} - T_{ws}) \\ \dot{Q}_{ws,out} &= h_{ws,out} \cdot A_{ws} \cdot (T_{amb} - T_{ws}) \end{aligned} \tag{3.15}$$

$$\begin{aligned} \frac{\partial T_{ws}}{\partial t} =& \frac{1}{\rho_{glass} \cdot A_{ws} \cdot d_{ws} \cdot c_{glass}} \cdot \\ & \Big[h_{ws,in} \cdot A_{ws} \cdot (T_{defrost} - T_{ws}) + h_{ws,out} \cdot A_{ws} \cdot (T_{amb} - T_{ws}) + \dot{Q}_{ws,weather}\Big] \end{aligned} \tag{3.16}$$

The temperature of the air reaching the middle part of the windscreen is lower than at the outlet. This is due to the heat transfer to the (here assumed) colder glass. This will be taken into account with a simple estimation using the already calculated mean convection heat transfer coefficient at the inner windscreen (equations 3.10 and 3.13) for half the windscreen.

$$T_{defrost} = T_{in} - \frac{h_{ws,in} \cdot A_{ws}}{2 \cdot c_{p,air} \cdot \dot{m}_{air,in}} \cdot (T_{in} - T_{ws}) \tag{3.17}$$

There are two errors that are made in this equation. $h_{ws,in}$ is higher in the lower parts of the windscreen due to higher air speeds. On the other hand, the air temperature difference $(T_{in} - T_{ws})$ driving the heat transfer diminishes towards the middle. Therefore, this estimation should not be used for precise calculations but can be integrated into a controller due to its simplicity.

Now, the windscreen temperature can be written as a function of the ambient and defrost temperatures and the air speeds on the windscreen. The windscreen constants are assumed to be known.

$$\frac{\partial T_{ws}}{\partial t} = f(T_{amb}, T_{in}, v_{car}, v_{air,defrost}) \tag{3.18}$$

3.1.5 Time constant considerations

The systems described are of first order. A main characteristic of such systems is the time constant giving an indication of how fast the system reacts to external changes. Although the found systems are not time invariant, boundaries can be given.

For a linear time invariant (LTI) first order system the following can be written with τ being the time constant and K being the gain.

$$\tau \cdot \dot{y}(t) + y(t) = K \cdot u(t)$$

Finding the time constants for the four systems presented before gives the following results:

$$\tau_{therm} = \frac{m_{air,cab} \cdot c_{V,air} + \sum_i (m_i \cdot c_i)}{(100\% - \mu_{recirc}) \cdot \dot{m}_{air,in} \cdot c_{p,air} + \frac{A_{cab}}{R_{cab}}} \tag{3.19}$$

The varying parameters here are the air flow and the fraction of recirculation. The minimum time constant is found by using no recirculation and the maximum air flow. With the parameters found for the *MUTE* car described in Chapter 10 (see also Appendix C.1), a minimum of $\tau_{therm,min} \approx 288\,\mathrm{s}$ and a maximum of $\tau_{therm,max} \approx 754\,\mathrm{s}$ can be estimated. This is due to the high amount of thermal energy stored in the car material. The air itself will react faster. Without the interior thermal mass these times reduce to 12 and 33 seconds.

For the humidity and carbon dioxide concentration the influence of the same parameters can be seen.

$$\tau_w = \frac{m_{air,cab}}{(100\% - \mu_{recirc}) \cdot \dot{m}_{air,in}} \tag{3.20}$$

$$\tau_{CO_2} = \frac{m_{air,cab}}{(100\% - \mu_{recirc}) \cdot \dot{m}_{air,in}} \tag{3.21}$$

The maximum time constant is easily identified to equal infinity. This is the case if no air is exchanged with the environment and nothing is changing. Furthermore, the minimum values are found to be (neglecting the water mass in the air) $\tau_{w,min} = \tau_{CO_2} \approx 29\,\mathrm{s}$ for the *MUTE* car. A much faster reaction is seen as no further "storage" exists apart from the air.

For the windscreen temperature the changing variables are the convection heat transfer coefficients.

$$\tau_{ws} = \frac{\rho_{glass} \cdot A_{ws} \cdot d_{ws} \cdot c_{glass}}{(h_{ws,in} + h_{ws,out}) \cdot A_{ws}} \tag{3.22}$$

The highest time constant is found with a standing car giving $\tau_{ws,max} = 616\,\mathrm{s}$. Looking for the maximum, the estimation of $h_{ws,out}$ (equation 3.10) needs to be consulted with the maximum car speed (here 100 $\frac{\mathrm{km}}{\mathrm{h}}$ is chosen). In this way a $\tau_{ws,min}$ of approximately 51 seconds is obtained.

These values are used for controller sample time considerations and give an indication what type of control can be used. Due to the involved car parameter they will be different between car types. Moreover, some (as the infinity) will not occur in reality due to air leakages not considered here. Consequently some values might be higher than in a real car. The calculations still give a rough estimation of the timescale in which changes in the systems occur. The results show that these happen in the range of several seconds.

3.2 The HVAC-unit

The HVAC-unit is the actor in the cars thermal system. It draws the air from the outside or the car cabin (recirculation), cools and/or heats it up and defines the way to blow it into the cabin. The heat sources (and sinks) are regarded in the following Section 3.3 for a heat pump system.

For an HVAC-unit several types and layouts exist. The most common type, the air mix type, is shown in Figure 3.4. The air is drawn by a fan from the outside or the car - chosen by the recirculation flap. Before flowing through the fan, a filter (not drawn in the picture) prevents dust and other pollution from entering the car. The air passes

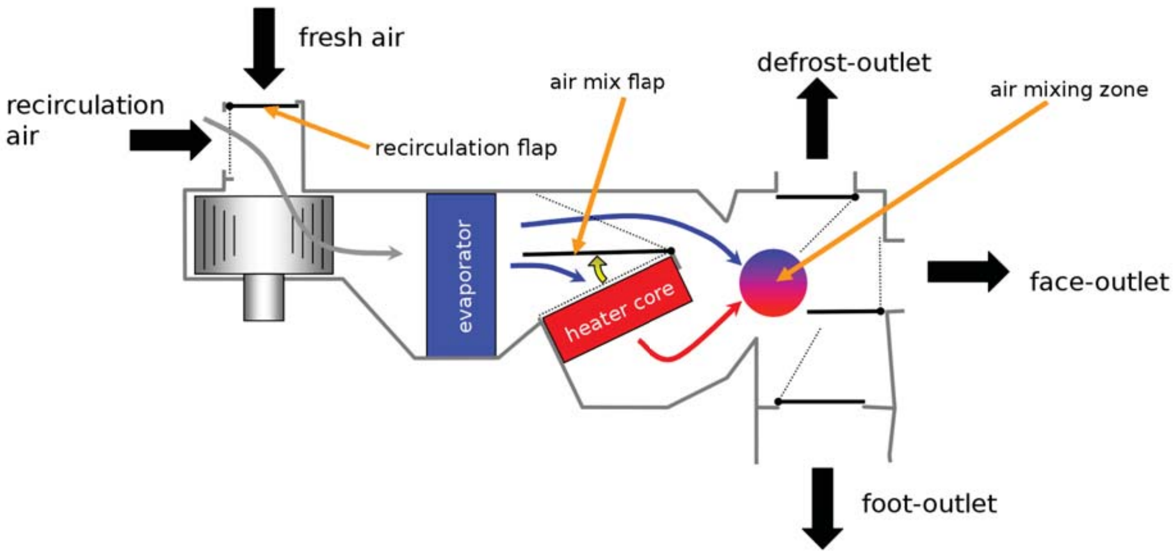

Figure 3.4: A schematic drawing of an air mix type HVAC-unit. [2]

the evaporator and is - if the evaporator is activated - cooled down and dehumidified. A part of it is then, depending on the air mix flap, heated by the engine's waste heat and/or another heating source (typically a PTC). Finally the air is (partly) mixed and distributed to the different outlets. Different temperatures for the outlets can be achieved by a good duct design and not fully mixing the cold and hot air. The foot area is usually tempered by hotter air than the face outlets which blow directly to the passengers. To defrost and defog the front windscreen, the defrost outlets are used.

Even if the layout in an electric car may change, some basic equations can be given.

3.2.1 The fan

Each fan has a characteristic curve determining the pressure drop depending on the air flow. This curve varies according to the applied voltage. A characteristic curve relating the pressure drop and the air flow can also be found for the HVAC system including the air ducts, the filter, the heat exchanger and the vents. The intersection of both curves determines the air flow into the car. An example is seen in Figure 3.5.

Several “disturbances” change the characteristic curve of the HVAC system. Some of the causes are very hard to take into account, such as blocked out- or inlets or other unpredictable events. With measurements in numbers the influence of the different ducts

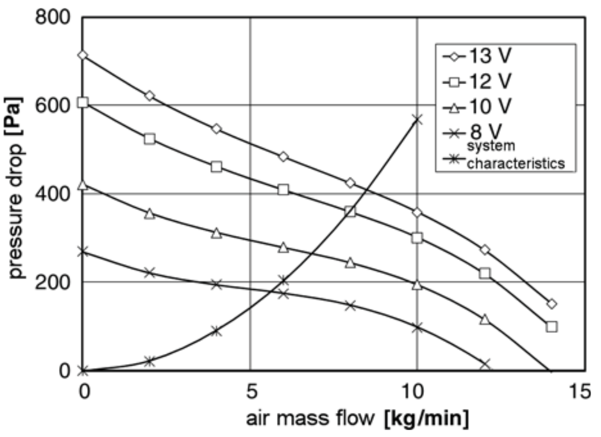

Figure 3.5: System and fan characteristics in a car for different fan voltages. [1]

through flap position changes could be included. One factor that can be at least estimated is the inlet pressure change due to the cars speed [1].

$$\Delta p = C_{inlet,p} \cdot \rho_{air} \cdot \frac{1}{2} \cdot v_{car}^2 \tag{3.23}$$

Δp	Pressure rise at the air inlet [Pa]
$C_{inlet,p}$	Pressure coefficient [-]
ρ_{air}	Air density $[\frac{\mathrm{kg}}{\mathrm{m}^3}]$
v_{car}	The cars speed $[\frac{\mathrm{s}}{\mathrm{m}}]$

The pressure coefficient is given by Großmann with a value between 0.1 and 0.3. This pressure rise is only valid for full fresh air. For a partial recirculation a lot depends on the geometry of the flap at the inlet. For this reason no general relation can be given. Some cars have a so-called “ram door”, a flap at the fresh air inlet, to reduce the influence of the car speed and prevent air flow into the cabin through the recirculation path. For a good air flow estimation without any flow or pressure sensors in the car a lot of experiments and curves are needed.

The fan’s power consumption is governed by the desired air mass flow and by its motor control. In manual controlled HVAC-systems series resistors lowering the voltage to the fan are often used. This method is very cheap and sufficient for switching between three or four speeds. The resistance also consumes power, though, making this control not very energy efficient. The modern version is realising the motor control through pulse width modulation (PWM). By switching very fast between 0 and 12 Volt the device is able to make the fan "see" different voltages depending on the pulse width. The result is a very energy efficient, continuous control. It is, however, more expensive due to the required electronics.

3.2.2 Air mixing

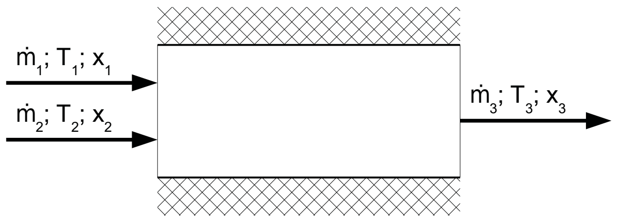

Figure 3.6: Adiabatic air mixing.

Fresh air and recirculated air are mixed at the recirculation flap. The resulting inlet air (subscript 3, see Figure 3.6) has the following properties:

$$\dot{m}_3 = \dot{m}_1 + \dot{m}_2 \tag{3.24}$$

$$x_{w,3} = (x_{w,1} \cdot \dot{m}_1 + x_{w,2} \cdot \dot{m}_2)\,\frac{1}{\dot{m}_3} \tag{3.25}$$

$$\dot{m}_3 \cdot (h_{1+x})_3 = \dot{m}_1 \cdot (h_{1+x})_1 + \dot{m}_2 \cdot (h_{1+x})_2 \tag{3.26}$$

with $(h_{1+x})_i = c_{p,air} \cdot T_i + x_{w,i}(\Delta h_v + c_{p,v} \cdot T_i)$

$$T_3 = \left[\frac{\dot{m}_1}{\dot{m}_3} \cdot (h_{1+x})_1 + \frac{\dot{m}_2}{\dot{m}_3} \cdot (h_{1+x})_2 - x_{w,3} \cdot \Delta h_v\right] \frac{1}{c_{p,air} + x_{w,3} \cdot c_{p,v}} \tag{3.27}$$

The same equations are valid after the air mix flap where warm air coming from the heat exchanger and cool air coming directly from the evaporator are mixed. The humidity of the air streams is equal in this case ($x_{w,1} = x_{w,2} = x_{w,3}$).

3.2.3 Dehumidification

Dehumidification happens in the evaporator if the air becomes colder than the dew point temperature (see Figure 2.1). This process is shown in Figure 3.7 and can be described

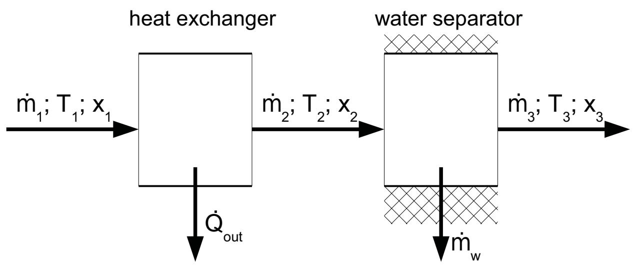

Figure 3.7: The dehumidification process.

by three equations [18]: Mass, water and energy balance.

$$\dot{m}_3 = \dot{m}_2 = \dot{m}_1 = \dot{m}_{air} \tag{3.28}$$

$$x_{w,3} = x_{w,2} - \frac{\dot{m}_w}{\dot{m}_{air}} \tag{3.29}$$

$$(h_{1+x})_3 = (h_{1+x})_1 - \frac{\dot{Q}_{out}}{\dot{m}_{air}} - \frac{\dot{m}_w}{\dot{m}_{air}} \cdot h_w \tag{3.30}$$

The enthalpy of the condensed water h_w is dependent on its temperature. If all possible water in the air is condensed, $x_{w,3}$ will be saturated $x_{w,3} = x_{w,sat}(T_2)$. The amount of condensed water can then be estimated with the following equation (assuming that the air in point 2 was oversaturated, otherwise $\dot{m}_w = 0$).

$$\dot{m}_w \approx (x_{w,1} - x_{w,sat}(T_2)) \cdot \dot{m}_{air} \tag{3.31}$$

This gives a temperature at point 3 of

$$T_3 = \left[(h_{1+x})_1 - \frac{\dot{Q}_{out}}{\dot{m}_{air}} - (x_{w,1} - x_{w,sat}(T_2)) \cdot h_w - x_{w,3} \cdot \Delta h_v \right] \frac{1}{c_{p,air} + x_{w,3} \cdot c_{p,v}} \tag{3.32}$$

with $(h_{1+x})_i = c_{p,air} \cdot T_i + x_{w,i}(\Delta h_v + c_{p,v} \cdot T_i)$

3.2.4 Heating

Heating can be expressed quite easily compared to the other cases, since the humidity and the mass flow do not change.

$$\dot{m}_2 = \dot{m}_1 = \dot{m}_{air} \tag{3.33}$$

$$x_{w,2} = x_{w,1} \tag{3.34}$$

$$(h_{1+x})_2 = (h_{1+x})_1 + \frac{\dot{Q}_{in}}{\dot{m}_{air}} \tag{3.35}$$

The heated air has a temperature of

$$T_2 = T_1 + \frac{\dot{Q}_{in}}{\dot{m}_{air} \cdot (c_{p,air} + x_{w,3} \cdot c_{p,v})} \tag{3.36}$$

3.2.5 The flaps

Different models of flaps or air doors exist. An overview and a comparison of the different types can be found in Figure 3.8. The most common type is the plate door.

	SLIDE DOOR	FILM DOOR	FLEXIBLE DOOR	MULTI BUTTERFLY DOOR	PLATE DOOR
FIG.	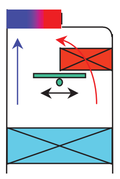	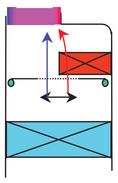	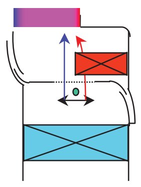	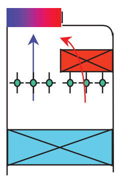	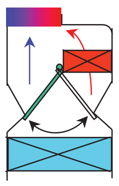
Space	+	+ +	+	+	-
Temp. Control	-	+ +	+ +	+ +	+

Figure 3.8: An overview and comparison of different flap types. [2]

In general each flap can be represented by a function describing the amount of air going through it. The shape of the curve will differ by the type and the position towards the air flow direction. It is also dependent on the air speed. Neglecting other possible influences like air temperature it can be written as follows:

$$\frac{\dot{m}_{air,through}}{\dot{m}_{air,in}} = \mu_{flap} = f(\alpha_{flap}, \dot{m}_{air,in}) \tag{3.37}$$

This relationship can be measured and put into a look-up table. Another way are predefined and limited flap positions which are calibrated once and then only used in combination. This is found in many cars as a control option for the air distribution and in its simplest case for the recirculation flap (full/none).

3.3 The heat pump

The heat pump is based on a thermodynamic cycle that is able to transport heat efficiently by the means of a compressed (and condensed) refrigerant and a subsequent expansion. One example is the cooling in today's cars which is done this way. The simplified functioning of such a cycle is seen in Figure 3.9.

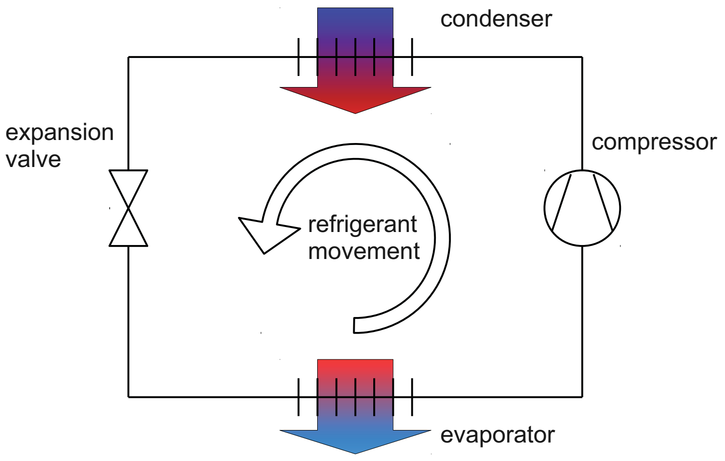

Figure 3.9: A simple vapour-compression refrigeration cycle diagram.

In an electric car the same concept as for the cooling should be used for the heating in one single cycle. This requires a more complex system, additional valves and slightly different components. Even more complexity is added by using the electric components as a heat sink (and source) as well and not only the ambient air

Such a complex heat pump cycle with all its valves (in Figure 3.10 denoted as "V"), expansion valves ("EV") and an internal heat exchanger ("IHX") to increase efficiency is shown in Figure 3.10 in two different operation modes (valve positions). This complex structure has a lot of potential to save energy. In winter “waste heat” from the electric components can help to give a comfortable climate in the car. Moreover, no additional cooling mechanism for the components is required since this can be done with the heat pump as seen in 3.10(b). Dehumidification becomes much more efficient if not the cooling *and* the heating energy have to be provided but only the difference.

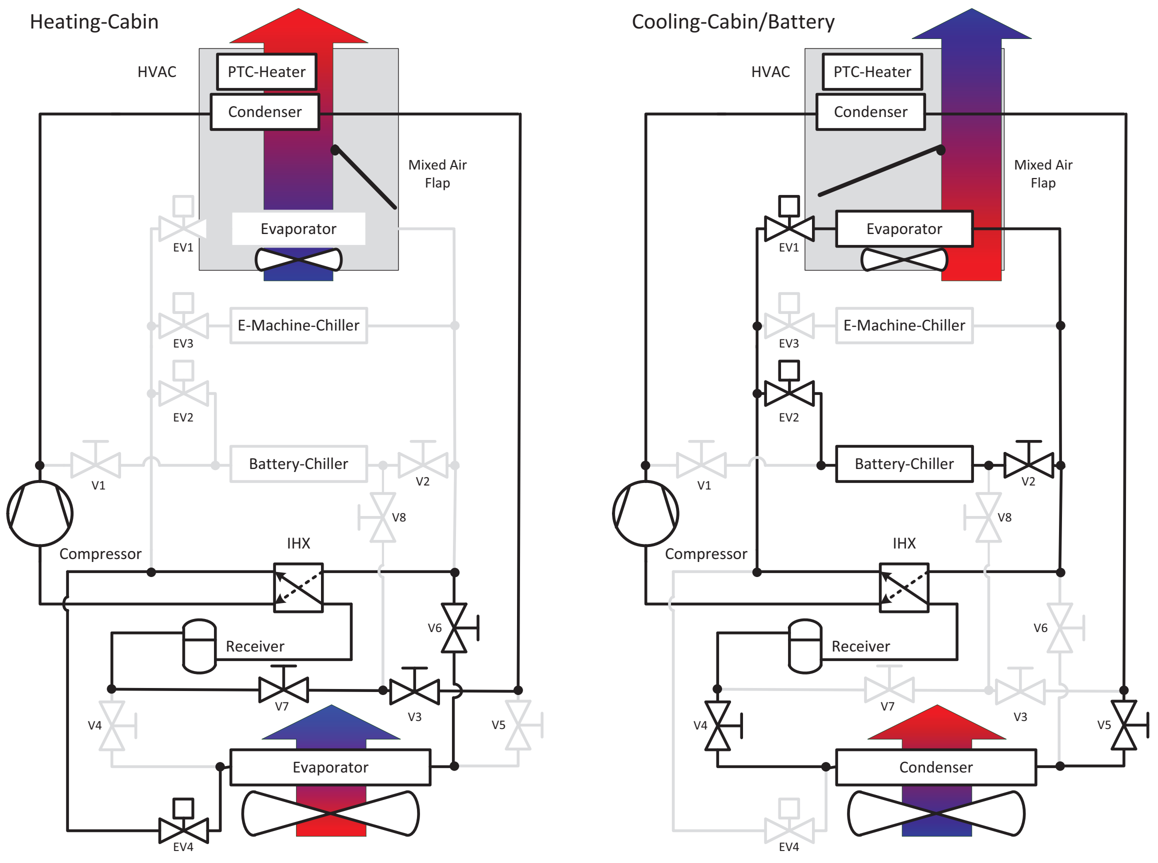

(a) Heating the cabin (b) Cooling the cabin and the battery

Figure 3.10: The heat pump system planned for the ePerformance project. [19]

Such a system also has its drawbacks. Apart from the higher material costs which are due to the big number of components, a more complicated and sophisticated control system is required to manage all these possibilities and different needs and requirements. In the following chapters the way how to include a heat pump will be mentioned. However, no detailed formulas or implementation will be given because this would go beyond the scope of this work.

3.3.1 Energy efficiency

Because of the heat transport a heat pump can “produce” more heat energy than it consumes through the compressor in the form of electricity. The efficiency is therefore indicated by the so-called *coefficient of performance* (COP) [20]. It is defined as the energy Q_{heat} delivered (in the heating case) divided by the electric energy $W_{compressor}$ consumed by the compression. A physical upper limit is given by the ideal (lossless) COP of a Carnot process.

$$COP_{heating} = \frac{Q_{heat}}{W_{compressor}} \leq \frac{T_{sink} + 273.15°\text{C}}{T_{sink} - T_{source}} \tag{3.38}$$

For the cooling case the extracted heat Q_{cool} is compared to the compressor energy. An upper limit can be given by the ideal process.

$$COP_{cooling} = \frac{Q_{cool}}{W_{compressor}} \leq \frac{T_{source} + 273.15°\text{C}}{T_{source} - T_{sink}} \tag{3.39}$$

This means the closer both temperature levels of the heat sink T_{sink} and its source T_{source} are, the better the COP can be.

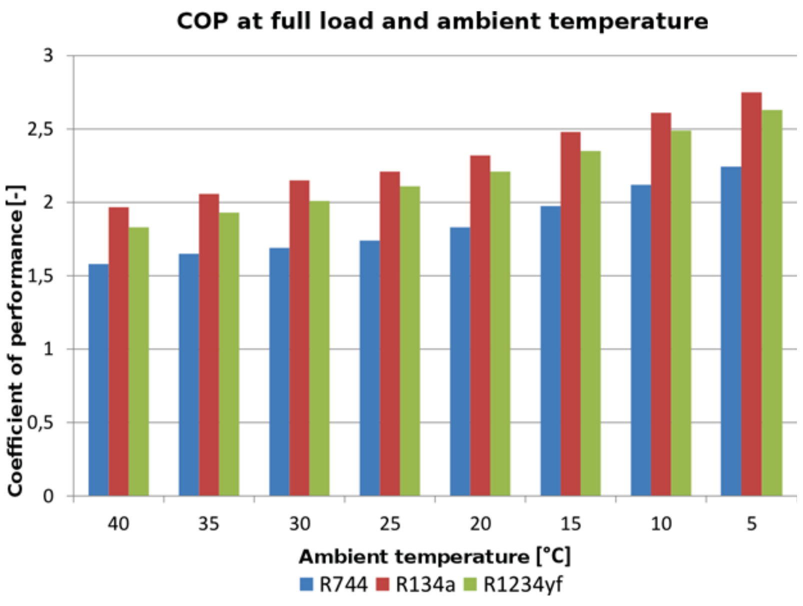

Figure 3.11: Comparison of refrigerants for the cooling case. [19]

The efficiency also depends on the refrigerant and the compressor. They give the limits for T_{sink} and T_{source} and an optimal working point. Examples of coefficients of performance for three refrigerants and different ambient temperatures are shown in Figure 3.11. A typical COP around 2 can be seen.

3.3.2 Heat exchanger icing

One main problem for the use of a heat pump in cars is the icing of the front (ambient air) heat exchanger. Acting as an evaporator when heating the cabin, its temperature has to be lower than the ambient air in order to extract heat from it. Given a humid autumn or winter weather this can easily lead to condensation of water and - below zero degree - to the development of an ice layer. This ice will prevent air flow through the structure and decrease the heat transfer (and with it the COP) dramatically. This is not acceptable since a car heating system has to be able to provide warm air under all circumstances to defog the windscreen - especially when it is cold and humid outside.

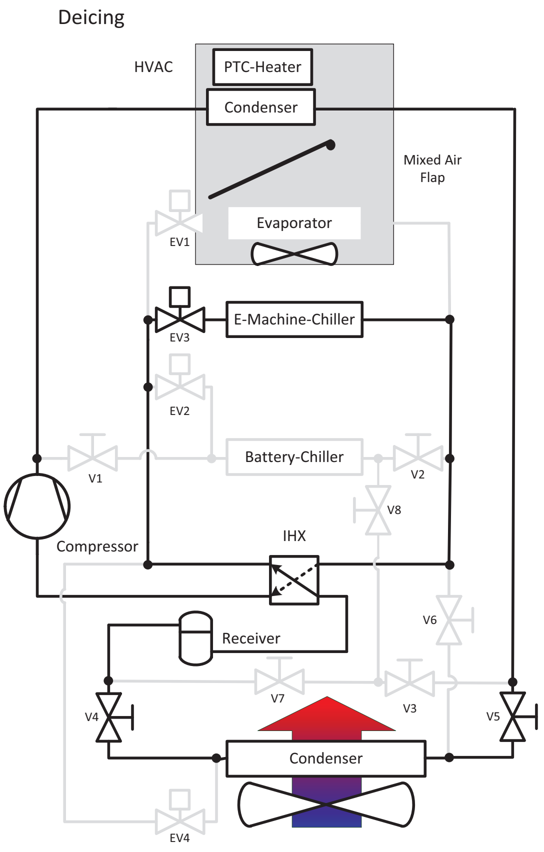

Figure 3.12: The de-icing mode in the ePerformance heat pump system. [19]

One solution to this problem taken in the ePerformance system [21] is to temporarily switch to another heat source to heat and de-ice the front heat exchanger if serious icing is detected. The source could be the electric motor as shown in Figure 3.12. Ice detection can be made directly by observing the pressure drop through the evaporator and indirectly through the COP of the heat pump.

To build up models for the icing in order to simulate or even predict it is subject to research at the moment.

4 Control strategy

The main goal of this thesis is to design a control strategy that fulfils the control objectives described in Chapter 2 in the best possible way.

4.1 Existing control structures

As pointed out in Section 1.1 most of the automatic "climate" control systems include only automatic *temperature* control. These controllers are often quite simple in order to require less powerful computing hardware. A simple hand-tuned relation between ambient, cabin and outlet temperature is used. Linearly to the output temperature the fan speed is set. Static rules are implemented to handle situations when for example the coolant is too cold. This approach does only partially reflect comfort (by a fixed temperature) and does not reduce energy consumption if possible.

An approach based on a CO_2 sensor [3] only uses full recirculation or fresh air, but not a mixture of both. It also does not include other objectives than the air quality. Another automatic defog control by Wang et al. (2004) [22] simply overrides the normal control. The integration into a control system is done by Jung, Lee and Jang [23], but apart from a PID-estimator in the fog-detection no details are given. In general these developments focus on single parts of the control, but not on an all-encompassing approach.

Information about the core algorithms difficult to obtain, since they are mostly kept as business secrets. One published approach by Wang et al. [24] uses an energy balance model and look-up tables to determine the required outlet air flow and its temperature to maintain a comfortable cabin. To this a transient part used to heat up (or cool down) the cabin is added. In this way a simple model based control is implemented. However, such a design is not capable of handling more than one object. Anti-fog strategies have to be implemented separately, added to the existing control and tested for interference.

Another control concept in use is fuzzy control [25], which uses (human) experience for the control of complex systems. Verbal formulated control rules are brought into a mathematical form. Several control laws like “if the temperature is high, blow in cool air” are combined. The fuzzy logic then makes smooth transitions. In this way no model of the controlled system is required. However, it still represents a sort of look-up table with no means of determining by itself whether the solution found is “good” since it incorporates no system model. One design by Farzaneh and Tootoonchi [26] compensates for this to a certain extent. Here parts of the fuzzy settings are optimised by using the PMV and compressor power as indicators for comfort and energy consumption. This allows the use of a fuzzy control while still achieving solutions close to an optimal one. This applies only to the circumstances it was optimised for, though, and it cannot be expected to provide efficient and comfortable output in all situations.

In some approaches the separation between the outer loop determining the outlet air parameters and the (mostly not shown) inner controller realising these with the HVAC-hardware is seen. This inner control is mostly open-loop control and adapted to each HVAC-model. With a high number of sold units the expensive and time-consuming finding of control curves pays off and is usually done therefore in industry.

The outer loop, which is often provided by an other enterprise than the HVAC-system manufacturer, may include a simple model. However, it is often based on empiric curves to adapt for example the set-point temperature to the ambient temperature, as seen in the previous paragraphs. None of the found controllers includes all of the objectives identified in Chapter 2.

4.2 Climate control in buildings

Multiple objectives like comfort and energy consumption are also a challenge in the building climate control. The total energy consumption (not the one per person, see Section 2.3) is higherhere and the use is more steady (or cyclic). Therefore, lowered energy costs pay off faster. Energy consumption requirements are also tighter and energy consumption limits are directly given for climatisation. For cars only an indirect regulation through fuel consumption and CO_2 emissions exists. Finally, there are less restrictions on weight or vibration behaviour while those are more on durability. This allows the use of advanced control algorithms and led to more research in this field in recent years.

In addition, most of the comfort experiments are done for indoor environments to quantify and improve the ease of persons in their homes or offices. Based on theri results, controller ideas have been tested. In the examples presented by Freire, Oliveira and Mendes, the PMV (predicted mean vote) is calculated with the available data and used as a control variable of a closed-loop control [27]. The control algorithms used were a PID, a fuzzy control and a model predictive control (MPC). Carbon dioxide concentration sensors have been taken as base for the control, too [13].

Multi-objective solutions do not take account of only one objective as air-quality or thermal comfort, but they add other goals as low power consumption. One approach by Freire, Oliveira and Mendes was using common MPC [27] but also the use of a genetic algorithm [28] was tested by Nassif, Kajl and Sabourin. Both try to minimise the energy demand while maximising the comfort in a building. They are used to optimise the set-points of a second loop, controlling the HVAC-system.

While coming close to a suitable controller scheme for the vehicle application, these strategies cannot simply be used as they are in a car. Lower computational power limit the complexity. Moreover, the thermal system “car” is unsteady compared to a building.

4.3 The control concept

The system which has to be controlled is nonlinear and non-stationary (in contrast to a building, for example). It can easily be separated into two components, as it was described in Chapter 3 and as implemented in commercial products (cf. Section 4.1). This gives the structure of a cascade control as seen in Figure 4.1. The HVAC-unit determines the air flow and its temperature, and is the “actuator” for the cabin system. It has to be controlled to reach desired input conditions to the cabin in the best possible way. In the outer loop these values for the input air have to be determined.

The objectives for this are competing. Accordingly, the best possible compromise

Table 4.1: Influence matrix of the controllable parameters and the control objectives.

Inlet air parameters	T_{in}	$\dot{m}_{air,in}$	$x_{w,in}$	μ_{recirc}	$\mu_{foot}/\mu_{defrost}$
Fogging affinity	■	■	■	□	■
Thermal comfort	■	■	■	□	■
Humidity comfort	■	■	■	□	□
Air quality	□	■	□	■	□
Air speed comfort	■	■	□	□	■
Energy consumption	■	■	■	■	□

■: has direct influence on the objective
□: has no direct influence on the objective

between them has to be found. It can be seen in Table 4.1 that it is not possible to control one independently of the others. In common climate control systems this is often solved by ignoring all objectives except the one most important at the moment (or not regarding some at all). While this leads to easier controllers it affects the overall performance since only one objective is (mainly) regarded at a time. In order to achieve the best performance an integral solution is needed.

A quite important difference to usual automatic control problems is that it is not precision that is most important. Correct decisions have to be taken dependent on many inputs. Due to thermal resistances and storage, time requirements are also comparably low (cf. Section 3.1.5).

The solution presented here consists of an estimator generating required values that are not directly measured to improve the quality of the model predictions. The outer loop controller is an optimiser, trying to find the best compromise between the objectives under given conditions. The third component uses the given optimised set-point to control the HVAC-unit fan, heater and cooler. A simplified scheme of this concept is shown in Figure 4.1.

The downsides are that it is computationally expensive, mainly because of the optimiser. On the other hand, computational power gets cheaper very quickly. The flexibility is an advantage: Objectives can be added without much trouble because of a model-based and modular design. Compared to a separate controller for each objective, the results of which are blended, it allows smooth transitions without a lot of tuning. Advantages over a fuzzy-logic are the flexibility and the model instead of the experience-

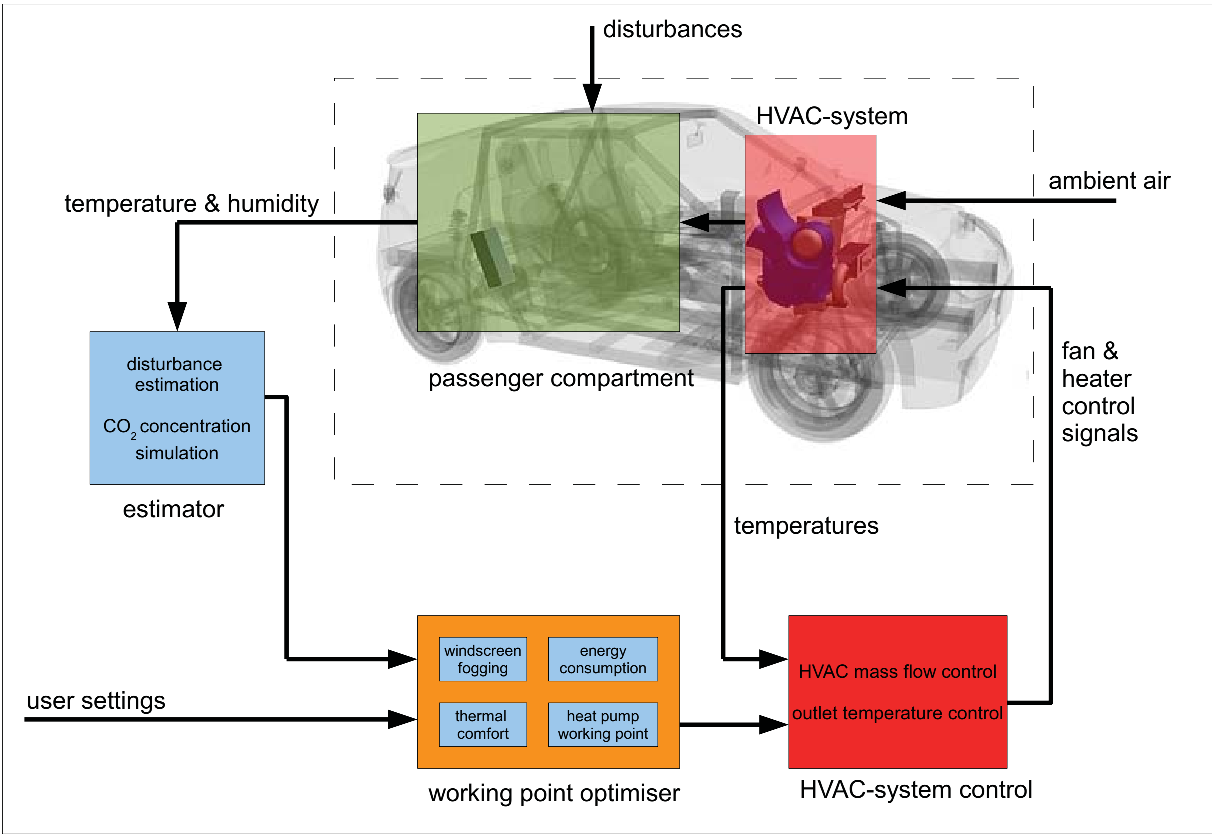

Figure 4.1: The simplified control concept.

based approach, giving good signals without requiring rules. The trade-off between the solution quality and the computational effort can be adapted with parameters for the optimisation algorithm.

4.4 The disturbance estimator

As sensors and their integration cost money, it is preferable to have as few as possible. Furthermore, some influences onto the system do not have to be known exactly or cannot be measured (in a reasonable way). Disturbances of the ideal models like air leakage or quantities as the human water emission are not known or captured by a sensor. Therefore, they are estimated.

The disturbance estimator filters the desired information out of the measured signals with the help of the system model. If the constants of the car used in equation 3.5 and the cabin temperature are known, it can be used to calculate the heat loss (or heat gain through radiation) which can be seen as the disturbance on the (simplified) model. Through humidity observation it can identify the total amount of water emitted by the passengers and even try to estimate the number of persons in the car. On the windscreen the disturbances through rain and sun can be calculated.

When these disturbances to the ideal system are known (or approximately known), they lead to an improved prediction of the system and thereby to improved control. The controller will have reduced stationary errors and react faster.

Another task is to estimate the CO_2 concentration in the cabin. Usually no sensor which would allow to control the amount of recirculation without impairing air quality is available. However, the concentration of carbon dioxide can be simulated based on the (estimated) number of persons and the amount of recirculated air. Even if the result is not accurate, it gives qualitative information about the air indicating when to stop using recirculation.

4.5 The working point optimiser

Optimisation of the HVAC-system set-points has been done in buildings in various ways as seen in Section 4.2.

This concept of optimisation will be adapted for the use in a car. Computational power is available today in more compact and energy efficient units making them suitable for vehicle applications where they are already used for entertainment. The comfort demand is less strict as in a building, as no one expects a car to have perfect comfortable climate from the first minute. Moreover, the system mostly is not safety critical. A cabin temperature which is some degrees above or below the ideal temperature or slightly cold feet will not present a safety risk. Only the windscreen fogging remains to be prevented. The timescale of the controlled systems in a car still is in the range of seconds (cf. Section 3.1.5) and permits the use of a more complex and computation time consuming algorithm.

The objectives, presented in Chapter 2, are mostly the same as in a building. They contain mathematically complex expressions like in the thermal comfort calculation. The optimiser has to find the best compromise between them.

As result a set-point for the HVAC-control is given defining the air blown into the cabin. This set-point is given by so-called *design variables*. In our case these are:

T_{in}	Temperature of the air blown into the cabin [°C]
$\dot{m}_{air,in}$	Mass flow into the cabin [$\frac{\mathrm{kg}}{\mathrm{s}}$]
$x_{w,in}$	Absolute humidity of the air [$\frac{\mathrm{g}}{\mathrm{kg}}$]
μ_{recirc}	Relative mass flow being recirculated [%]
μ_{foot}	Relative mass flow going to the foot outlets ($\frac{\dot{m}_{air,foot}}{\dot{m}_{air,in}}$) [%]
$\mu_{defrost}$	Relative mass flow going to the defrost outlets ($\frac{\dot{m}_{air,defrost}}{\dot{m}_{air,defrost+face}}$) [%]

Another choice of design variables is possible. Instead of the inlet temperature (T_{in}) and the humidity of the air going into the cabin ($x_{w,in}$), the cooling and heating power could be used as well. However, since temperatures and humidity are directly measured they are better suited as control set-point for the HVAC-system controller. If a heat pump with multiple sources is used this degree of freedom has to be integrated into a design variable as well. A logical value indicating when to de-ice the front heat exchanger is useful in this case, too (see Section 3.3.2).

The optimiser is working in the following way (seen in Figure 4.2): It includes a system model that predicts the system states for the car cabin found in Chapter 3. Those are the cabin air temperature and its humidity, but also others like the power consumption that are required for the objective computation and directly influenced by the HVAC-system output. It simulates how an air flow affects the cabin air and the other states in a given period of time. Even if this is done in a simplified way, it gives an indication which effects an action will have.

With this information the values indicating the degree of fulfilment for objectives and hardware constraints can be calculated. Based on these a set of design variables is rated, which cannot be used if it does not fulfil one or more constraints. The set of design variables with the best result with respect to the objectives has to be determined. The definition of "best" and how this is achieved is found in Chapter 6.

This so-called *predictive control* needs to simulate a model several times each sample. This causes the already mentioned computational demand.

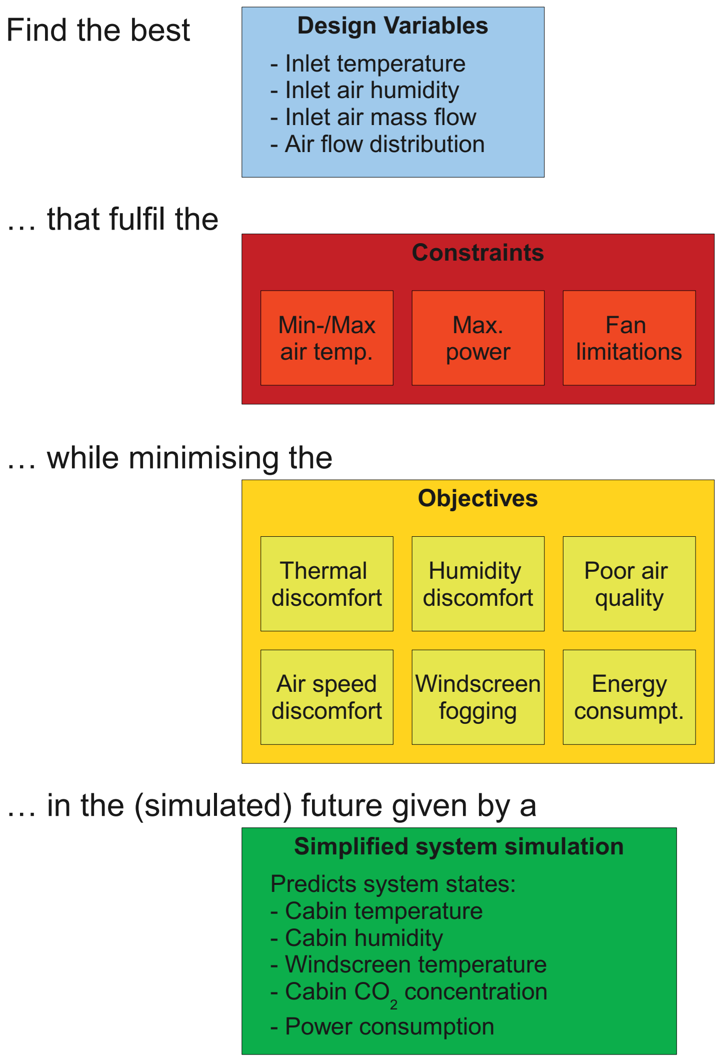

Figure 4.2: The basic concept of the optimiser.

4.6 The HVAC-system control

The optimised set-point should be realised as fast as possible. Therefore, the HVAC-system controller will run with a higher frequency than the optimiser.

For the fan control usually no flow sensors are available (even though they exist), so open-loop control is used with the help of the fan characteristics and known pressure drops. The temperature and humidity are measured which permits closed-loop control. Fast reaction is possible if this is combined with a feed-forward control. The temperature distribution is usually realised in hardware through guiding ducts and cannot be controlled.

The desired inlet air temperature cannot be reached at once, especially during a heat-up. The fan, in contrast, is reacting much faster. To avoid an inrush of uncomfortable cold air a *cold air prevention system* is added. It limits the fan while the air is too cold.

5 The disturbance estimator

The structure of the systems seen in Chapter 3 is nonlinear with many time dependent values. An observer requires a certain structure or linearisation of the model. The structure is not given. Linearisation would have to be repeated whenever a bigger change is detected and is for this reason supposed to be too calculation expensive. Therefore, a simpler approach is taken here.

5.1 Estimation of disturbances

All effects not taken into account by the system model and errors in the parameters are regarded as disturbances. For the thermal cabin system from equation 3.5 this would be $\dot{Q}_{others}$ which represents heat sources like the passengers, electronics or heat loss through air gaps. Here the sun is also included in this term, which has to be done if no solar radiation sensor is available.

$$\begin{aligned}\dot{Q}_{disturb} = \; & \tfrac{\partial T_{cab}}{\partial t}\left[m_{air,cab} \cdot c_{V,air} + \textstyle\sum_i (m_i \cdot c_i)\right] - \\ & \left[\dot{m}_{air,in} \cdot c_{p,air} \cdot (T_{in} - T_{cab}) + \tfrac{A_{cab}}{R_{cab}} \cdot (T_{amb} - T_{cab})\right]\end{aligned} \tag{5.1}$$

The disturbance in the car cabin air humidity represents the humidity sources, called $\dot{m}_{w,pas}$ in equation 3.8. It also covers humidity loss through air gaps or open windows.

$$\dot{m}_{w,pas} = \left[\tfrac{\partial x_{w,cab}}{\partial t} \cdot m_{air,cab} - \dot{m}_{air,in} \cdot (100\% - \mu_{recirc}) \cdot (x_{w,amb} - x_{w,cab}) + \dot{m}_{w,cond}\right] \tag{5.2}$$

External heat fluxes disturbing the windscreen system that were called $\dot{Q}_{ws,weather}$

in equation 3.16, are estimated by this equation:

$$\begin{aligned}\dot{Q}_{ws,weather} = & \tfrac{\partial T_{ws}}{\partial t}\left(\rho_{glass} \cdot A_{ws} \cdot d_{ws} \cdot c_{glass}\right) \\ & - h_{ws,in} \cdot A_{ws} \cdot \left(T_{defrost} - T_{ws}\right) - h_{ws,out} \cdot A_{ws} \cdot \left(T_{amb} - T_{ws}\right)\end{aligned} \tag{5.3}$$

When all the temperatures and humidity values as well as the material and car constants are known, the only the derivatives are left to calculate. Since sensor values are usually noisy, a robust way has to be found in order not to amplify these disturbances and introduce oscillations into the controller. The way taken here is to employ the slope of a linear regression as derivative. This permits to use a (configurable) number of samples and thus reduce noise.

Having n measurement values taken with a sample time Δt at times $t_i = i \cdot \Delta t$ the slope is calculated by:

$$\frac{\partial x}{\partial t} \approx \frac{n \cdot \left(\sum_{i=1}^{n} x_i \cdot t_i\right) - \left(\sum_{i=1}^{n} t_i\right)\left(\sum_{i=1}^{n} x_i\right)}{n \cdot \left(\sum_{i=1}^{n} t_i^2\right) - \left(\sum_{i=1}^{n} t_i\right)^2} \tag{5.4}$$

Approximations of higher order can be used as well, but are not regarded any further in this context. The increased accuracy does not justify the more complicated calculation and may even counteract the low-pass filtering.

For the other inputs to the equations, n values are averaged as well to keep the influence of noise or input jumps low. With the choice of n the amount of this low-pass filtering can be adapted.

5.2 Simulation as replacement for sensors

Some of the information required by the objectives might not be available in a normal car. One sensor which is only found in very few vehicles, but quite important when trying to safe energy and using recirculated air, is the carbon dioxide sensor.

Simulating this state entirely can give an idea whether the CO_2 concentration is high or not. However, one has to keep in mind that this will represent only a rough estimation. Generally, the real concentration will be lower due to air leakage - which is not taken into account here.

To realise this simulation equation 3.9 has to be implemented. As a starting value the environmental concentration $x_{CO_2}(t = 0) = x_{CO_2,amb} \approx 700\,\frac{\mathrm{mg}}{\mathrm{kg}}$ can be used. In order to estimate the human emission $\dot{m}_{CO_2,pas}$ the number of "standard persons" can be obtained from $\dot{m}_{w,pas}$ calculated in equation 5.2. By this disturbance in the humidity in the car divided by the average human water emission through respiration the number of persons can be estimated.

6 The optimiser: an evolutionary algorithm approach

The optimiser is the most complex part of the control structure as seen in Section 4.3. It has to find the best compromise between the objectives. To do so it calculates predictions for the system “cabin”. The resulting control output has to respect certain limits, meaning safety has to be assured. For example, a perfect temperature is useless if the carbon dioxide concentration gets too high.

Doing all this the computational effort has to be limited. Even if faster processors can be integrated into new cars, there will still be a cost pressure and a time limit for the computation.

6.1 The optimal control problem

In control engineering the optimal control problem can be stated as follows [29]:

$$\begin{aligned} &\min \int_{t_{start}}^{t_{end}} L(\boldsymbol{x}(\tau), \boldsymbol{u}(\tau))d\tau + \phi(\boldsymbol{x}(t_{end})) \\ &\dot{\boldsymbol{x}}(t) = \boldsymbol{f}(\boldsymbol{x}(t), \boldsymbol{u}(t)) \\ &\boldsymbol{u}(t) \in \mathbb{U}, \quad t_{start} \leq t \leq t_{end} \\ &\boldsymbol{x}(t) \in \mathbb{X}, \quad t_{start} \leq t \leq t_{end} \\ \boldsymbol{x}(t_{start}) &= \boldsymbol{x}_0 \end{aligned} \tag{6.1}$$

Where $L(\boldsymbol{x}(\tau), \boldsymbol{u}(\tau))$ stands for the trajectory cost, meaning the cost of bringing the states $\boldsymbol{x}$ from its starting values $\boldsymbol{x}_0$ to the final values $\boldsymbol{x}(t_{end})$ with the control signal $\boldsymbol{u}$ or other costs arising during this time. $\phi(\boldsymbol{x}(t_{end}))$ is the final cost, for example the distance of the states $\boldsymbol{x}(t_{end})$ from a desired value. $\mathbb{U}$ and $\mathbb{X}$ represent the restrictions on the control and the system states, also called boundaries or constraints (for varying limits).

Usually this is used to offline generate optimal reference trajectories employed as feed-forward control. An approach to use optimal control in online applications in a closed loop is called *model predictive control* (MPC) [30]. Here the starting time t_{start} is set to the actual time t. The end time t_{end} is set to a time $t + t_{horizon}$. This is also called *receding horizon control*. In the controller the system and its (usually piece-wise constant) control output is simulated and optimised for this horizon $t_{horizon}$. Then, the first output is taken and applied to the system.

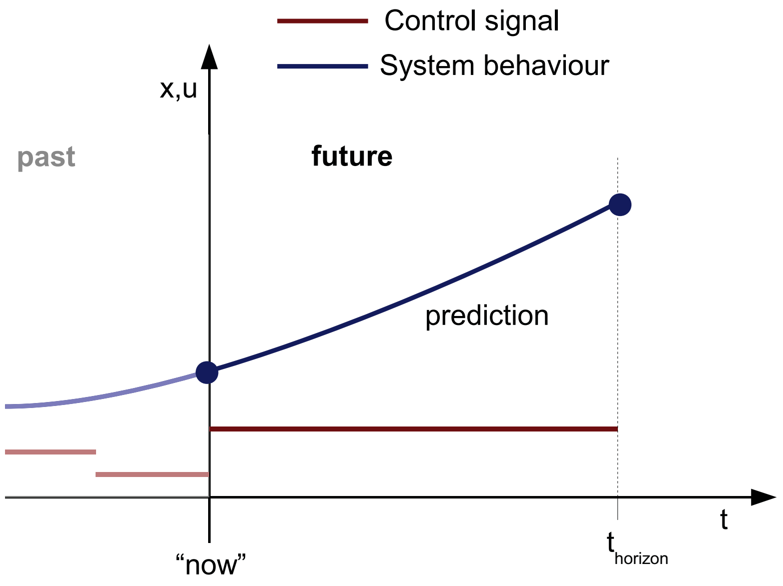

Figure 6.1: The functioning of (simplified) *model predictive control*

For the case of the climate control some assumptions and simplifications to this general formulation are made. For the objectives described in Chapter 2 the only true trajectory cost would be energy consumption. Here the simplification is made that it does not matter at which time the energy is used or the system is heated. This is not completely valid (as described in Section 2.3), but situations like recuperating happen in a much larger timescale than the horizon and can as well not be predicted. Moreover, the heat transfer to the interior components changes depending on the air flow. This could however be implemented in the thermal model.

With this change made, all objectives are only dependent on the states at the end time, leading to the following formulation, which is visualised in Figure 6.1.

$$
\begin{aligned}
&\min \phi(\boldsymbol{x}(t + t_{horizon}), \boldsymbol{u}(t + t_{horizon})) \\
&\dot{\boldsymbol{x}}(\tau) = \boldsymbol{f}(\boldsymbol{x}(\tau), \boldsymbol{u}(\tau)) \\
&\boldsymbol{u}(\tau) \in \mathbb{U}, \quad t \leq \tau \leq t + t_{horizon} \\
&\boldsymbol{x}(\tau) \in \mathbb{X}, \quad t \leq \tau \leq t + t_{horizon} \\
&\boldsymbol{x}(t) = \boldsymbol{x}_0
\end{aligned}
\tag{6.2}
$$

Since the cost is only dependent on values at the end time the control signal can be kept constant during the simulated time $t_{horizon}$. Therefore, only one time step has to be simulated and optimised each run. This reduces the computational effort dramatically, since only one set-point and not an optimal trajectory has to be found.

6.2 Algorithm selection

In this problem formulation a numerical method is still needed to solve the (nonlinear) optimisation problem in each time step.

6.2.1 Selection criteria

The algorithm should fulfil certain criteria to be able to be used for a car climate control. Robustness is important since the car parameters will never be exactly known. A minimum number of (as cheap as possible) sensors is desired as well, which reduces the data quality. In all those cases the algorithm has to provide reasonable solutions. Those should of course never cause a danger to the passengers. This means that the control has to respect limits and prioritise objectives in certain situations. For example the inlet temperature should never be below zero degree at high inlet mass flows. In addition, the windscreen has to be kept free from fog even if this causes a temporary conflict with other objectives. To run on a system on a chip (SoC) in car at a reasonable frequency it has to have a low computational effort. The time scale of several seconds is relatively long for a control problem, but not that long for an optimisation task, especially as the objective formulations are nonlinear and can contain discontinuities. Finally, it is an aim that the algorithm can be used in future developments of the *MUTE* car (presented in Chapter 9). This may imply changes in the HVAC-system and integration of new components. The extension of the controller and its adaption should not be too complicated.

In summary the optimiser algorithm should fulfil the following criteria:

- Robust
- Safe
- Low computational effort
- Handles discontinuities
- Easy to extend

6.2.2 Gradient based algorithms

For the majority of online optimisation problems a so-called gradient method are used. A prominent and efficient gradient-based optimisation algorithm is sequential quadratic programming (SQP) [31]. SQP exploits the first and second order derivative information.

Compared to other algorithms, this generally leads to a lower number of function evaluations. On the other hand it imposes more requirements on the system and objective functions. As such it cannot handle non-continuous differentiable objective functions. Discrete variables are not applicable in this algorithm as well.

Due to these downsides no gradient based method is applied.

6.2.3 Evolutionary algorithms

Evolutionary algorithms (EA) are stochastic methods that were first developed in the seventies. They were used to solve stationary optimisation problems, for example in construction design.

This class of stochastic methods is inspired by biological evolution. A number of sets of design variables (so-called *individuals*) forms a *population*. Each of them gets assigned a *fitness* value with the help of the cost function z, which could also be a vector of objective functions. Based on this some are selected as parents. With different methods, new individuals are created through a *recombination* of the chosen parents. *Mutation*, the random change of design variables, is applied and the resulting population is evaluated. Finally, the *replacement* operator deletes the worst performing individuals.

An operation sequence of this basic evolutionary algorithm is found in Figure 6.2. Terms and definitions that will be used in the following which are used for evolutionary algorithms are explained in Table 6.1.

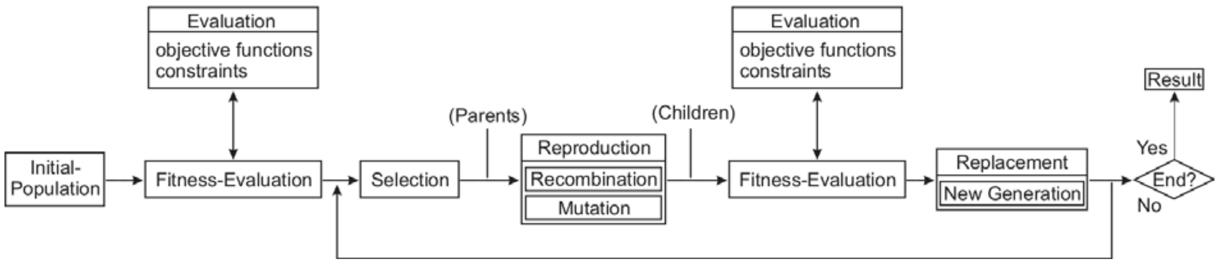

Figure 6.2: General operation sequence for an evolutionary algorithm. [31]

Based on the first representatives, evolutionary programming (EP) (Fogel, Owens, & Walsh, 1966), evolution strategies (ES) (Schwefel, 1965; Rechenberg, 1973), genetic algorithms (GA) (Holland, 1975), and genetic programming (GP) (Koza, 1992), a broad variety of algorithms with bigger or smaller changes and improvements exists. Some can handle multiple objectives and provide the pareto front - the set of the best compromises. More and more feature elitism, where the best parents are stored and inserted before the replacement operation.

It is one characteristic of this class of methods is that, due to its heuristic nature, one run is not repeatable. The solution is never exactly the same if performed twice. They proved to be very robust and are able to handle discrete variables as well as non-continuous objective functions because of the this property, too. However, there is no indication that a found solution is optimal.

The fact that these algorithms are working with a group of points permits an independent evaluation of the fitness and makes them perfectly parallelisable, which is important for multi-core processors or clusters. On the other hand, the number of required function evaluations is quite high. For this reason, special care has to be taken that the resulting algorithm and the system simulation is not too computationally expensive.

Table 6.1: Terms and definitions used for evolutionary algorithms.

Design variable	parameter which is modified in order to find the optimum
Individual	complete set of *design variables* for an optimisation problem
Population	group of *individuals*
Parents	*individuals* chosen for the generation of *children*
Children	new generated *individuals* through recombination of *parents*, and mutation
Generation	the process of *parent* selection and *children* creation
Fitness	figure to compare which *individual* is closer to the optimum
Objective (func.)	function that the optimiser seeks to minimise
Design space	n_{DV}-dimensional search region (n_{DV} is the number of *design variables*)
Constraint	technical or physical limit to the *design space*
Pareto front	all *individuals* where the improvement of one objective would lead to the impairment of another

Because of the population approach with many individuals at a time there is not only one solution to choose the control signal from, but several. This is advantageous if there are criteria that cannot (or should not) be integrated into the optimisation.

Examples of evolutionary algorithms in control systems engineering are found in a survey by Fleming and Purshouse [32]. In general, they report the application for control design, but they also mention some online applications. For a heating system, a PI-controller was online tuned with an EA (Ahmad, Zhang, & Readle, 1997)[33]. In another example the temperature profile of an ethanol fermentation process was optimised online with an EA by Moriyama and Shimizu (1996) [32].

Optimal control algorithms of this type have already been used in climatisation. In a building, Nassif et al. [28] used a NSGA-II algorithm for set-point optimisation of a multi-zone HVAC system with regard to comfort and energy demand in a university building.

6.3 Design of an incremental micro evolutionary algorithm

While approaches of using evolutionary algorithms in online control have already been made, the circumstances in these cases are not comparable to the ones in car climate control. In the case of the building climate control [28] the population size was set to 100 and 500 generations were evaluated, which lead to a lot of function evaluations. This is possible in a building where more computing power is available, but in a car it is not (yet). The second example close to the planned control layout is the set-point optimisation for an ethanol fermentation process [32]. Here however, the sample time was thirty minutes. For an climate control application it should be not more than several seconds. Therefore, an adapted algorithm is required.

6.3.1 Overview of IMEA

In the design of the evolutionary algorithm for the car climate control optimisation particular attention is paid to the computation demand. In comparison to usual applications of EAs the simulated system is through the applied simplifications quite small and in the range of a simple MPC-problem. Thus, the computational effort of the algorithm itself cannot be neglected, as it is often done [34].

The main ideas of the developed *incremental micro evolutionary algorithm* are:

- Use a *small population* in order to reduce computing time.
- Have a fixed amount of function evaluations to give a *deterministic run time*.
- Ensure feasible solutions through a *base population* inserted at each run.
- *Adapt mutation* to the changes of the environment.
- Employ a *special ranking scheme* to penalise exceeded limits differently.
- Augment efficiency through *elitism* (storing the best individuals for the next run).
- Avoid double entries and keep *diversity* to be able to react to changes.

- *Select the control values* with respect to the last one applied to avoid jumps.
- Prevent control outputs which exceed limits by replacing them with *panic handlers*, i.e. special outputs.

A flowchart of the algorithm is found in Figure 6.3. The methods applied are described in detail in the next sections.

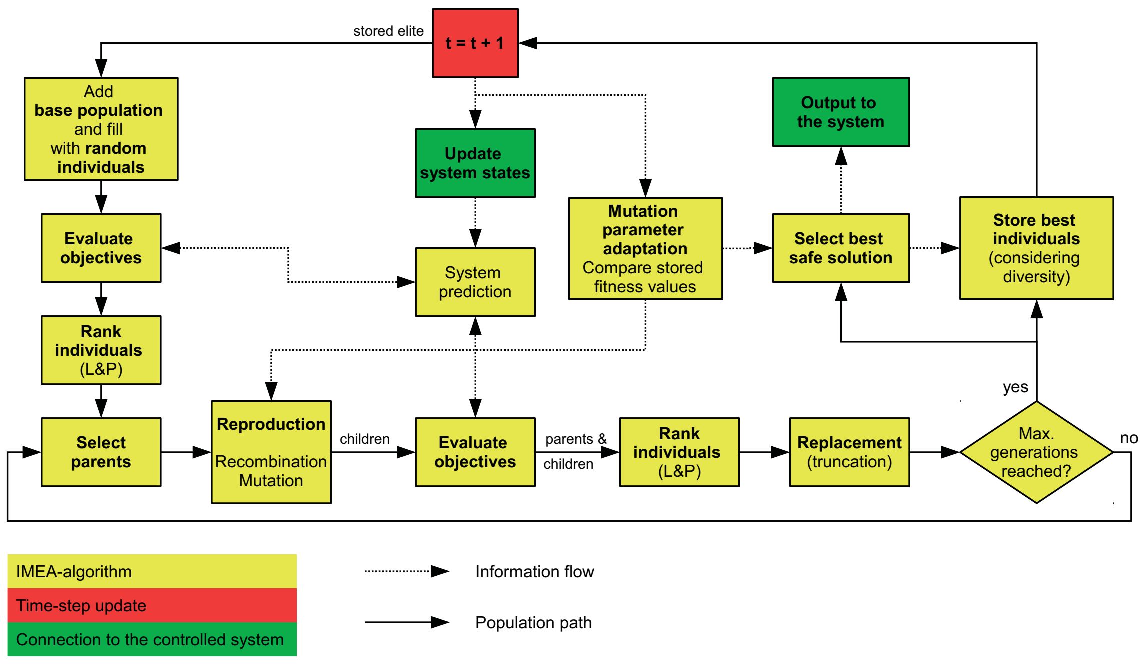

Figure 6.3: Flowchart of the incremental multi-objective evolutionary algorithm.

At the start of each time-step the system states (temperatures, humidity and other sensor values) are updated. They are then used in the system prediction. The population is built up by the *elite* from the last run and a constant *base population*. The remaining individuals for the population are randomly chosen from the design space. Using the system model, the future states are *predicted* for each individual. Based on these the objectives are *evaluated* and the results stored. In the following step the population is compared using the *limits and priorities ranking scheme*.

The ranking is decisive for the *selection* as parent. The parent couples are *recombined* and the resulting offspring *mutated*. The objectives are *evaluated* for the children and a *ranking* together with the parent generation is conducted. Finally this ranked list is *truncated* to the original population size. To obtain a better result, more generations can be realised with the algorithm. If this is desired, parents are chosen again from the population and a new offspring is created.

After the set number of generations the most suitable individual is *selected as control output*. This output as well as the best individuals that are not too close to the base population are selected as elite and *stored* for the next run.

6.3.2 Design variable coding

The algorithm is designed to work with continuous design variables. They are "coded" as real numbers, which is sufficient for the application as it is the most comprehensive and the simplest way. Discrete design variables, however, are possible with some extensions to the algorithm as it is done for GAME by H. Langer [34].

6.3.3 Generation of the initial population

The creation of the initial population has to fulfil two objectives: On the one hand it should be as close as possible to the optimum in order to find the best possible solution. On the other the non-stationary environment requires it to be widespread to be able to cope with changes.

The presumptive closest individuals to the optimum that are known, are the fittest ones from the last run. Those have been stored (see also 6.3.6) and can be used now. If the boundaries changed these elite individuals have to be adapted. This is done by simply setting these values onto the limit that are out of bounds.

In order to be able to track environment changes two mechanisms are used. Reasonable starting values for the most common cases are implemented. If these are spread over the design space and adapted to changing boundaries, they can assure good coverage and give faster reaction of the algorithm. The implementation of fixed individuals called *base population* was already done by Lennon and Passino for a brake system control application [32].

The population is completed with random individuals, called *random immigrants* by Grefenstette [35]. These give another means of diversity and make it possible to find the (changed) optimum.

6.3.4 System simulation and objective evaluation

For each individual a simulation is done first, predicting the system states if it would be employed as output (cf. Figure 6.1). The simulated time span is usually longer than an control output actually will be applied to the system. This is done to see differences better than with short horizons. Moreover, some effects only show after a certain (simulation) time (e.g. defogging). On the other hand, it some assumptions decrease the prediction quality of a longer simulation. For example environment parameters like the ambient temperature change during one optimisation run, but are assumed to be constant in the simulation.

The prediction is one of the most computational expensive parts of the algorithm. This requires the simulated horizon (and its quality!) to be bound. The simulation of the system in the form $\dot{\boldsymbol{x}}(t) = \boldsymbol{f}(\boldsymbol{x}(t), \boldsymbol{u}, [\boldsymbol{x}_0, parameters])$ is done using a simple Euler method:

```
for $(t = 0; t < t_{horizon}; t = t + \delta t)$
    $\boldsymbol{x}(t + \delta t) = \boldsymbol{x}(t) + \delta t \cdot \boldsymbol{f}(\boldsymbol{x}(t), \boldsymbol{u})$
```

This technique is of the first order, leading to higher errors for small δt than higher order methods. However, the trend will be given correctly. Moreover, a perfect estimate is not possible due to changing environmental influences. Other integration methods could be applied as well.

The predicted states are fed into the objective functions. The obtained objective ratings are stored to be compared in the next step.

$$\phi_i(\boldsymbol{u}) = \phi_i(\boldsymbol{x}(t + t_{horizon}))$$

6.3.5 Ranking and constraint handling

The implemented ranking scheme is based on the weighted sum approach and the *goals and priorities* ranking developed by Fonseca and Fleming (1993) and used in GAME [34].

They group the objectives and constraints into more important (higher priorities) and less important (lower priorities). Additionally, a goal value allows to not regard an objective if its target value is reached. As last decisive factor Fonseca and Fleming use pareto ranking. In the control case a (here changing!) pareto front is not of interest, since only one control output is needed. Therefore, this mechanism is replaced by the comparison of the weighted sum of the objective function results. The trade-off for the optimum will be given by pre-defined weights.

In addition, objective goals are less important than limits that should not be exceeded in a control purpose. These limits can be objectives that are important for functioning, safety or constraints. If the weighted sum the total score is low, but one objective is unacceptably high, an individual with a higher score but no broken limit should be preferred. For example is it not acceptable to have a fogged windscreen. The objective goal "as good as possible" is always desired.

This is illustrated in a small example, found in Table 6.2. Individual a is preferred to individual b because of its lower weighted sum. The sum is even lower for individual c, but because its fogging risk is above the acceptable limit, it is ranked last.

Table 6.2: Example for the *limits and priorities* ranking.

	Fogging risk	Energy consumption	Weighted sum	Rank
Individual a	80	50	130	0
Individual b	75	75	150	1
Individual c	101	0	101	2

Red numbers mean the objective is above the its limit. Both weights are 1.

To simplify the calculation, it is not differentiated which objective limit is exceeded, but only the number of exceeded limits at each priority level. A constraint (treated as objective in the following) is realised through a high priority and a limit and weight equalling zero. An objective has a weight which is not zero (meaning it is minimised) and a limit adapted to it, which can be very high to realise "no limitation".

Two individuals $\boldsymbol{a}$ and $\boldsymbol{b}$ are compared with regard to their objective values

$$\begin{aligned}\boldsymbol{a} = &\ \boldsymbol{\phi}(\boldsymbol{u}_a)\\ \boldsymbol{b} = &\ \boldsymbol{\phi}(\boldsymbol{u}_b)\end{aligned}$$

Each of the objectives has its assigned priority value p. These values are collected in the priority vector

$$\boldsymbol{p} = [p_1, \ldots, p_{n_{ob}}]$$

The weight vector is of the same length n_{ob}, which represents the number of objectives.

$$\boldsymbol{w} = [w_1, \ldots, w_{n_{ob}}]$$

The limits finally represent the values which should not be exceeded.

$$\boldsymbol{l} = [l_1, \ldots, l_{n_{ob}}]$$

The subvectors of objective values and their limits with the same priority p are indicated with $\boldsymbol{a}_p$ and $\boldsymbol{l}_p$, respectively. The symbol "$\underset{\boldsymbol{l}}{\prec}$" reads as "is preferred to with respect to $\boldsymbol{l}$". With those symbols this *limits and priorities* approach can be formulated as follows:

$$\begin{aligned}&\boldsymbol{a} \underset{\boldsymbol{l}}{\prec} \boldsymbol{b}, \text{ if and only if:}\\ &\quad p = 1 \Rightarrow (|\boldsymbol{a}_p > \boldsymbol{l}_p| < |\boldsymbol{b}_p > \boldsymbol{l}_p|) \vee \left\{(|\boldsymbol{a}_p > \boldsymbol{l}_p| = |\boldsymbol{b}_p > \boldsymbol{l}_p|) \wedge \left[(\boldsymbol{a} \cdot \boldsymbol{w}^T) < (\boldsymbol{b} \cdot \boldsymbol{w}^T)\right]\right\}\\ &\quad p > 1 \Rightarrow (|\boldsymbol{a}_p > \boldsymbol{l}_p| < |\boldsymbol{b}_p > \boldsymbol{l}_p|) \vee \{(|\boldsymbol{a}_p > \boldsymbol{l}_p| = |\boldsymbol{b}_p > \boldsymbol{l}_p|) \wedge (\boldsymbol{a}_{1 \ldots p-1} \underset{\boldsymbol{l}_{1 \ldots p-1}}{\prec} \boldsymbol{b}_{1 \ldots p-1})\}\end{aligned} \tag{6.3}$$

First the objectives with the highest priority p are compared to their limits. If the number of exceeded limits is lower for $\boldsymbol{a}$ than for $\boldsymbol{b}$, $\boldsymbol{a}$ is preferred. If it is equal, they are compared in the same way for the priority $p - 1$. This is continued until $p = 1$. If at this lowest level no decision can be found, $\boldsymbol{a}$ is preferred to $\boldsymbol{b}$ if its weighted sum is lower. The rank of an individual is given by the number of individuals preferred to it.

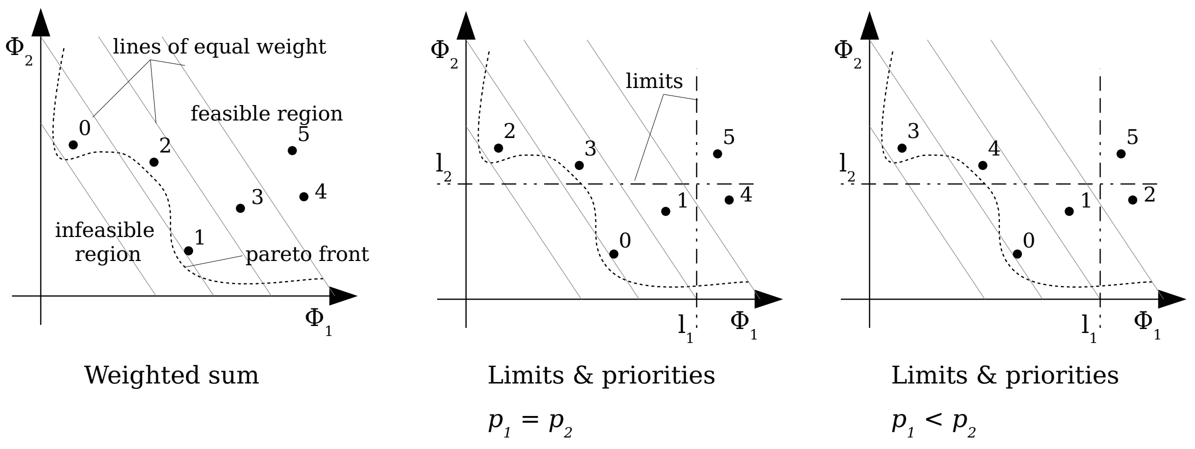

Figure 6.4: Illustration of the limits and priorities ranking for two objectives.

In Figure 6.4 an example for this ranking scheme is shown for two objectives and a small population. On the left is a simple weighted sum ranking. In the middle the limits are used with two objectives with the same priority. On the right the priority for objective ϕ_2 is higher than the one of objective ϕ_1, resulting in a different ordering.

By this approach it is guaranteed that the best individual represents the lowest found danger as it has the least broken limits. Among those with the same number it is the best performing with regard to the given trade-off.

6.3.6 Elitism and base population

Storing the best individuals of one run for the next one leads to a higher performance of the algorithm [34]. This elitism can as well reduce fluctuations in the output if the chosen output is available as output again and a solution close to it is found.

For the application in a non-stationary environment the best individuals are not necessarily good in the next run. However, in a slowly drifting environment (which can be assumed besides the user inputs) they can give a good indication. Important for the composition of an elite is a good diversity. Otherwise so-called “niching” occurs when only individuals close or equal to the best are chosen as elite in a period with very little changes. The resulting population then has a lower performance if more changes happen.

As these diversity algorithms are computationally quite expensive, a simpler approach is taken here. A certain diversity is already guaranteed by the base population and the random individuals added during the population initialisation described in Section 6.3.3. This could also be the main cause of niching (or double entries) since the base population is added in *each* run.

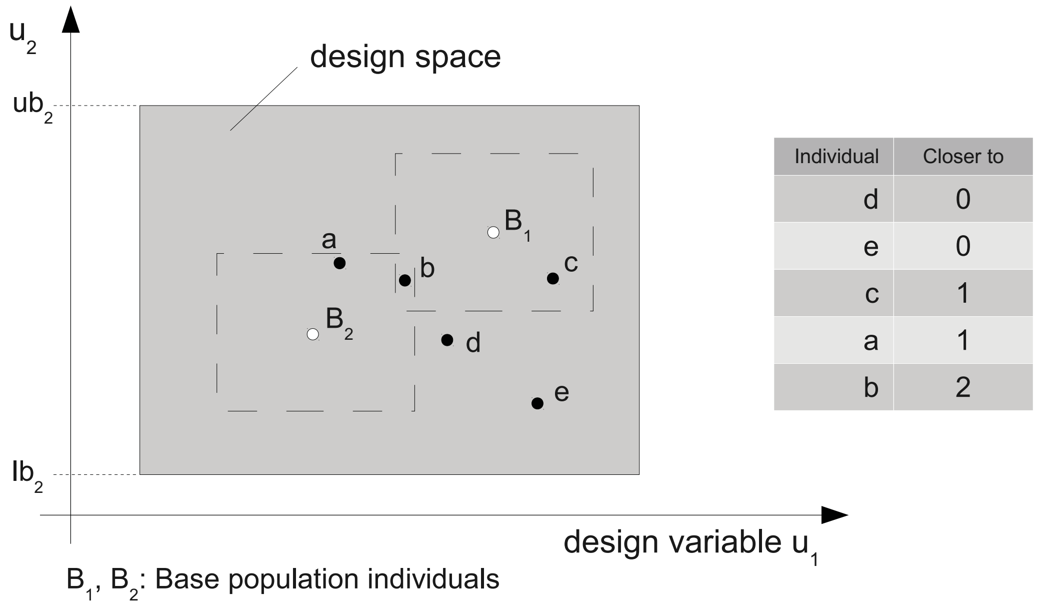

Individual	Closer to
d	0
e	0
c	1
a	1
b	2

Figure 6.5: Example for the elite selection with two design variables.

To choose the elite individuals, the population is compared to the base population and the chosen control signal. The number of individuals that are closer to each individual of the population than a certain threshold percentage ϵ_{thr} is stored. This procedure is illustrated in Figure 6.5. The population is then sorted with respect to this value and then according to their ranking. The first n_{elite} individuals are then chosen as elite. They are the best performing ones closest to the least number of base individuals. The chosen control signal is always stored.

6.3.7 Selection

For each child, a couple of two individuals has to be chosen from the population. Therefore, two times the number of children n_c has to be selected. For this two different algorithms are identified as best and presented by H. Langer for GAME [34]. The first is the tournament selection. Two randomly selected individuals are compared and the winner is chosen as parent. This method can also be performed in more stages to increase the selection pressure. The other algorithm is called *global stochastic remainder* selection. Based on the rank of the individuals, the expected number of copies is put into the parent pool. With a selection probability of $prob_i$ an individual is selected $n_{i,copies} = \text{floor}(prob_i \cdot 2 \cdot n_c)$ times. If (due to the floor operator) places are left, they are filled by a conventional roulette wheel selection [34]. There an individual is randomly chosen with a probability of $prob_i$. Finally, random couples are formed in the obtained parent pool.

This algorithm is chosen because of its simplicity (which means lower computational costs). Langer also states its reduced stochastic noise compared to a roulette wheel selection.

6.3.8 Recombination and mutation

Each found couple is combined to form a new individual. This is done through an arithmetic crossover for continuous variables [34].

$$\boldsymbol{u}_{c,i} = \boldsymbol{u}_{par,1,i} - r \cdot (\boldsymbol{u}_{par,2,i} - \boldsymbol{u}_{par,1,i}), \quad r = \mathrm{U}([0,1]) \tag{6.4}$$

r is a uniformly distributed random number between 0 and 1. This recombination is used to find the best solution possible with the "genetic material" available in the population.

In order to "explore" the design space the mutation operator is applied. Here a random number is added to the design variables of all child. In this case the random number is normally distributed with a standard deviation σ_i for each design variable u_i. This mutation was reported to have higher convergence rates and lower required population sizes than comparable binary genetic algorithms [34]. A common fraction s_x of the design space, limited by the lower ($\boldsymbol{lb}$) and the upper bounds ($\boldsymbol{ub}$), is taken for each design variable:

$$\boldsymbol{\sigma} = s_x \cdot (\boldsymbol{ub} - \boldsymbol{lb}) \tag{6.5}$$

s_x, the exploration factor, is important since it determines the scatter radius. Thus, for a population being far away from the optimum a high value is advantageous. This would be the case after a parameter or environment change. In a steady state - or close to the optimum - a lower spread would be more effective.

The common strategy is decreasing the s_x with the number of generations. To obtain a short execution time, however, each run can only include a low number. For the incremental algorithm, it is advantageous to adapt the exploration factor for each run not for each generation. A better way would be to base the mutation on environmental variations. These values, as temperatures, are directly measured and changes can be detected very fast. The problem here is that a relative change would be needed. Therefore, the measurements would have to be compared with a reference value. Since this has to be specified for each watched parameter, an easier approach is taken.

The idea of this so-called *hypermutation* [35] is to adapt the standard deviation with regard to the fitness (objective results). If the average decreases, a change is occurring and the s_x has to be increased to allow the search for better solutions. While Cobb and Grefenstette used a switching exploration factor, this is not done here. The algorithm is not supposed to find an optimal solution in one run, but incremental. Therefore, the adaption is done also step-wise. Instead of the average fitness - which is not a good indicator with random individuals introduced each run - the fitness, $fit_{control}$, of the chosen control signal is taken. Here the weighted sum of the objective results is taken as the fitness. This value is replaced by a the parameter fit_{limit} if no solution is found that does not exceed a limit.

$$s_x(k) = \begin{cases} s_{x,max} & \text{for } fit_{control}(k-1) = fit_{limit} \\ s_x(k-1) + \delta_{s_x} & \text{for } fit_{control}(k-1) > fit_{control}(k-2) \wedge s_x(k-1) < s_{x,max} \\ s_x(k-1) - \delta_{s_x} & \text{for } fit_{control}(k-1) < fit_{control}(k-2) \wedge s_x(k-1) > s_{x,min} \\ s_x(k-1) & \text{else} \end{cases} \tag{6.6}$$

In the time step k the exploration factor can be set to a maximum, if no acceptable solution has been found in the last run. Otherwise it is decreased or increased by a increment δ_{s_x}, depending if the fitness of the controlling individual $fit_{control}$ is lowered or not. Of course this adaption is limited by an $s_{x,max}$ and $s_{x,min}$. This gives a bigger (or equal) search area as long as the algorithm does not find a better solution.

With the mutation operator individuals can be shifted out of the design space. As a remedy these are simply moved back onto the boundary. This simple repair mechanism guarantees to have feasible individuals only.

6.3.9 Replacement

As replacement operator a simple truncation is applied. The children and the parent generation are joined and ranked. The best n_{pop} individuals are then transferred to the next generation or the control signal and elite selection.

6.3.10 Control signal choosing

Assuming that the found solutions are among the best that are available, the selection has to fulfil two goals: A solution which exceeds limits should never be applied. In such a case another solution has to be found to provide a secure output. Secondly fast changes should be avoided when being in a steady state. Even when a found solution is good a restriction is made limiting the jumps between the old and the new set-point. This gives smoother transitions and reduces the disturbances through sudden changes.

The allowed distance from the last control output is adapted with the same mechanism as for the mutation standard deviation. This allows bigger jumps when they are needed and changes are detected, and limits them in a stationary case. With the adapted change percentage s_x and the upper and lower limit the maximum changes for each design variable is determined.

$$\boldsymbol{\lambda_{change}} = s_x \cdot (\boldsymbol{ub} - \boldsymbol{lb}) \tag{6.7}$$

If the best solution is too far away from the last control output, the second best is tried. If in the population no solution close enough to the last signal can be found, the best is taken. In this way this mechanism gives smooth transition, if that is possible.

There is a weak point in the model predictive control, namely if an objective is saturated and the horizon is too short to find a solution going beyond that saturation point, for example when the windscreen is fogged or iced and cannot be defogged in the time $t_{horizon}$. Then solutions going in the "wrong direction" are likely to be preferred because the saturated objective is equal for all and will be not influence the decision. In this case a solution with only little cool air blown to the feet could be chosen as control in the fogged window example. In such a case it would help to modify the predicted time span. That would lead to increased (and varying!) computation time, which is not desirable. In addition, one could imagine a situation where this would lead to extreme, if not infinite periods which have to be simulated. Therefore, another method has been implemented here.

Each objective has its limit assigned which has already been used for the ranking. If this limit is exceeded it is usually close to saturation or in a state where counter measures have to be taken. Thus, for each objective a special control output is defined which is aimed at helping the controller to find a way to a secure state. If several limits are exceed at a time, an ordering ($\boldsymbol{o}$) gives an indication which to handle first. The weights used for the ranking can be applied for this purpose as well.

If the chosen individual is above a limit, the output will replaced with a *panic handler*.

$$\boldsymbol{u}_{output} = \begin{cases} \boldsymbol{u}_{control} & \text{for } \phi_i(\boldsymbol{u}_{control}) \leq l_i \ \forall \ i = 1 \dots n_{obj} \\ \boldsymbol{u}_{panic,i} & \text{for } \phi_i(\boldsymbol{u}_{control}) > l_i \wedge i \mid o_i = \max(o_j), j \mid (\phi_j(\boldsymbol{u}_{control}) > l_j) \end{cases} \tag{6.8}$$

This solution allows deterministic computation time since no change to the simulation is made. It also allows the control to handle extreme situations.

6.3.11 Final thoughts on the algorithm

The described methods were chosen with the information found in different publications. However, the optimisation of the algorithm and its parameters would go beyond the scope of this thesis.

The main drawback of the choice of a genetic algorithm is that the quality of the found solution cannot be guaranteed, but with the introduction of the replacement signals through *panic handlers* safe outputs are given at each time step. The deterministic run-time, efficient subroutines and the incremental functioning make it suitable for online optimisation with multiple objectives. The model based design and its flexibility are the main advantages.

7 The HVAC-system controller

The HVAC-controller receives its set-point from the optimiser. In the inner loop the task is to realise those inlet air conditions as fast and as good as possible with the available hardware. Here conventional automatic control objectives are of importance: speed, precision and accuracy.

As already mentioned in Section 4.1, this control has to be adapted to the hardware. Therefore, only general control structures will be shown in this chapter. If not stated otherwise a “standard” car HVAC-system is assumed as it is presented in Section 3.2.

7.1 Temperature and humidity control

In car HVAC-system heat and humidity control are usually coupled since the air is first cooled (and dehumidified) and then reheated. The humidity of the air after the evaporator is not measured, while its temperature has to be captured to avoid icing. This measurement will be used as indicator for humidity.

The here presented control design is based on feed-forward signals to allow fast reaction to set-point changes. To give accuracy and to compensate for model errors a closed-loop PI-controller is added.

A scheme for doing this in a standard HVAC-system is shown in Figure 7.1. Equations for the calculations are found in Section 3.2 describing the HVAC-hardware functioning.

The required temperature of the saturated air coming from the evaporator is calculated on the basis of the given x_{in}. If it is higher than or equal to than the ambient temperature, the evaporator can be switched off. This is due to the fact that no humidification is possible. A lower limit for the temperature should be around 4 degrees Celsius

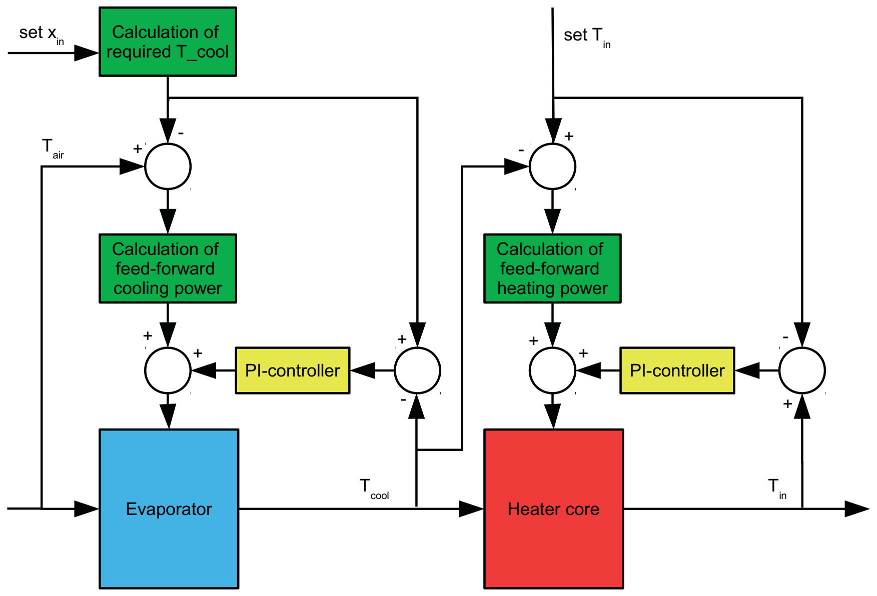
set x_{in}
Calculation of required T_cool
set T_{in}
T_{air}
Calculation of feed-forward cooling power
Calculation of feed-forward heating power
PI-controller
PI-controller
Evaporator
T_{cool}
Heater core
T_{in}

Figure 7.1: Scheme of the HVAC temperature and humidity control.

above zero in order to avoid icing on the evaporator [36]. Based on equation 3.32, a feed-forward value for the power needed to cool the air from its inlet value T_{air} to the desired T_{cool} can be determined. The difference between the calculated cool air temperature and the actual value is fed into a PI-controller. Its output is then added to the feed-forward control signal. This cooling power has to be translated to actor values, for example a valve setting and the compressor speed.

The principle for the heating power control is the same. The given set-point for the inlet temperature T_{in} and the temperature after the evaporator are used to calculate a feed-forward heater power. To this value the correction of the PI-controller, which is working on the error between the set and the actual T_{in} is added. Again, depending on the hardware, this power is translated, for example into an air mix flap angle.

If no cooling is available, the cooling part is simply removed and the T_{cool} temperature is replaced by the inlet value T_{air}.

7.2 Heat pump control

For a heat pump the scheme described before can be used as well. The cooling and the heating power have to be translated into hardware settings. The heat source or sink can be taken directly from the optimiser output if a design variable for this has been introduced (cf. Section 4.5).

The de-icing should be implemented by using a predefined program and by suspending the inlet temperature control. Therby, no interference with other control signals can happen during the heating and melting of the ice on the front heat exchanger. This avoids too short de-icing which would lead to fast ice re-accumulation.

7.3 Fan control

Normally no sensor is used for the air flow, so open-loop control is the only option. It is based on the fan characteristics as well as the system impedance of the HVAC-system. This gives one operating point (= air mass flow) for a given fan voltage, as shown in Figure 3.5 in Section 3.2.1. If these points are known, a fan voltage for a desired air flow can be given. In this way the air flow is controlled with the help of a look-up table.

However, there are a lot of disturbances making this approach inaccurate. As described in the system description in Section 3.2.1 countermeasures have to be realised depending on the geometry and HVAC-system. Even if some relations can be given, for example for the pressure rise at the air inlet, measurements (or simulations) are required to quantify the resulting influence on the air flow.

7.4 Flap control

The air mass flow percentage to the outlets (or passing the flap) has to be translated into a flap opening angle. This is done with look-up tables relating these two parameters. To obtain these, experiments for each flap have to be performed. For a mass-production vehicle this could also be implemented in hardware by a gear or a cam disc making the control “see” a (nearly) linear relation.

7.5 Cold air prevention system

The heating core is not able to deliver heat instantaneously. By contrast, the fan reacts much quicker to changes, so there has to be a mechanism preventing the passengers to be blown with cold air, which is not comfortable.

The cold air prevention system avoids this by reducing the fan control output when the outlet air is cold. The air speed-comfort relationship found in Section 2.2.2 can be used as a base. Air flow into the cabin colder than zero degree Celsius should be reduced to a minimum.

8 System and functionality integration

In this chapter the application of the optimiser algorithm for the car climate control will be shown. The equations for the objectives found in Chapter 2 and the system (Chapter 3) have to be brought into a suitable form for the algorithm. User control and different operating modes have to be integrated.

8.1 Objective implementation

The objectives are directly used as far as they can be expressed mathematically. The results are used in the algorithm, as seen in Section 6.3.5, in two ways. On the one hand, it is important if they exceed a limit. On the other hand, the weighted sum of all is used if the limit comparison gives no winner. In order to make the weight designation and the objective comparison easier it is advantageous to have a common maximum and minimum objective result. This avoids that one objective becomes too dominant. The minimum is set to zero, while for the maximum a parameter ϕ_{max} is used.

8.1.1 Windscreen fogging affinity

The basic equations to estimate the fogging affinity are given in Section 2.1. The finding of the minimum, however, is not suited for a control application. The distance calculated in equation 2.3 will be replaced by an estimation.

The idea is to approximate the closest point on the vapour saturation curve. This is done via a local linearisation of this curve as seen in Figure 8.1. Starting from a measured point A given through the water vapour pressure p_v and a temperature T the points B

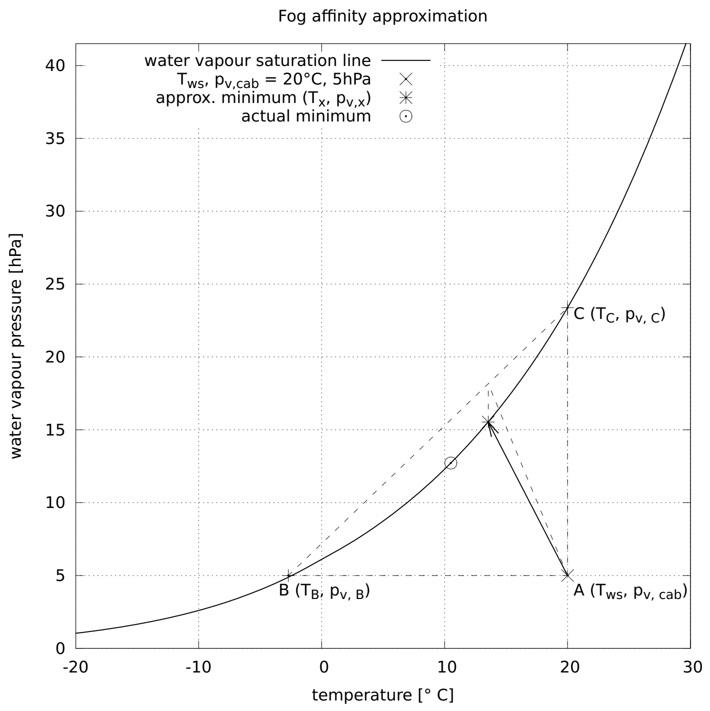

Figure 8.1: A way to estimate the fogging affinity given in equation 2.3.

and C are found by the vertical and horizontal crossings with the saturation function. They can be calculated with the help of equation 2.1, here referred to as $p_{sat} = f(T)$.

$$\begin{aligned} p_{v,C} = & \quad f(T_{ws}) \\ T_B = & \quad f^{-1}(_{v,cab}) \end{aligned} \tag{8.1}$$

There are small errors calculating T_B with the inverse function if $T_B < 0\,^\circ\mathrm{C}$ because of the switch in the parameters (see Table 2.1). They are not important to the estimation, though and do not justify a recalculation with changed parameters.

Having found these points, the temperature of the closest point to A on the segment $\overline{BC}$ is of interest. It is given by the following equation:

$$T_x = T_B + (T_{ws} - T_B) \cdot \cos(\sphericalangle(\overline{BA}, \overline{BC})) \tag{8.2}$$

The values of the points A, B, and C are inserted and the vapour pressure is scaled with the factor $a_{p_{sat}}$ from equation 2.2 in order to obtain a correct angle $\sphericalangle(\overline{BA}, \overline{BC})$ in the scaled coordinate system.

$$T_x = T_B + \frac{(T_{ws} - T_B)^2}{\sqrt{(T_{ws} - T_B)^2 + \left(\frac{p_{v,C} - p_{v,cab}}{a_{p_{sat}}}\right)^2}} \tag{8.3}$$

The corresponding vapour pressure value $p_{v,x}$ will be calculated via equation 2.1. Now the fogging affinity indicator κ can be approximated with

$$\kappa \approx \sqrt{\left(\frac{p_{v,x} - p_{v,cab}}{a_{p_{sat}}}\right)^2 + (T_x - T_{ws})^2} \tag{8.4}$$

The error made compared to the original equation is seen in Figure 8.2.

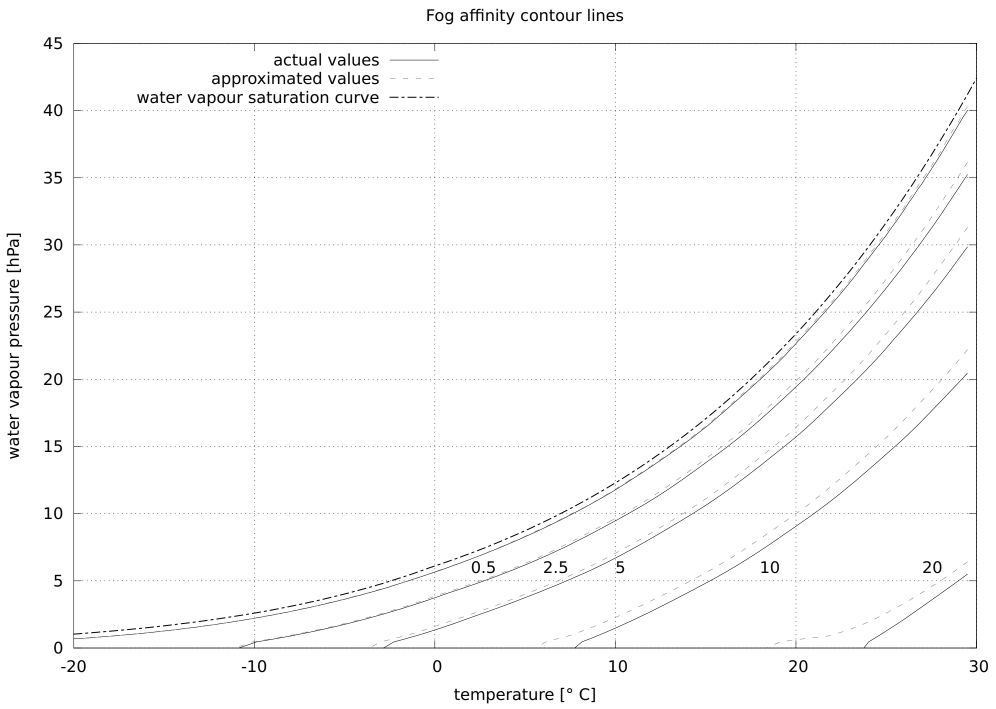

Figure 8.2: The contour lines of equations 2.3 and 8.4.

In order to get a result in the range $0 \ldots \phi_{max}$ with zero being the lowest fogging risk, κ has to be scaled. This requires the definition of a distance κ_{max}. This value defines when the system should begin to take countermeasures. Choosing a value which is too high makes the control act too early and may lead to higher energy consumption. A very low value risks to have a too small margin for measurement errors or sudden changes, which can lead to fogging. Here, a value of 5 °C will be used. It can be optimised through experiments. For higher distances the objective result ϕ_{fog} is 0. Below κ_{max}, the κ value will be scaled linearly to be ϕ_{max} on the vapour saturation curve. Above it, which can happen due to measurement errors, the result has to be the maximum, too.

$$\phi_{fog} = \begin{cases} 0 & \text{for } \kappa \geq \kappa_{max} \\ \left(1 - \frac{\kappa}{\kappa_{max}}\right) \cdot \phi_{max} & \text{for } \kappa < \kappa_{max} \\ \phi_{max} & \text{for } p_v \geq p_{sat}(T) \end{cases} \tag{8.5}$$

The limit for the objective depends a lot on the used sensors, their positioning and their response behaviour. Gühmann [6] used a distance below 1 ℃ to indicate fogging. As seen later in Figure 10.7 this could be reproduced in an experiment.

8.1.2 Thermal comfort

A simpler scaling than the one in equation 2.5 to obtain the *Predicted Mean Vote* can be used up to a metabolism of $M = 150\,\frac{\mathrm{W}}{\mathrm{m}^2}$ [1] to save some computation time.

$$PMV = \frac{3.8}{M}\{\dot{q}_H - \dot{q}_d - \dot{q}_{sw} - \dot{q}_{re} - \dot{q}_L - \dot{q}_R - \dot{q}_C\} \tag{8.6}$$

Of the used parameters in equations 2.6 and 2.7 all the passenger related parameters are not directly available (e.g. from sensors) in a car. The clothes, age, sex and, most importantly, the metabolism (seen in Figure 2.2) differ among humans but vary for one person in time as well. Therefore, a parameter to compensate for these changes should be provided.

User adaption

The two parameters available in the model are the clothing insulation r_{cl} and the metabolism M. The external work is assumed to be zero ($W = 0$) since the power transmitted to the car is comparably small. In order to keep it simple to use and parameterise, one parameter to bias the comfort model should be chosen.

As an assumption the worn clothes will be expressed by a function of the ambient temperature. The simplest way would be to set it to a fixed value, corresponding to a passenger being equally dressed the whole year while driving the car. Another option is a user dressed according to the ambient temperature. In summer one usually wears light clothes, so an r_{cl} of 0.30 clo [7] is taken for temperatures above 25 ℃. In winter, pullover, long trousers and better insulating boots are probably also worn in cars, resulting in a higher value. Therefore, below a temperature of -5 ℃ the maximum for casual clothes stated in [7] of 1.50 clo is taken. Between these extreme values a linear interpolation is done. The resulting function is shown in Figure 8.3.

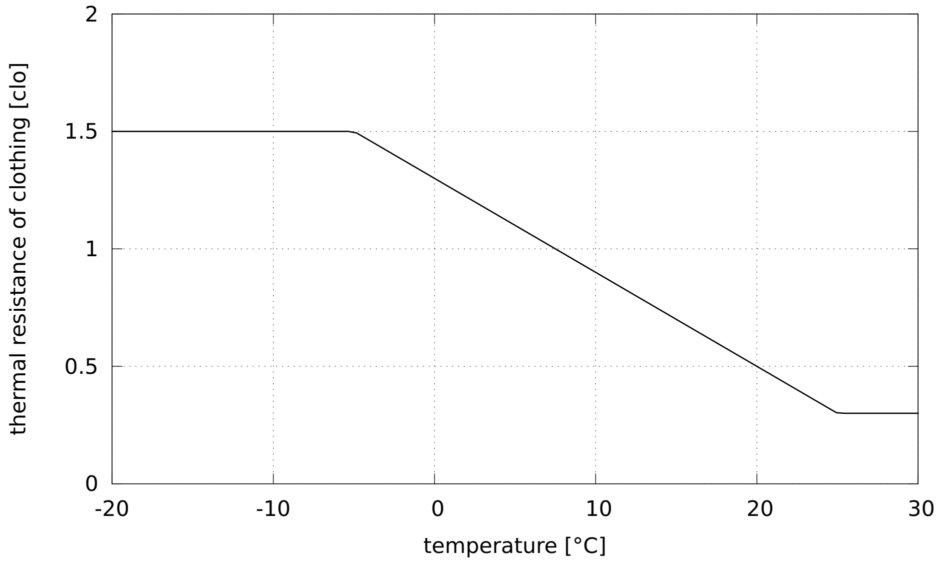

Figure 8.3: Assumption for clothes insulation as a function of ambient temperature.

The comfort temperature (PMV = 0) was calculated depending on the ambient temperature for both options. The metabolism was set to 1.2 met, 50% relative humidity and no air flow was applied. The mean radiation temperature was calculated using an estimation for the heat transfer of the car driving 50 $\frac{\text{km}}{\text{h}}$ as described in the following section. The result in Figure 8.4 shows that the fixed clothing gives a higher comfort temperature in winter than in summer. This setting is usually applied today [2] and is close to the recommendation of DIN 1946-3 [11]. Most likely equal clothing has been used for all ambient temperatures in these comfort observations. The adapted clothing factor gives (in the relevant temperature range) the opposite - a higher comfort temperature at a higher ambient temperature. This setting might not be accepted by everyone, but - as the clothes are adapted to the season - it will require less energy for cooling and heating.

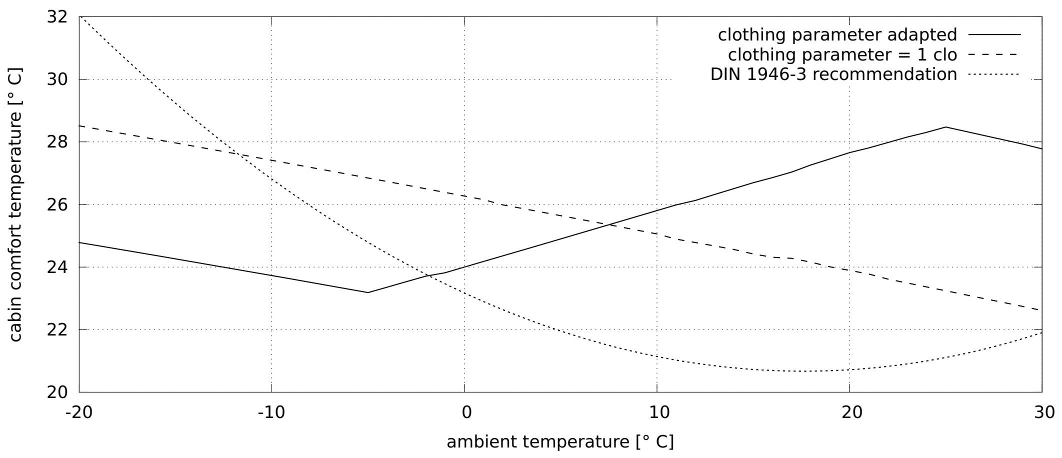

Figure 8.4: Comparison of the comfort temperatures for different clothing adaptions.

As an option for the controller, the parameters (upper and lower clothes insulation) can be adapted to the desired behaviour.

The metabolism value is used to let the user influence the temperature. This is a good choice since its magnitude is highly dependent on the person. Even if single values are given in EN ISO 7730 [7], these are only mean values. In an annotation it is already mentioned there that elderly people have lower metabolisms. Moreover, a woman's energy consumption is calculated differently from a man's. Other parameters in the *Harris-Benedict-Formula*, used to estimate the metabolism, are age, weight and body size [37]. By simulations metabolisms from 0.75 met to 2.25 met have been found as a suitable range. Changing this value represents an indirect means of controlling the cabin temperature and can be used to manually compensate possible errors made in other parameters. A lower value will automatically lead to a higher comfort temperature. An advantage of this kind of user control is that the comfort temperature is automatically adapted to the ambient temperature and the air flow. A scaling with 100 being 0.75 met and 0 equalling 2.25 met is done in order to obtain a simpler scale and the relation of a higher value leading to a higher temperature.

Mean radiant temperature

The mean radiant temperature T_r also has to be estimated. It is approximated by the mean surface temperature of the surrounding environment. In a car a major part of it is the car body. Its inner surface temperature $T_{surface}$ is usually not measured and will be estimated in the following.

The transfer through a plate is expressed as follows [17]:

$$\frac{T_{amb} - T_{surface}}{R_{cab,out} + R_{body}} - \frac{T_{surface} - T_{cabin}}{R_{cab,in}} = \dot{q}_r \tag{8.7}$$

The influences of solar radiation are covered by $\dot{q}_r$. The absorptance has to be observed when inserting (measured) radiation values here. The thermal resistance of the car body material R_{body} can be used directly. The other two have to be calculated first:

$$R_{cab,out} = \frac{1}{h_{cab,out}} \tag{8.8}$$

$$R_{cab,in} = \frac{1}{h_{cab,in}} \tag{8.9}$$

With the help of equation 3.10, $h_{cab,in}$ and $h_{cab,out}$ are approximated. For the outer heat transfer coefficient the air speed is close to the car speed $v_{air} \approx v_{car}$. This applies at least for the roof which has a high share of the car body surfaces surrounding the passengers. Inside the car cabin the air is not moving fast, so a constant heat transfer coefficient of $6.2\,\frac{\mathrm{W}}{\mathrm{m^2 \cdot K}}$ will be assumed (cf. equation 3.10).

Joining equations 8.7 - 8.9, the inner surface temperature of the car body can be estimated:

$$\begin{aligned} T_{surface} = \frac{1}{R_{tot}} [&T_{amb} \cdot R_{cab,in} + T_{cabin} \cdot (R_{cab,out} + R_{body}) \\ &+\dot{q}_r \cdot R_{cab,in} \cdot (R_{cab,out} + R_{body})] \end{aligned} \tag{8.10}$$

With R_{tot} being $R_{tot} = R_{cab,out} + R_{body} + R_{cab,in}$.

Without a solar sensor this estimation can be made, but it will not give a good estimation when the solar radiation is high. For the windscreen and the windows the temperature can be obtained in a similar way if no temperature sensor is available. Interior equipment surfaces are supposed to have the same temperature as the cabin air. This will not be the case while the cabin air is heating up, but for materials with low thermal masses the temperature will be close.

The obtained values have then to be averaged and weighted by their area respective to the passenger.

$$T_r = T_{surface} \cdot w_{body} + T_{glass} \cdot w_{glass} + T_{interior} \cdot w_{interior} \tag{8.11}$$

with $w_{body} + w_{glass} + w_{interior} = 1$.

Scaling and weight

As scaling a figure based on the PMV, called the *predicted percentage of dissatisfied* (PPD) could be used. It is defined as

$$PPD = 1 - 0.95 \cdot e^{(-0.03353 \cdot PMV^4 - 0.2179 \cdot PMV^2)} \tag{8.12}$$

This gives as result of the thermal comfort objective function

$$\phi_{therm} = PPD \cdot \phi_{max} \tag{8.13}$$

In DIN 7730, appendix D [7], an implementation of a thermal comfort calculation is found.

8.1.3 Air speed comfort

As mentioned in Section 2.2.2, the air speed itself can cause discomfort. Using a different comfort model, this objective could be included in a general thermal aspect. Here it has to be implemented in a separate function.

The air speed towards the passengers is calculated by the air volume going through the face-outlets divided by their area. When reaching the persons the maximum speed $v_{air,face}$ is reduced with a distance x (assuming circular outlets with a diameter D_{outlet}) [16].

$$v_{air,face} = 6.3 \cdot \frac{D_{outlet}}{x} \cdot \frac{\dot{m}_{air,in}}{A_{outlets,face} \cdot \rho_{air}} \tag{8.14}$$

The temperature change in the jet is not taken into account here.

Based on Figure 2.3 an air speed comfort area is defined. Similar to the fogging

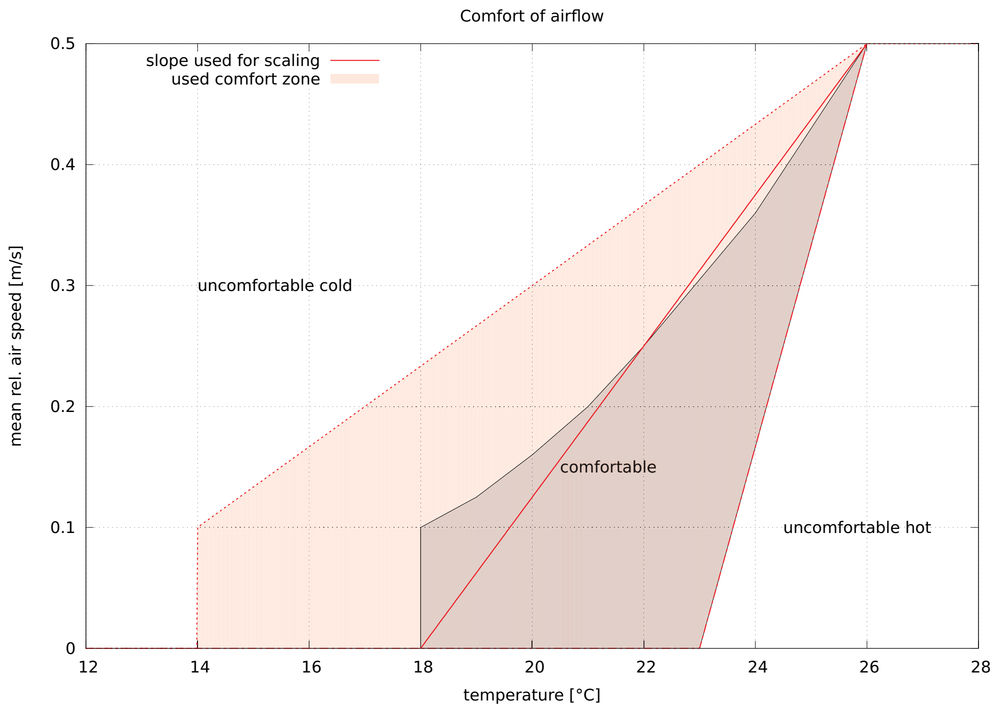

Figure 8.5: Comfort range of air speed used for the objective.

risk, a scaling factor (here $a_{airspeed} = 16\,\frac{°C\cdot s}{m}$) for the air speed is introduced. This is necessary to compensate for the different units. Finally the distance from the defined comfort zone is calculated.

The comfort area from Figure 2.3 is extended to allow lower temperatures. This might be necessary when the climate control needs to compensate for solar radiation. A linear upper boundary is chosen which simplifies the calculation and is closer to the shape of the contour lines of the formula of ISO 7730 (cf. Figure 2.4). The resulting area is shown in Figure 8.5.

$$\begin{aligned} v_{high}(T_{in}) &= \begin{cases} 0\,\frac{m}{s} & \text{for } T_{in} < 14\,°C \\ 0.4 \cdot \frac{T_{in}-14}{12} + 0.1\,\frac{m}{s} & \text{for } T_{in} \geq 14\,°C \end{cases} \\ v_{low}(T_{in}) &= \begin{cases} 0\,\frac{m}{s} & \text{for } T_{in} < 23\,°C \\ 0.5 \cdot \frac{T_{in}-23}{3}\,\frac{m}{s} & \text{for } T_{in} \geq 26\,°C \end{cases} \end{aligned} \tag{8.15}$$

Based on these limits the air speed comfort objective result $\phi_{airspeed}$ is calculated. A speed distance of v_{max} from the comfort region gives maximum penalty. A user adaption

v_{pas} will be introduced (set to 0 in Figure 8.5).

$$\phi_{airspeed} = \begin{cases} \frac{14 - T_{in}}{v_{max} \cdot a_{airspeed}} \cdot \phi_{max} & \text{for } T_{in} < 14\,^{\circ}\mathrm{C} \\ \frac{v_{low}(T_{in}) - v_{in} + v_{pas}}{v_{max}} \cdot \phi_{max} & \text{for } 14\,^{\circ}\mathrm{C} \leq T_{in} \leq 26\,^{\circ}\mathrm{C} \wedge v_{face} < v_{low}(T_{in}) + v_{pas} \\ \frac{v_{face} - v_{high}(T_{in}) + v_{pas}}{v_{max}} \cdot \phi_{max} & \text{for } 14\,^{\circ}\mathrm{C} \leq T_{in} \leq 26\,^{\circ}\mathrm{C} \wedge v_{face} > v_{high}(T_{in}) + v_{pas} \\ \frac{14 - T_{in}}{v_{max} \cdot a_{airspeed}} \cdot \phi_{max} & \text{for } T_{in} > 26\,^{\circ}\mathrm{C} \\ 0 & \text{else} \end{cases} \tag{8.16}$$

This relationship can be used to implement a simple air speed consideration. Values above ϕ_{max} need to be set to ϕ_{max}. The limits may be adapted and tested. A v_{max} of $0.3\,\frac{\mathrm{m}}{\mathrm{s}}$ is chosen to avoid reaching the maximum of $0.82\,\frac{\mathrm{m}}{\mathrm{s}}$ proposed in ISO 7730 [7].

8.1.4 Humidity comfort

As seen in Section 2.2.3, an established mathematical formulation of a comfortable air humidity does not exist. Therefore, using the chart by Leudsen and Freymark and the limits given in DIN 1946-3, a comfort figure for the humidity is created.

As general limits for the relative humidity 30% as lower and 70% as upper boundary have been chosen. A slope fitting the one of Leudsen and Freymarks graph is chosen, while the upper limit is adapted to the DIN recommendations. As a result, an upper φ_{high} and a lower φ_{low} comfort limit is obtained.

$$\begin{aligned} \varphi_{high} &= \begin{cases} 70\% & \text{for } T_{cab} < 12^{\circ}\mathrm{C} \\ (-1.2 \cdot T_{cab} + 84.0)\% & \text{for } T_{cab} \geq 12^{\circ}\mathrm{C} \end{cases} \\ \varphi_{low} &= \begin{cases} (-0.44 \cdot T_{cab} + 45.7)\% & \text{for } T_{cab} < 35^{\circ}\mathrm{C} \\ 30\% & \text{for } T_{cab} \geq 35^{\circ}\mathrm{C} \end{cases} \end{aligned} \tag{8.17}$$

T_{cab} is the actual cabin temperature in degrees Celsius. The comfort area can be seen in Figure 8.6. With these limits the humidity comfort (ϕ_{hum}) is defined. It expresses how far away from a comfortable humidity the actual condition is. In order to respect personal

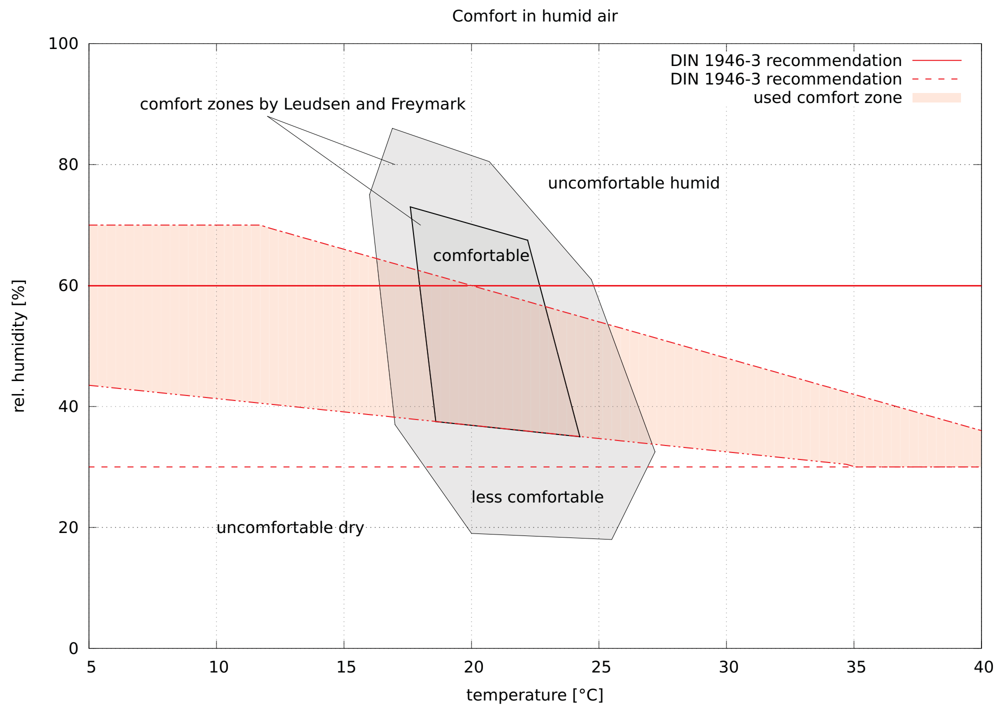

Figure 8.6: Comfort range of air humidity used for the objective.

preferences of the passengers a user control φ_{pas} biasing the limits is introduced.

$$\phi_{hum} = \begin{cases} \phi_{max} \cdot (\varphi_{cab} - \varphi_{high} + \varphi_{pas})/30 & \text{for } \varphi_{cab} > \varphi_{high} + \varphi_{pas} \\ \phi_{max} \cdot (\varphi_{cab} - \varphi_{low} + \varphi_{pas})/30 & \text{for } \varphi_{cab} < \varphi_{low} + \varphi_{pas} \\ 0 & \text{else} \end{cases} \tag{8.18}$$

φ_{cab}	Relative humidity in the car cabin [%]
φ_{pas}	Passenger humidity biasing ($-30\% \ldots + 30\%$) [%]

The passenger influence is limited to 30% to stay within the physical limits. This distance of 30% is also the distance giving the maximum value ϕ_{max}.

8.1.5 Air quality

The concentration of carbon dioxide in the air can be used as an indicator for air quality, as seen in Section 2.2.4. Even if it is not measured it can be estimated and used as an objective to ensure fresh air supply.

Based on the relation shown in Figure 2.6 the air quality objective result (ϕ_{CO_2}) is calculated.

$$\phi_{CO_2} = \begin{cases} 0 & \text{for } x_{CO_2} < x_{CO_2,min} \\ \phi_{max} \cdot \left[1 - \left(\frac{x_{CO_2} - x_{CO_2,min}}{x_{CO_2,max} - x_{CO_2,min}}\right)^2\right] & \text{for } x_{CO_2,min} \leq x_{CO_2} \leq x_{CO_2,max} \\ \phi_{max} & \text{for } x_{CO_2} > x_{CO_2,max} \end{cases} \quad (8.19)$$

x_{CO_2}	Carbon dioxide concentration in the cabin $[\frac{\mathrm{mg_{CO_2}}}{\mathrm{kg_{air}}}]$
$x_{CO_2,min}, x_{CO_2,max}$	Carbon dioxide concentration limits $[\frac{\mathrm{mg_{CO_2}}}{\mathrm{kg_{air}}}]$

As minimum CO_2 concentration the value for ambient air, 390ppm $\approx 700\frac{\mathrm{mg_{CO_2}}}{\mathrm{kg_{air}}}$, is taken. As maximum a value of 2000ppm $\approx 3600\frac{\mathrm{mg_{CO_2}}}{\mathrm{kg_{air}}}$ will give the highest weight of ϕ_{max}. This value is proposed as a maximum for hygienically acceptable air quality [13]. A comparison with the equation given in the European Guidelines for Ventilation Requirements in Buildings [14] is seen in Figure 8.7.

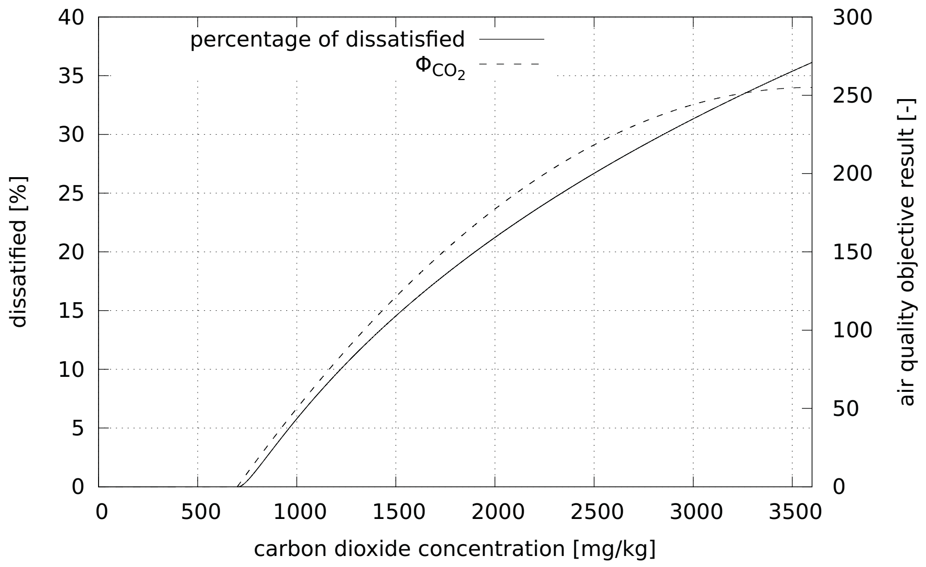

Figure 8.7: The air quality objective result ($\phi_{max} = 255$) compared to the percentage of dissatisfied people [14].

8.1.6 Power consumption

Based on a previous determined maximum P_{max} the electric power consumption objective result ϕ_{el} is calculated with the predicted power consumption P_{el}.

$$\phi_{el} = \frac{P_{el}}{P_{max}} \cdot \phi_{max} \tag{8.20}$$

Here a linear scale is applied. Other weightings could be used if it makes a difference if high power is drawn over a short period of time or a low power is consumed over a longer one. The predicted power is based on a model for each component, estimating the energy consumption needed to provide the inlet air properties (represented by the design values).

In addition to this objective a second one can be defined if fuel based heating is used. The use of two separate objectives allows to influence the electric power consumption without interfering with the heating. As before, the required power to generate the heat is predicted, here by means of equation 3.36. It is scaled by the maximum power of the heater and multiplied by the maximum rating to obtain the fuel consumption objective result ϕ_{fuel}.

$$\phi_{fuel} = \frac{\dot{Q}_{fuel}}{\dot{Q}_{max,heater}} \cdot \phi_{max} \tag{8.21}$$

8.1.7 Component thermal management

One approach to consider the thermal requirements of other components, if they are included in the same cycle, are tolerance windows. These have an optimal point and a tolerance area. Possible physical representations for these are the component temperature, the cooling/heating power or more advanced the coolant flow and its temperature. The last option is planned for the ePerformance prototype [21] and shown in Figure 8.8. Such a window could be easily translated into a limit and an objective function.

8.2 Constraint formulation

Constraints model the limits of the hardware. Limits are given since the fan, the heater and the cooler cannot output “negative power” and have a maximum power .

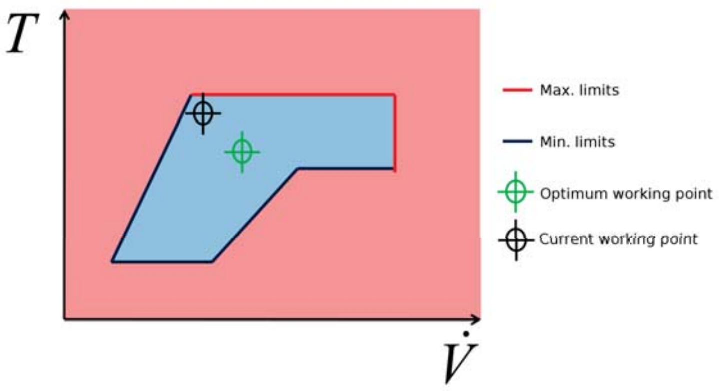

Figure 8.8: The thermal requirements interface to the components in the ePerformance project. [21]

Constraints are typically brought into such a form that their output is below or equal zero but greater than −1 when fulfilled. Results above zero indicate an exceeded constraint.

If only heating is available, the minimal physical possible air outlet temperature $T_{min,phys}$ is given by the ambient temperature T_{amb}. If cooling is available, too, it is also dependent on the air flow and the evaporator power. A lower comfort limit is assumed at 5 ℃. $T_{max,phys}$ depends on the heater core power and temperature. As maximum comfort limit 55 ℃ is taken. The minimal and maximal temperatures are found by comparing the feasible temperatures and the comfort limits.

$$\begin{aligned} T_{in,max}(\dot{m}_{air,in}, \mu_{recirc}) &= \min\{T_{max,comfort}, T_{max,phys}(\dot{m}_{air,in}, \mu_{recirc})\} \\ T_{in,min}(\dot{m}_{air,in}, \mu_{recirc}) &= \max\{T_{min,comfort}, T_{min,phys}(\dot{m}_{air,in}, \mu_{recirc})\} \end{aligned} \tag{8.22}$$

This ensures that the persons in the car are not frozen or burnt and that the optimiser only gives feasible outputs.

$$g_{tl} = \frac{T_{in,min}(\dot{m}_{air,in}, \mu_{recirc})}{T_{in}} - 1; \quad g_{tu} = \frac{T_{in}}{T_{in,max}(\dot{m}_{air,in}, \mu_{recirc})} - 1 \tag{8.23}$$

The water amount in the inlet air is also limited. Since there is no means of humidification in a car, the maximum is determined by

$$x_{w,in,max}(\mu_{recirc}) = \mu_{recirc} \cdot x_{w,cab} + (1 - \mu_{recirc}) \cdot x_{w,amb} \tag{8.24}$$

The lower bound is given by the amount of water in the saturated air at the evaporator. This is dependent on the temperature of the evaporator and therefore on the cooling power. It is also a limiting factor if the heating power needed to re-heat the air is available. Another limit to respect is that the evaporator temperature should not be below zero degree to avoid icing.

$$x_{w,in,min}(T_{in}, \dot{m}, \mu_{recirc}) = x_{w,sat}(\dot{Q}_{cool,max}, \dot{Q}_{heat,max}) \tag{8.25}$$

The constraints then look similar to the ones on the temperature

$$g_{hl} = \frac{x_{w,in,min}(\mu_{recirc})}{x_{w,in}} - 1; \quad g_{hu} = \frac{x_{w,in}}{x_{w,in,max}(\mu_{recirc})} - 1 \tag{8.26}$$

The lower limit of the air mass flow is 0 $\frac{\text{kg}}{\text{s}}$, but since a low air flow is always desired, the air flow when the fan starts spinning is taken instead. The physical upper limit depends on the fan and the HVAC-unit, the duct and the outlet pressure drop. Another limitation is given by the cold air prevention system (see Section 7.5). Here the lower of both limits has to be chosen as $\dot{m}_{air,in,max}$.

$$g_{fl} = \frac{\dot{m}_{air,in,min}}{\dot{m}_{air,in}} - 1; \quad g_{fu} = \frac{\dot{m}_{air,in}}{\dot{m}_{air,in,max}} - 1 \tag{8.27}$$

Since the flap passage percentage is defined as mass flow to a certain output divided by mass flow before the flap, the μ cannot be negative and is 100% maximum.

$$g_{vl} = -\mu_x; \quad g_{vu} = \mu_x - 1 \tag{8.28}$$

In an electric vehicle power management is important. Therefore, it is good if systems which are not safety-critical, like heating and ventilation, can be restricted in power consumption. This results in a constraint that the actual drawn power $P(T_{in}, x_{w,in}, \dot{m}_{air,in})$ has to be less then the given (and changing!) limit P_{lim}.

$$g_{pow} = \frac{P(T_{in}, x_{w,in}, \dot{m}_{air,in})}{P_{lim}} - 1 \tag{8.29}$$

Additional constraints may be necessary depending on the HVAC-system. For example a constraint for the icing if a heat pump is employed. The icing can be integrated into the energy consumption objective function by a modified efficiency of the heat pump. However, to force de-icing above a certain limit in order to avoid damage to the components, a separate constraint is advisable. Its limit can then be set without interfering with the objectives while it is not exceeded.

8.2.1 Integration as boundaries

Some constraints vary, while others are fixed. These - as the flap passage and fan limits - can be given as boundaries for the design space. Upper and lower limits for the other design variables have to be set in order to limit the search area. A smaller design space leads to faster results as unusable results are not considered.

These boundaries may be adapted by external signals or user settings in order to force a different minimum or limit one variable. However, they may not depend on other design variables or predicted states. In Table 8.1 an overview of the standard values is given.

Table 8.1: Overview of the objectives and their corresponding parameters.

Design variable	lower bound	upper bound
T_{in}	$T_{min,comfort}$	$T_{max,comfort}$
$\dot{m}_{air,in}$	$\dot{m}_{air,in,min}$	$\dot{m}_{air,in,max,phys}$
$x_{w,in}$	0	$x_{w,amb}$
μ_{recirc}	0	1
μ_{foot}	0	1
$\mu_{defrost}$	0	1

Boundaries for the de-icing switch and source selection are not required. Due to their discrete nature only available values can be chosen.

8.2.2 Integration as objectives

All the constraints depending on design variables or predicted states have to be evaluated for each individual. Therefore, they have to be implemented as special objective, as described in Section 6.3.5. The functions, as shown above, return a value between -1 and

0 if the constraint is satisfied and values greater than zero if not, as it is common for optimisation problem formulations [31].

The constraints for the temperature and the humidity of the inlet air are limited through the maximum heating/cooling power and depend on the air flow. Equation 3.1.1 and equation 3.2.3 can be used to implement a maximum and minimum temperature constraint as well as a minimum humidity.

The electric power limitation and the upper air flow limit given by the cold air prevention have to be realised in this way, too. Other limitations for connected design variables, for example icing can be integrated by a special objective.

8.3 Parameters for the objectives

In the following Table 8.2 an overview of the objectives so far presented and their scaling method is given. The scaling can be important for the compromise finding in combination with the weight. Moreover, possible priorities, weights and limits are shown. Objectives regarding the application of a heat pump in a more general thermal management are not listed since they depend a lot on the system.

The objectives derived from the constraints are the simplest to parameterise. They have the highest priority, are not weighted and have - with the standard formulation as used before - the limit zero.

For the objectives, a ϕ_{max} of 255 is used. Therefore, listed limits of 255 mean “no limit” since they cannot be exceeded. For the power consumption objectives it is not useful to set a limit since the calculation is based on the maximum powers. The air speed objective does not require any limit since it is not very important. The humidity control will also not be limited as it is limited by physics (0-100% relative humidity). Another factor for this decision is that it is not completely controllable (cf. Section 8.2). For the fogging affinity a limit is given by the sensor accuracy to predict fogging. The air quality is required to stay below the OEL-value (cf. Section 2.2.4). In the case of the thermal comfort, a limit is used together with its *panic handler* (see Section 6.3.10) in order to guide a way out of a very uncomfortable state.

Priorities are chosen by importance. Safety related objectives, fogging and air

Table 8.2: An overview of the objectives with parameter examples.

Objective	**Scaling**	**Priority**	**Weight**	**Limit**
Fogging affinity	linear, κ_{max}	3	3	230
Thermal comfort	PPD	1	2	254
Air speed comfort	linear	1	1	255
Humidity comfort	linear	1	1	255
Air quality	neg. quadratic	2	2	250
Power consumption (electric)	linear, P_{max}	1	1	255
Power consumption (fuel)	linear, $\dot{Q}_{max,heater}$	1	0.2	255
Min. inlet temperature (constr.)	linear	4	0	0
Max. inlet temperature (constr.)	linear	4	0	0
Min. inlet humidity (constr.)	linear	4	0	0
Max. electric power (constr.)	linear	4	0	0
Cold air prevention limit (constr.)	linear	4	0	0

quality, have the highest priority. The others are regarded as equal.

The weights determine the position of the control solution on an imaginary pareto front. A high value, for example on the fuel power consumption objective, will lead to quite a cold experience in winter. Therefore, a trade-off has to be found and tuned to fit the desired behaviour. In the exemplary values shown here, passenger related values are regarded as most important.

As for the boundaries these values can also be changed online through control settings.

8.4 User control

The passenger has to be able to adapt the states of the cabin air, the temperature and the humidity, to the desired values. This is achieved indirectly by modifying the humidity φ_{pas} for the humidity objective (cf. Section 8.1.4) and the metabolism M for the temperature (cf. Section 8.1.2).

The disadvantage of this approach is that no direct resulting value can be given for example no direct set-point temperature, which might be unfamiliar to some people. However, in today's cars a set temperature will be modified already depending on the environment temperature, leading to a higher cabin temperature in winter and a colder on hot days (see Figure 8.4).

The advantage of an indirect setting is that the adaption is based on measurements and established comfort calculation instead of a simple relation with the ambient air temperature. This should cause less need to change the settings and thus less distraction. The air flow towards the passenger can also be adapted using the v_{pas} variable. Persons very sensible to air flow can reduce the direct draught in this way.

As examples three special modes are presented here: Recirculation-, defrost- and precondition-modes. Recirculation is desired in case of odours entering the car from outside, for example when driving through a tunnel. Here a switch is used to force air recirculation. This is realised with changed boundaries by setting the lower boundary for the recirculated air percentage μ_{recirc} to 100%. A sensor in the air inlet could automatically activate this mode if needed.

Defrosting the windscreen might have to be available manually if the glass is iced and fast heating up of the window is desired. In this case again changing the boundaries gives the desired result. All air needs to go to the defrost outlets, which is done by setting the maximum air fraction to the feet μ_{foot} to zero. A high air flow is desired in order to bring in heat fast and give a high heat transfer. Therefore, the air flow minimum is set to a higher value (e.g. half the maximum) and the minimum temperature is raised. Finally, there is an increased fogging risk with full recirculation. This is avoided by guaranteeing a minimum of fresh air and by setting the upper bound for μ_{recirc} to a value below 100%, for example 50%.

The last mode, preconditioning, is used to heat (or cool) the car before starting a journey. With a remote control this can be activated just like auxiliary heating in conventional cars. To achieve this it would be sufficient to start the automatic climate control, but in order to be more efficient and faster it is useful to modify the weights. Air quality is not regarded at this point of time, since no human is in the car. This allows the algorithm to use full recirculation all the time, making heating and cooling efficient. Moreover, the thermal comfort can be favoured in comparison to the fogging affinity since no water sources are in the car. Less aggressive heating of the windscreen gives lower heat losses through the glass.

With the presented algorithm, of course many more settings and modes would be possible. Through changing weights the system can be adapted online and a personal trade-off between the objectives could be set. However, this would lead to a very complex control, which is not desired. New ideas for user control can be realised in a simple way, though.

Finally, the car should have the possibility to give manual control to the passenger. Some people like to influence the climatisation directly and do not want to give an algorithm full control (although this is what a designer of such a program wants to make superfluous). Additionally it is useful in case of a hardware (sensor) or software failure. Therefore, manual control has to be made available in parallel to the automatic control.

8.5 System simulation

For the system simulation the differential equations derived in Chapter 3 can be directly used in the given integration scheme from Section 6.3.4. Starting values are obtained by the sensors or the estimation ($x(t = 0) = x_{sensor}$).

A good choice for a predicted horizon is in the range of the system time constants (estimated in 3.1.5) in order to cover the system behaviour. To keep the computation time small, the choice of very few steps is proposed here. This makes the prediction inaccurate for bigger changes, but this is supposed to be acceptable since accuracy is only required when reaching a steady state value with little changes in the system states.

8.6 Optimiser algorithm parameters

The optimiser algorithm needs to be parameterised in order to be adapted to the problem. The parameters affect the computation time as well as the solution quality.

8.6.1 Population size

The population number consists of three figures:

$$n_{pop} = n_{base} + n_{elite} + n_{random}$$

The base and the elite population as well as the random immigrants size have to be balanced in order to give a good reaction speed and a proper solution quality.

First a set of base settings or *base population* has to be identified, as described in Section 6.3.3. These should cover reasonable set-points for common situations. A defog-preset should be present as well as settings for heat-up and cool-down. Other options like a low fresh air supply and a standard steady state input can be defined. Doing these definitions it is good to make them dependent on the boundaries (or other parameters) to allow the functioning of the modes described in Section 8.4. In this way it is also guaranteed that they are included in the design space. It is recommended to spread them across the design space, which happens automatically when defining set-points for different conditions. Then the base population can fulfil its task to speed up the optimisation by providing good starting points for most situations.

The second influence on the population size is the number of elite-individuals that are transferred from the last run. A high number increases the probability of a suitable solution among them, but it also leads to mediocre individuals being evaluated in every run. It also reduces the number of new, random individuals being introduced into the population.

For the controller values around $n_{base} = 5$, $n_{elite} = 3$ and $n_{random} = 2$ have been chosen and gave good results.

8.6.2 Other settings

Another important setting is the number of children. A high number will give higher chances to find a better solution, but it increases the computational effort, too. Connected to this setting is the number of generations, n_{gen}. Each generation a new offspring is created, so the overall number of system and objective evaluations n_{eval} for one optimiser run (each sample) is

$$n_{eval} = n_{pop} + n_{gen} \cdot n_c$$

Since in each generation the diversity is reduced, a high number of generations will lead to a more precise solution, while a reduced number (with the same number of function evaluations) will have a higher search area. Both numbers represent the trade-off between exploration and precision. Two generations and 20 children are chosen as suitable values.

In the domain of the exploration control another factor can be influenced. The s_x value determines how big mutations are applied and how big steps in the control output are allowed. According to equation 6.6 a step δ_{s_x} is added or subtracted depending on the fitness development. In order to always allow some mutation, but to not create too many individuals out of the design space, an upper and a lower limit for this adaption are defined.

Values of 0.1 as a minimum factor, 0.6 as a maximum and a step size of 0.05 have found to be suitable.

9 The *MUTE* project

In the *MUTE* project a cooperation of 20 departments of the TU München and partners from industry want to show the feasibility of a usable and competitive electric car through innovative and new technology. Therefore, a *MUTE* prototype car is developed at the moment.

9.1 The electric car *MUTE*

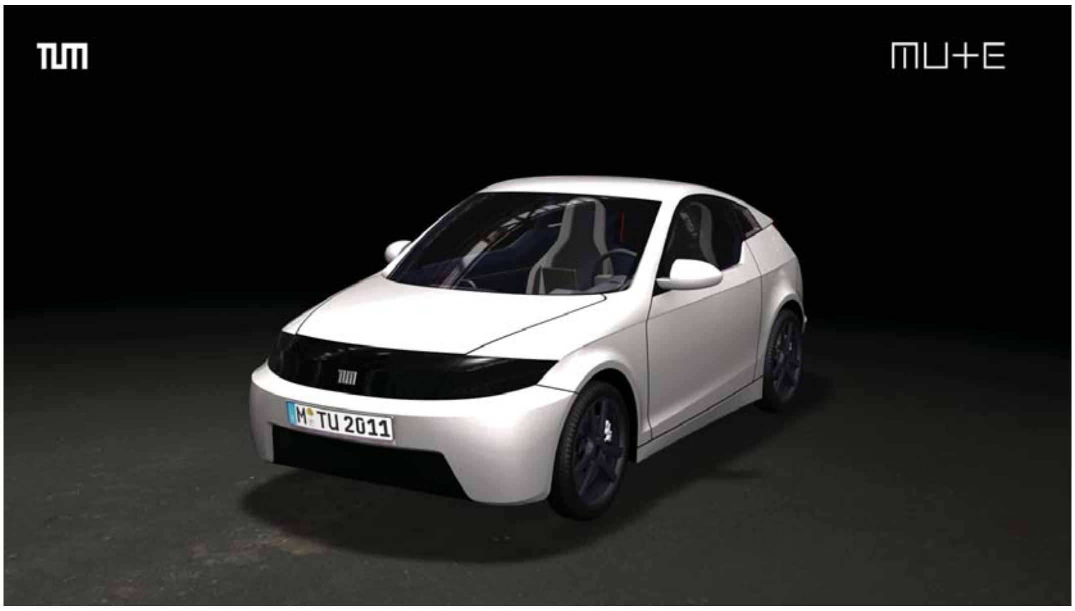

Figure 9.1: The MUTE car design. [38]

A preliminary rendering of the design is shown in Figure 9.1. The car can transport two persons and two pieces of luggage. This limitation makes a design possible that is small and lightweight enough to be registered under the L7E license (subcompact car). This leads to reduced tax paying for the customer and lower technical requirements. In order to fit into this car class the vehicle has to have a weight below 400 kg (the *MUTE* car will add 100 kg of battery to this) [38]. The engine output is limited to 15 kW as well.

The guaranteed range, which is an important figure for an electric car, is planned to be 100 km. This is realised by a rechargeable battery and - for exceptional cases - an electric range extender, which consists of a normal battery. The planned top speed is 120 $\frac{\mathrm{km}}{\mathrm{h}}$. The batteries are the main cause for high prices of electric (and hybrid) cars today available, but lower energy costs can compensate for these over their live-time. The project's goal is to reach a TCO (total cost of ownership) equalling the on of a today's compact car. Focus for the product design is the middle European market.

Apart from these "basic" features, innovative ideas are going to be realised. A mobile internet connection allows to use web-based applications and the car can be remote controlled. A new developed aluminium frame and car casing made completely out of carbon composite are used for the passenger cabin in order to save weight.

This makes the plan different from the car manufacturers' electric cars, where the fuel engine is replaced by an electric one, but not a lot more changed. However, the concept of the TU München has still to proof that it is usable in reality.

9.2 Climatisation in the *MUTE* car

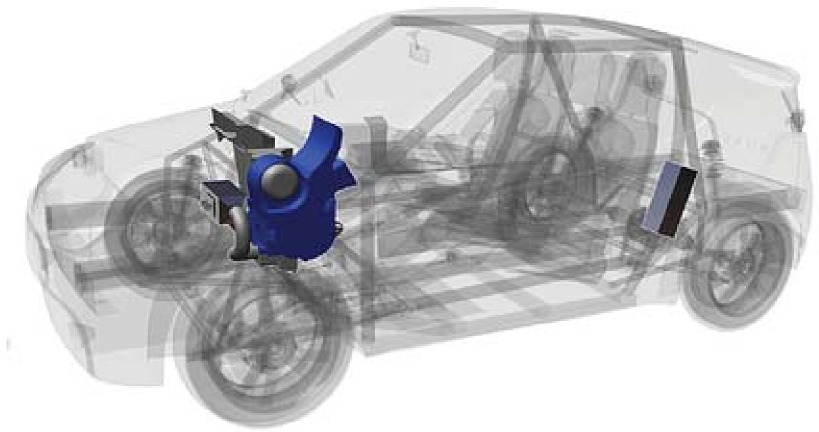

Figure 9.2: The *MUTE* car HVAC-system. [38]

The HVAC-hardware has to be as lightweight as possible since weight is an important factor for the *MUTE* development. Therefore, it was decided to only have basic functionality in the car. The first prototype will not include an air cooling, because of its electric energy demand and weight. For the heating, a bio-ethanol powered air-heater is employed. The preliminary position of the HVAC-unit and the heater in the front of car can be seen in Figure 9.2.

10 Hardware and characteristics of the *MUTE* prototype

The developed climate control concept is realised for the use in the TU München's electric car prototype. The car will be small, low-cost, but implement new ideas, as described in Chapter 9. Therefore, some hardware will not be included due to the budget and/or the weight restriction.

10.1 The car interior

The car is built up upon an aluminium frame with a body made out of carbon fibre laminate. The main parts (roof, floor) consist of two 1.2 mm strong layers with 5 mm air in between. The windscreen and the side windows are made out of 3.85 mm thick laminated safety glass. The rear windows material is approximately 4 mm thick polycarbonate.

A geometrically simplified model (Figure 10.1) has been derived from the CAD data for simulation and parameter estimation purposes. The air volume in the cabin is approximately $2\,\mathrm{m}^3$, the windscreen has a surface of $0.84\,\mathrm{m}^2$. The overall surface of the model is $11.0\,\mathrm{m}^2$, $2.3\,\mathrm{m}^2$ of which are windows.

The thermal conductivity of carbon fibre reinforced plastics (CFRP) depends a lot on the structure of the laminate and the used matrix and fibre materials. Since it will be much higher than the one of the air in between it can be neglected for an estimation, though. For the safety glass, the thermal characteristics of normal glass (found in Appendix A) are assumed. The heat transferbetween the cabin and the ambient air depends on the air speed on the surfaces and the geometry as described in Section 3.1.1. For an existent car measurements could be made finding the coefficients and implement

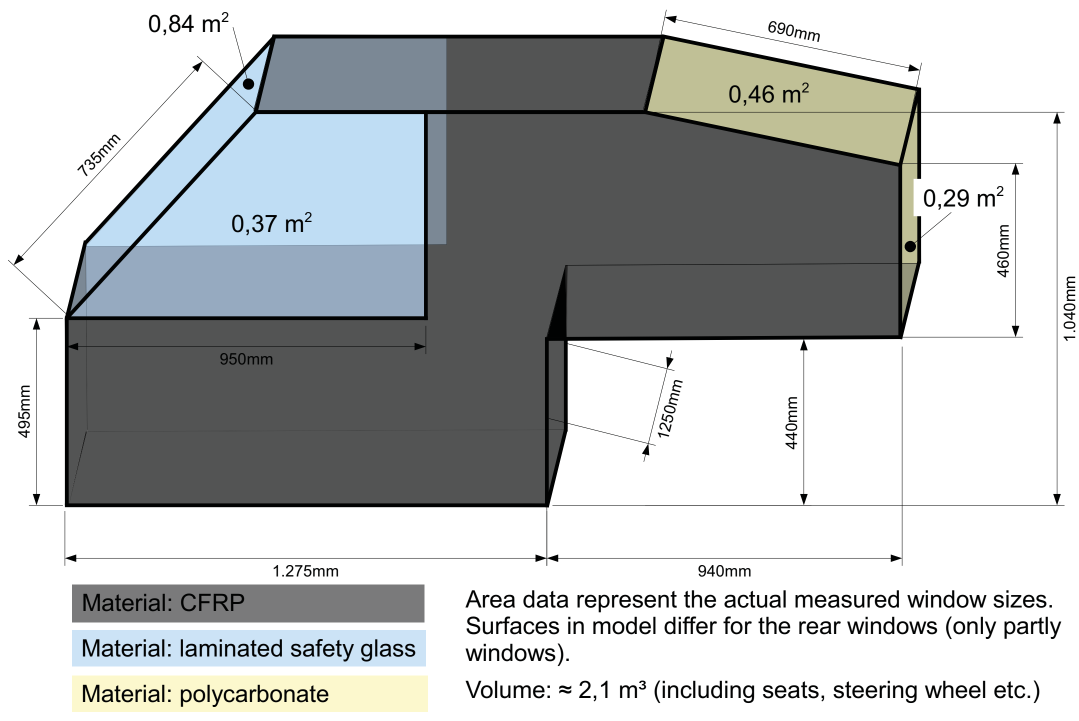
0,84 m²
690mm
0,46 m²
735mm
0,37 m²
0,29 m²
460mm
1.040mm
950mm
495mm
1250mm
440mm
1.275mm
940mm
Material: CFRP
Material: laminated safety glass
Material: polycarbonate
Area data represent the actual measured window sizes. Surfaces in model differ for the rear windows (only partly windows).
Volume: ≈ 2,1 m³ (including seats, steering wheel etc.)

Figure 10.1: A reduced model of the *MUTE* car cabin.

equation 3.3. As this is not possible yet for the *MUTE* car, a standard value [1] is taken and scaled for the car size as proposed.This value of 52 $\frac{\mathrm{W}}{\mathrm{K}}$ is used as a constant and changes have to be considered by the disturbance estimator.

The interior parts are mainly made out of synthetic material. Only a rough estimation can be made since not all the parts are constructed and the materials (at least for the prototype car) are not defined, yet. For the interior part a mass of 25 kg and an average heat capacity of 1.5 $\frac{\mathrm{kJ}}{\mathrm{kg \cdot K}}$ are assumed. Only the surface of these parts interact with the air and has a temperature close to the cabin air temperature. Therefore, the thermal mass is reduced to a replacement value of 100 $\frac{\mathrm{J}}{\mathrm{K}}$.

With the dimensions taken from the CAD-model (seen in Figure 10.1) the following area weighting factors (cf. equation 8.11) were obtained for an average passenger position:

$$\begin{aligned} w_{body} &= 0.365 \\ w_{glass} &= 0.274 \\ w_{interior} &= 0.361 \end{aligned}$$

The defrost air outlets consist of three vents, each has an outlet size of 32 cm^2 and a width (nozzle size d) of 15.6 mm. In addition, two vents towards the side windows with a size of 16.8 cm^2 are supplied by this outlet. There are two foot outlets as well. Their sizes are not required for the system equations, their pressure drop, however, will influence the air flow.

The pressure coefficient on the windscreen (cf. equation 3.11) will be estimated with the help of computational fluid dynamics simulations by the *Institute of Aerodynamics and fluid mechanics* at the TU München. As long as the results are not known a value of 0.75 [15] is assumed.

10.2 The HVAC-unit

The HVAC-unit is taken from a smart-fortwo and is one of the smallest ones available today. It was modified to be able to implement a more sophisticated control and fuel based air heating. A schematic of the air flow in it is shown in Figure 10.2.

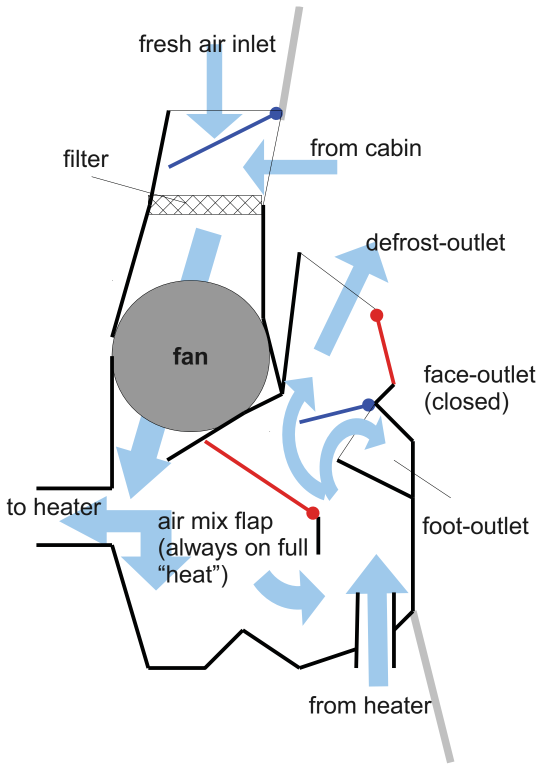

Figure 10.2: Schematic of the modified HVAC-hardware used in the *MUTE* car.

The evaporator and the heat exchanger have been removed. The recirculation flap and the defrost/foot outlet selector flap are equipped with a Johnson Electric 180°-servo motor to permit continuous and independent settings. The other two flaps are fixed and not used. The air mix flap is not needed anymore since the amount of heating is controlled by the external air heater. Face outlets could not be realised because of package collisions in the car. Their opening is closed permanently as well. Therefore, the air speed v_{air} felt by the passengers (see Section 2.2), is estimated by the air from the defrost vents. Its speed is reduced by a factor obtained by equation 3.12 giving 0.3 for a distance to the outlets of two meters.

The air that is heated is drawn right after the fan and blown into what was originally the hot air path. The connection to the heater can be seen in Figure 10.3.

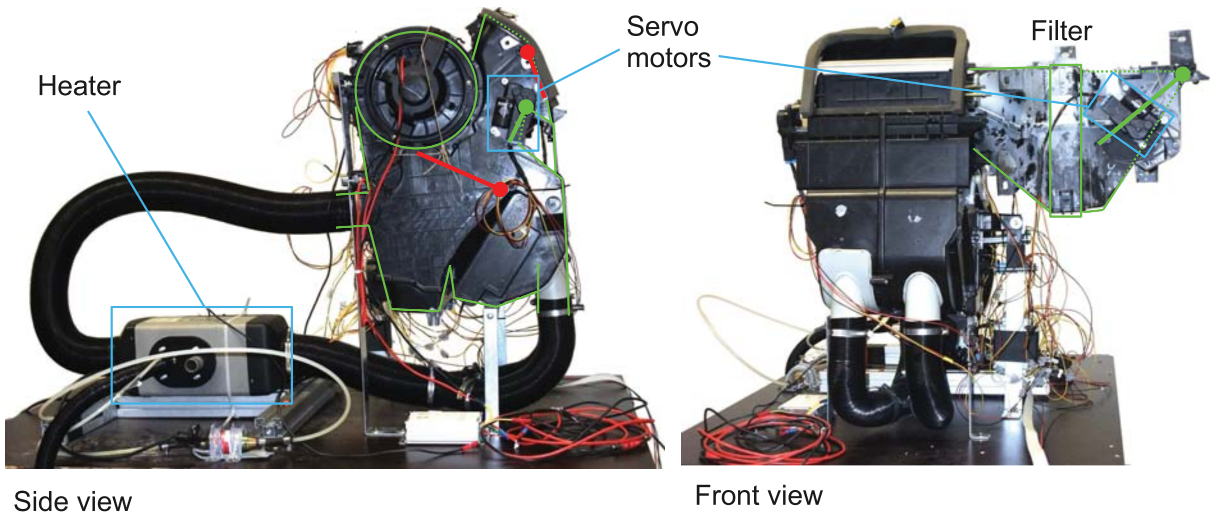

Figure 10.3: The complete HVAC-hardware for the *MUTE* prototype.

The fan motors four steps series resistor control is replaced with a stepless pulse width modulation electronic. For the open-loop control of the air flow, measurements of the fan characteristics are required. The data for the use in the car can only be obtained by measurements including the final air ducts and outlets. For the simulation, preliminary values were obtained by simulating these pressure drops through reduced outlet sizes. These values are shown in Figure 10.4 and have been achieved with the defrost outlet selected and a cover with defined cut-out openings.

The outlet measurements with the 99 cm^2 opening are taken for the simulations

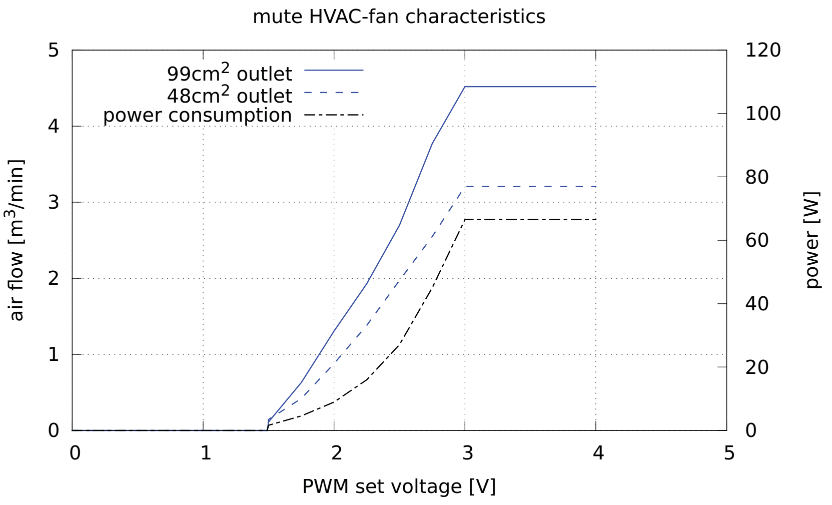

Figure 10.4: Power consumption and air flow of the used HVAC-fan for different outlet sizes.

since they are closest to the real outlet size (found in Section 10.1). This curves do not respect influences by recirculation or car speed. These depend on the geometry and the air flow and could not be obtained so far.

The modified HVAC-unit permits to test partial recirculation and offers a lightweight yet very basic climatisation for the *MUTE* car. However, nowadays' HVAC-components are highly optimised concerning air temperature layering (cf. Section 2.2.2). Therefore, it is likely that the intended temperature distribution (hot to feet and defrost, cooler to face) is not present anymore in the modified air path.

10.3 The heating unit

A Webasto Air Top 2000 ST prototype air heater is used to heat the incoming air. It is fuelled with bio-ethanol and has its own integrated fan (see Figure 10.5). Normally these units are used to heat up caravans, boats or small cabins [39].

The electric power consumption is given as 14 - 29 W (see Table 10.1). This is, however, only valid as long as the glow plug is not active. When starting, it draws a power up to 100 Watt over a period of around 160 seconds. When stopped the glow plug is also used to burn remaining fuel in the combustion chamber for approximately 34 seconds.

The manufacturer was not able to provide the necessary information and material

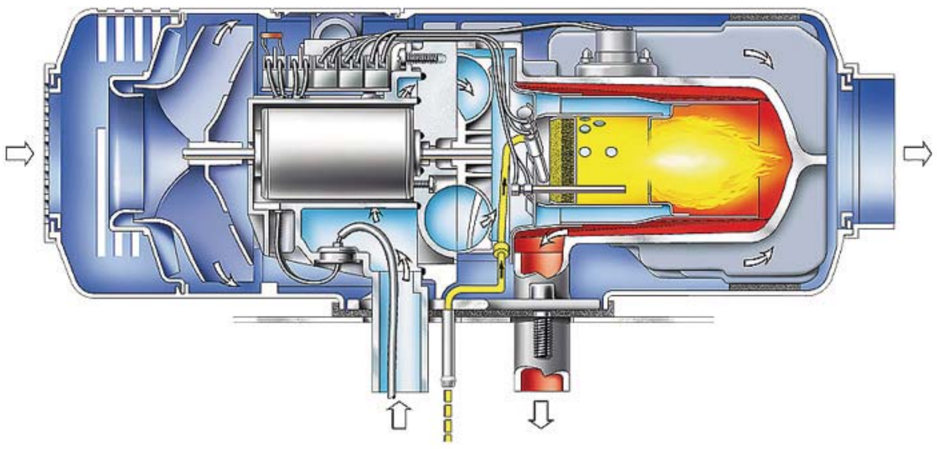

Figure 10.5: The Webasto Air Top 2000 ST functioning. [39]

to directly control the heating power. Therefore, the temperature control had to be realised by the heater integrated control. The control range of the system originally was +5 to +35 ℃ as seen in Table 10.1. By modifying the external temperature sensor with an 3.9 kΩ resistor, a suitable range for a car climate control of +10 to +58 degrees Celsius were obtained. In this way, the desired temperature of the air coming into the cabin is given as set-value for the heater control which is then controlling the heating power with the help of its own (modified) sensor.

Table 10.1: Technical specifications of the Webasto Air Top 2000 ST B. [39]

Heating performance (kW)	1.0 - 2.0 kW
Fuels	Gasoline (Bio-ethanol for the prototype)
Fuel consumption (kg/h)	0.1 ... 0.2 (0.14 ... 0.27 l/h)
Nominal power consumption (W)	14 ... 29 W
Heating flow rate (m^3/h)	93 (towards 0.5 mbar)
Control range for cabin temperature (℃)	+5 ... +35 (modified to +10 ... +58)
Measurements L x W x H (mm)	311 x 120 x 121
Weight (kg)	2.6

This air heating is lighter and slightly more efficient [2] than a water-heat exchanger solution, but it takes more space since the heater is not integrated into the HVAC-unit (see Figure 10.3). Another drawback is the slow control which is caused by the detour over the internal control of the heater, which is not suited for this application. However, a proof-of-concept will be possible with the available components, but a production vehicle will need a new developed design.

10.4 The sensors

The temperature is measured at five positions. The heater inlet and outlet temperature is captured in the HVAC-system in order to be able to detect a heater fault. The air temperature at the outlet to the cabin is needed for the heater control and the cold air prevention system. For fog prediction and prevention, the windscreen temperature is required. Finally, a combination of relative humidity and temperature measurements is applied to determine the state of the cabin and the ambient air. The heater fuel reservoir fill level is also observed by a sensor.

As temperature transducers Analog Devices AD22100 temperature sensors are employed. They cover a range from -50 to +150 ℃ and feature a voltage output that is linearly proportional to the temperature. Both humidity sensors are of the type Honeywell HIH-4000. They use capacitive sensing and give a near linearly voltage output in relation to the relative humidity. There is no solar sensor in the *MUTE* prototype.

Care has to be taken when positioning the sensors. Bad placing can lead to complete useless measurements if the signal is disturbed too much. This would be the case if the cabin temperature sensor is positioned in the flow of one of the air outlets or exposed to direct sun light.

The ambient temperature and air humidity is usually measured behind (or in) the front bumper. The placing of the measurement devices in the cabin is more difficult due to the inhomogeneous climate. Today, the sensors are mostly placed in the control unit in centre console and are often vented by a small fan. In the *MUTE*, a position without direct influence from the outlets that is not exposed to solar radiation and is quite central in the car was found below the mounting for the user interface (see Figure 10.6).

The windscreen temperature sensor has to be attached to the glass. In existing cars it is placed in the rear view mirror fixture or close to it. They all have in common the position at the top of the windscreen since this is the coldest part (neglecting a small area

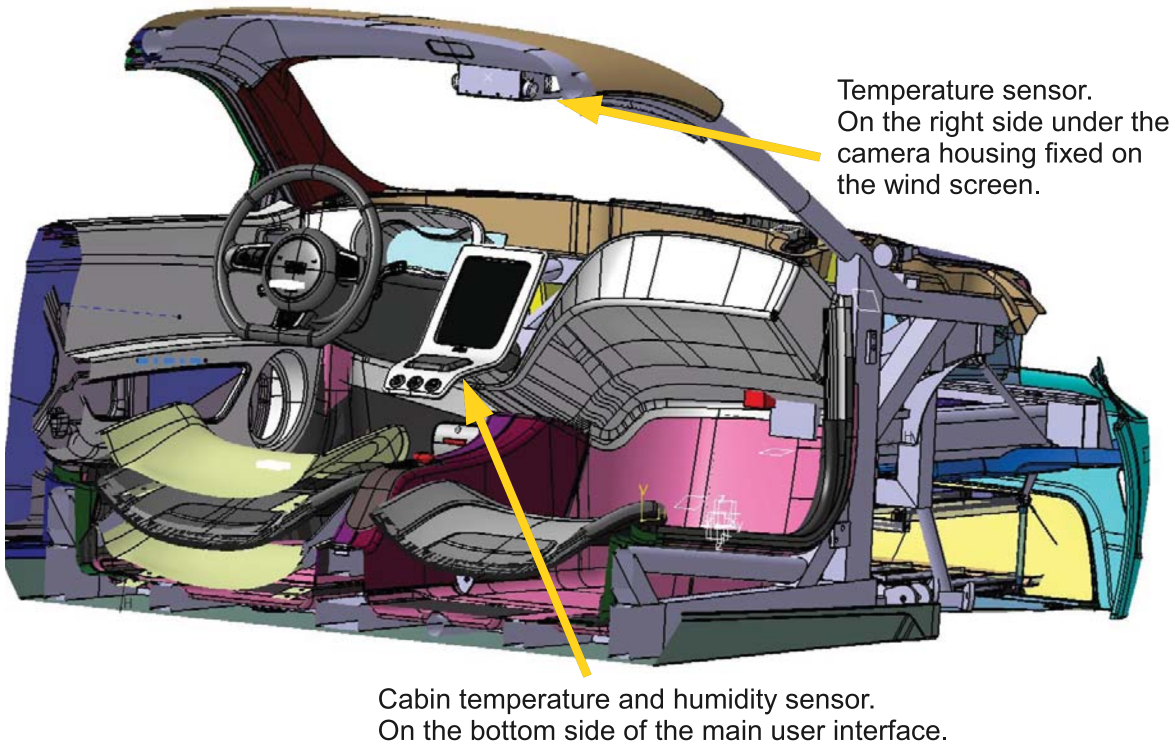
Temperature sensor.
On the right side under the camera housing fixed on the wind screen.
Cabin temperature and humidity sensor.
On the bottom side of the main user interface.

Figure 10.6: The sensor positions in the *MUTE* cabin.

in the bottom corners) and the fogging will start here. An insulation against the (warm) defrost air is necessary for the employed sensor in order to obtain good results. This was shown in experiments (see test results in Figure 10.7). 10.7). Thermal adhesive could be used to attach the sensors on the glass. A position on the right of the box containing the camera for remote controlled driving in the centre of the car in front of the windscreen was chosen in order to affect the drivers view as little as possible (see Figure 10.6).

The sensor values are read through a multiplexer. In this way only on analogue input is occupied, but the sample time for each sensor is reduced by eight (the number of multiplexer inputs).

10.5 Other available information

There is other information available that is useful (or even needed) for the climate control. A power limit and consumption manipulation information is given by the low-voltage sys-

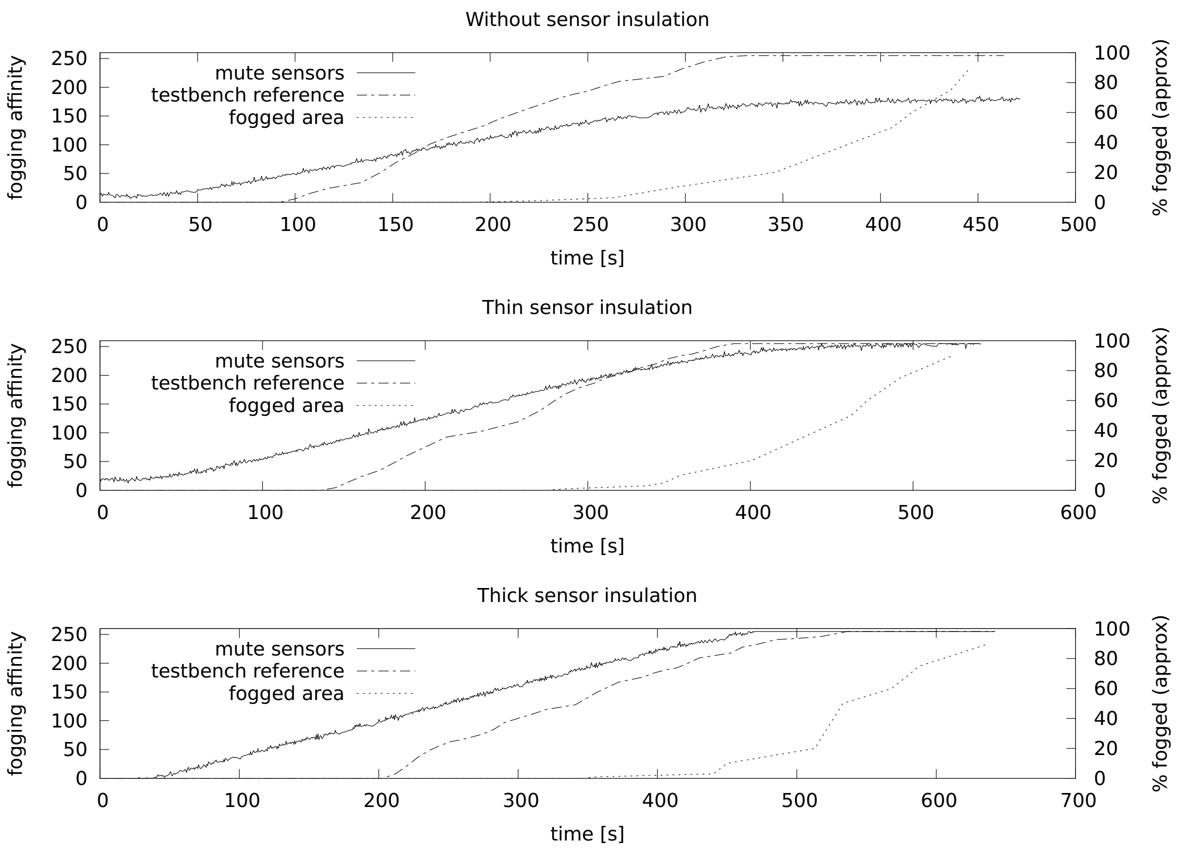

Figure 10.7: Measurements of the fogging affinity (as described in Section 8.1.1) with different sensor insulation on a test bench.

tem control. The signal `HEI_P_sollMaxLeist` contains the maximum electric power that the climatisation may consume. `HEI_rel_Energieverbr` indicates whether saving energy is important at the moment. A special solution for the battery cooling in the *MUTE* car requires knowledge about the air flow there. The air used to cool (or heat up) the battery pack, which is located behind the passenger seats, is taken from the cabin and blown off outside. This requires the HVAC-ventilation to deliver at least as much fresh air into the car as the battery cooling takes out. Otherwise underpressure leading to air coming in elsewhere and a decreased battery air flow would be the consequence. The air flow of the four battery fans can be estimated using their control signal, `KLI_rel_BattKuehlung`, combined with a look-up table. This data however can only be obtained by measurements in the car including the air ducts.

Another signal that is available is `INF_STb_istPersInFzg`. It indicates if there is a person in car. It is used to stop the CO_2 simulation if, for example, the car is remote controlled in order allow more fuel saving recirculation. A list of all available in- and outputs is found in Appendix B.

10.6 The user interface

The user interface will be realised on an Apple iPad 2. The control signals are sent over a wireless network and a car-bus system to the controller. A proposal for the interface with the options defined in Section 8.4 can be seen in Figure 10.8.

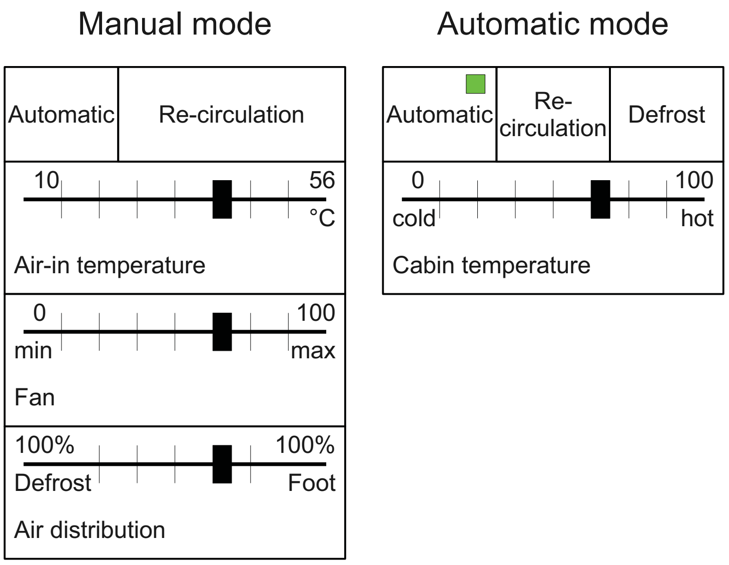

Figure 10.8: A proposal for the user interface.

In the manual mode all the outputs (heater, fan, air distribution) can be directly controlled giving a maximum of control to the user. Only the air recirculation control was for simplicity reduced to the common "yes or no" button. The goal in automatic mode is to have only the necessary options in order to distract as little as possible. Consequently, as the *MUTE* has no means of dehumidification, the humidity adaption is not available (the objective still is implemented). The air speed objective is not available as no direct air flow towards the passenger exists. Only the temperature preference can be set. The defrost mode is available in the automatic mode in order to force the control to bring warm air to the windscreen, for example if the fogging detection fails.

In addition, the precondition mode is realised, used to create a comfortable climate in the car before the passenger starts driving. It can be activated by a signal coming from the remote control.

10.7 Computer and electrics

The climate control software (as well as the other real-time components) was built in Matlab Simulink. In the prototype it will run on a dSpace MicroAutoBox 1401. This platform for in-vehicle function prototyping offers interfaces to all major automotive bus systems and digital as well as analogue in- and outputs. It integrates an IBM PPC 750FX processor running at a frequency of 800 MHz. The main memory is 8 megabytes and the nonvolatile flash memory 16 megabytes big.

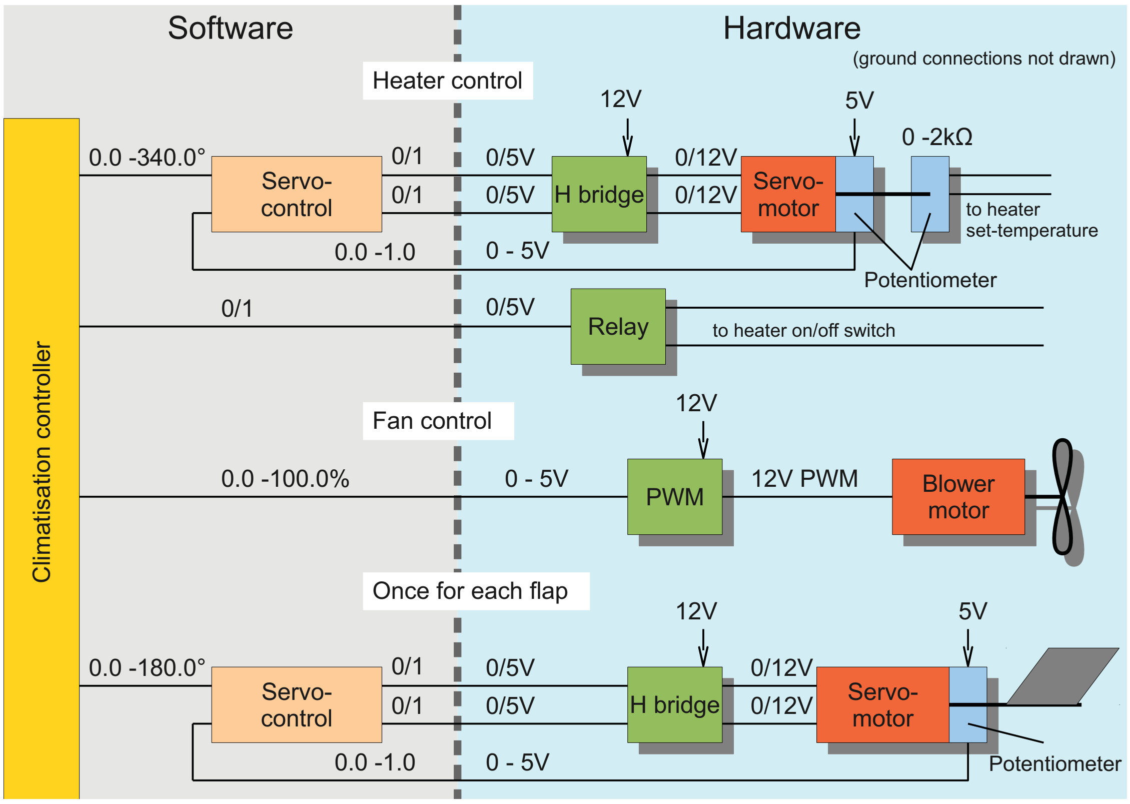

Figure 10.9: Overview of the output interface and its hard- and software components.

In Figure 10.9, an overview of the output interface with the involved software and electric components is shown. The servo motors driving the flaps and the potentiometer setting the set-temperature for the heater require another small controller. It takes the set-angle value from the climate control and outputs the logical signals “turn clockwise” and “turn counterclockwise”. These are fed to H bridges[1], which power the motors which are running on 12 Volt. The main fan is driven by a 12 V PWM signal whose active cycle is given by an analogue output. The servo motor - potentiometer combination for the heater control might be replaced with a digital potentiometer integrated circuit.

10.8 Parameterisation for the *MUTE* car

Some parameters related to the *MUTE* car could only be estimated since the car is not built, yet. They have to be measured and adapted once a prototype exists in order to achieve the best control.

The heat transfer can be measured by testing how much heating power is required to keep the car’s interior at a constant temperature. A better estimation of the heat capacity of the interior parts (seats etc.) built into the prototype a can be done.

The fan characteristics in the system with all ducts and outlets attached has to be measured and the curve (shown in Figure 10.4) has to be adapted. Moreover, the relationships between the flap opening angles and the air mass flow percentage passing it have to be quantified with the ducts attached (cf. Section 3.2.5). All other air flow related values in the objectives could be corrected as well. The air speed on the windscreen (equation 3.11 and the air speed towards the passengers (cf. Section 10.2) can be adapted to measurement data.

One important relationship to find is the one between the battery cooling air flow and its PWM-set value (see Section 10.5). The heater potentiometer angle to set-temperature will also need calibration.

[1]A semiconductor device used for motor control.

11 Matlab implementation

The climate controller is integrated into the Matlab Simulink model for the *MUTE* car control. All time critical tasks like the driving functionality are done in this program running on the dSpace MicroAutoBox. The in- and output specifications for the climate control block can be seen in Appendix B.

11.1 Model structure

The sensor input values will first enter a block called *input validator* (in Figure 11.1 yellow on the left side). The containing routines check, if the data is within the sensor limitations and if the servo motors are working. The scaling of the values into the later assumed ranges and unit conversion are done as well. The servo motor positions are transferred into percent of air flow trough them. The absolute humidity of the cabin and the ambient air is calculated. Found errors and the sensor values (or replacements) are the output.

The model has three working modes: Automatic, manual and off. A logic (grey block on the left in Figure 11.1) decides which one of them is active. Disabling not used mode-blocks is done to safe computing time. The second grey block uses these activation signals to forward the desired control signal to the output. If the controller is switched off (at start-up or during shut-down) the *off-settings* (cyan, at the bottom) are activated. Fan and heater are turned off and the air inlet flap brought to the full recirculation position. The *automatic control* in the upper cyan block becomes active if the controller is switched on and the automatic or the precondition mode is chosen. Its structure will be described in Section 11.2. The activation of the *manual mode* permits the user to directly control the output temperature and air flow as well as the outlet (foot/defrost).

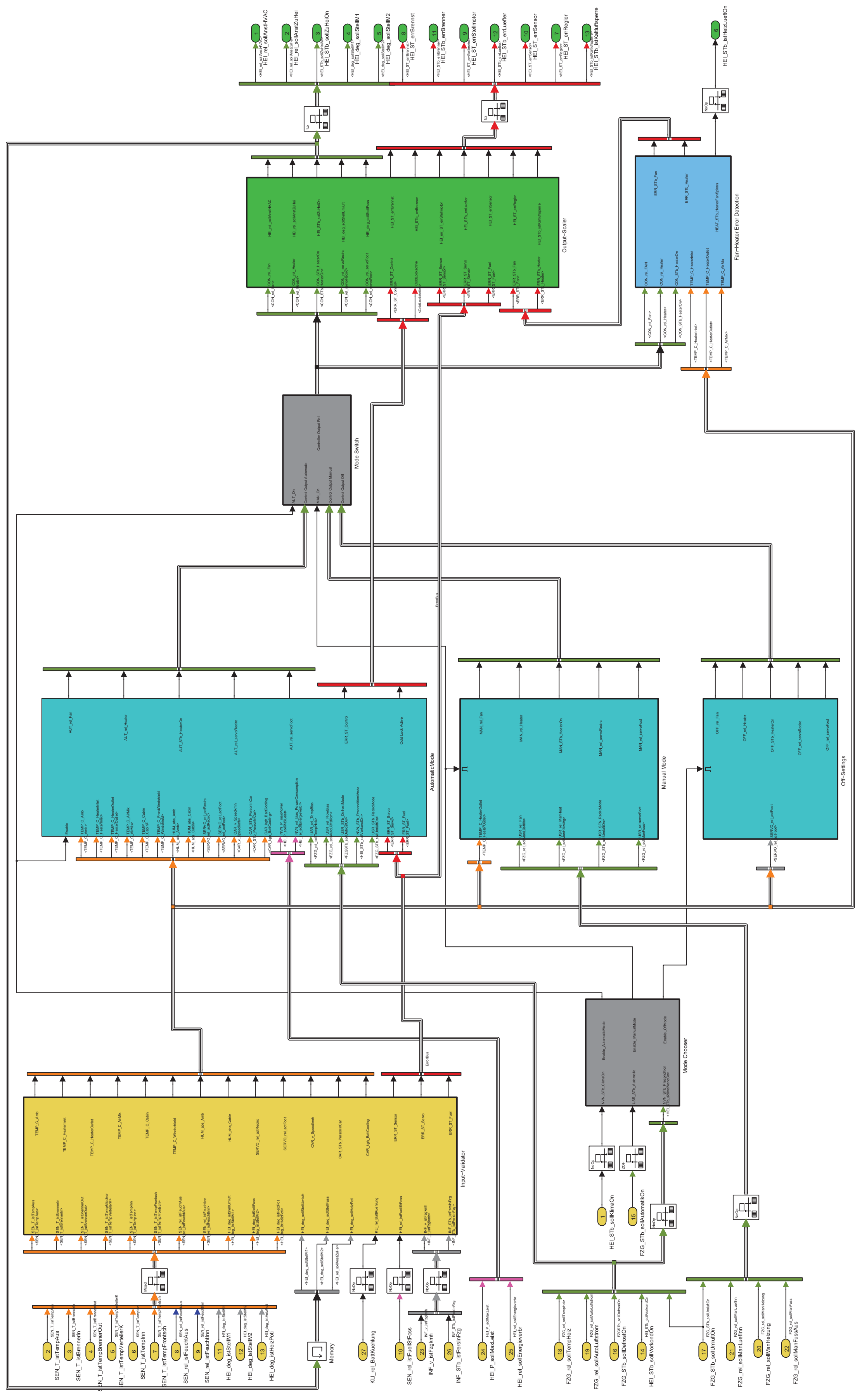

Figure 11.1: The controller overview in Matlab Simulink.

Only recirculation can only be switched on or off. The manual mode is implemented in the middle cyan block.

The *output scaler* in the green block on the right brings the control signals to the dimensions required by the output definitions. The flap opening and heater set-temperature in percent are scaled to a servo angle. Moreover, the fan PWM set-value is given in percent and scaled to the required voltage output with the needed offset (cf. Figure 10.4). Another task is to intervene if errors occur. If the heater fails, the output is set to zero to prevent further damage. Severe automatic control errors lead to a fail-save default setting.

The last block drawn in blue on the bottom right in Figure 11.1 is the *heater and fan error detection*. Temperature sensors are used to detect if the air is getting warmer or not to check if the heater is working, but to discover a fan malfunction is difficult. The only means for this is to detect with the help of the temperature sensors if cool air is mixed to the warm air coming from the heater. Another output generated by this block is the "heater fan spinning"-signal. The heater fan needs to continue to spin for around three minutes after the device has been turned off in order to cool it down. This signal is used to prevent the car control from cutting the power to early.

11.2 Automatic mode

The automatic mode block implements the controller design presented in Chapter 4. The system states are the cabin temperature T_{cab}, and absolute humidity $x_{w,cab}$, the windscreen temperature T_{ws} and the carbon dioxide concentration $x_{CO_2,cab}$. Internally also a power consumption is used which is directly derived from the input air settings. These are - used as design variables - the input air mass flow $\dot{m}_{air,in}$, the air temperature T_{in}, the fraction of the air being recirculated μ_{recirc} and the relative amount going to the foot outlets μ_{foot}. This reduced set is related to the hardware used in the *MUTE* car. No cooling, as stated in Section 9.2, and thus no active influence on the air humidity is possible. Moreover, no face outlets are available (cf. Section 10.2).

The disturbance estimator, presented in Chapter 5, predicts model errors and simulates not measured system states. It is implemented in the two light blue blocks on the

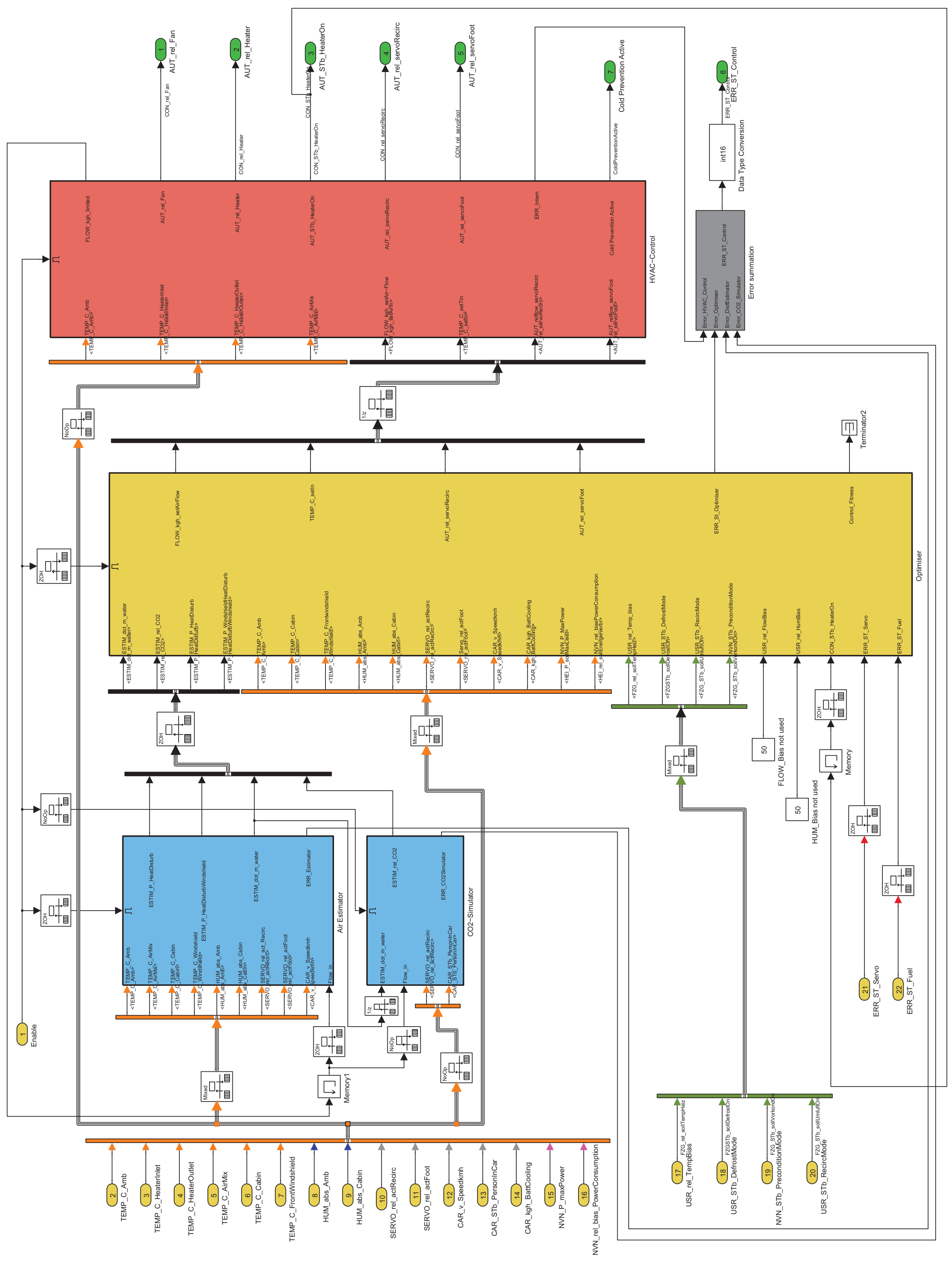

Figure 11.2: The automatic control implementation in Matlab Simulink.

left in the Simulink model shown in Figure 11.2. The upper one estimates the model errors for the cabin humidity and temperature as well as for the windscreen temperature. The lower one contains a simulation of the carbon dioxide concentration in the cabin air as no sensor is available.

The yellow block in the middle is the core of the controller, the optimiser. It includes a general implementation of the IMEA-algorithm presented in Chapter 6. The cabin system is coded into a function as well as each objective. The used system parameters are recapitulated in a table in Appendix C.1. The set of objectives presented in Chapter 8 is reduced by the ones not applicable. The humidity minimum cannot be changed. No air flow is directed towards the passengers as well. On the other hand, a battery air flow constraint described in Section 10.5 is added. An overview of the objectives and the used (standard) priorities, weights and limits are found in Appendix C.2. The design variables related and general controller settings can be found there, too. Some objective parameters (e.g. the power consumption weight) and design variables boundaries are adapted online to the environment conditions and user or system settings, as described in the Sections 8.4 and 8.2.

Finally, the set-point values for the inlet air are translated into control output values in the rightmost, red block. Here, no closed-loop control is involved since the fuel heater is not suited for this use (see Section 10.3). With look-up tables the physical values are translated into a percentage of fan PWM, heater set-point and flap opening angle outputs. A cold air prevention mechanism, as explained in Section 7.5, is implemented. The desired output air mass flow is fed back to the simulator since no measured information about this value is available. The status of the heater (on/off) is fed back to the power estimation in the controller's system simulation, which then can tell whether the glow plug needs to be activated.

Warnings are generated by the blocks if an estimation limitation was reached or a *panic* (exceeded objective limit) occurred in the controller. An error signal is indicated if the control is not able to allocate the required memory. These signals are joined into one number and output as the controller error signal.

11.3 Programming

The controller layout is completely done in Simulink's graphical programming. The disturbance estimator and the optimiser, as the most complicated parts, are entirely written in C-code.

The optimiser code is distributed over five files in order to increase the readability and re-usability. A chart showing this structure, the containing functions and the dependencies is found in Figure 11.3.

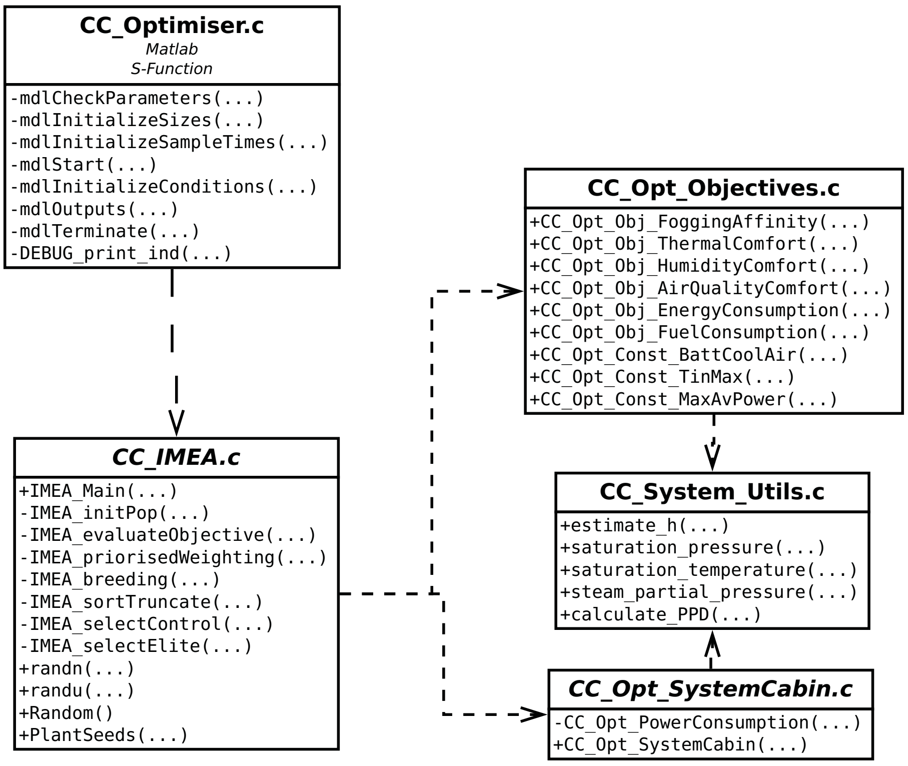
CC_Optimiser.c
Matlab
S-Function
-mdlCheckParameters(...)
-mdlInitializeSizes(...)
-mdlInitializeSampleTimes(...)
-mdlStart(...)
-mdlInitializeConditions(...)
-mdlOutputs(...)
-mdlTerminate(...)
-DEBUG_print_ind(...)
CC_Opt_Objectives.c
+CC_Opt_Obj_FoggingAffinity(...)
+CC_Opt_Obj_ThermalComfort(...)
+CC_Opt_Obj_HumidityComfort(...)
+CC_Opt_Obj_AirQualityComfort(...)
+CC_Opt_Obj_EnergyConsumption(...)
+CC_Opt_Obj_FuelConsumption(...)
+CC_Opt_Const_BattCoolAir(...)
+CC_Opt_Const_TinMax(...)
+CC_Opt_Const_MaxAvPower(...)
CC_IMEA.c
+IMEA_Main(...)
-IMEA_initPop(...)
-IMEA_evaluateObjective(...)
-IMEA_priorisedWeighting(...)
-IMEA_breeding(...)
-IMEA_sortTruncate(...)
-IMEA_selectControl(...)
-IMEA_selectElite(...)
+randn(...)
+randu(...)
+Random()
+PlantSeeds(...)
CC_System_Utils.c
+estimate_h(...)
+saturation_pressure(...)
+saturation_temperature(...)
+steam_partial_pressure(...)
+calculate_PPD(...)
CC_Opt_SystemCabin.c
-CC_Opt_PowerConsumption(...)
+CC_Opt_SystemCabin(...)

Figure 11.3: The structure and dependencies of the optimiser C-code.

The *IMEA* optimiser code was kept as general as possible to be able to use it without much effort in other projects or even for other purposes. Its main function is called by a Matlab S-function which can, due to its special structure and containing functions, be integrated with a block into Simulink models. This file prepares the input values for the optimiser, adapts the limits and parameters and hands them through pointers onto special structures to the optimiser. The objective function and the system simulation are given by function pointers. This allows easy integration of additional objectives or different system simulations. The objective and system functions are called by the `IMEA_evaluateObjective` function. The data structures and the complete code of the optimiser is found in Appendix E.

The disturbance estimator is integrated directly into one S-function. The carbon dioxide concentration simulation is programmed graphically in Simulink since it only contains standard elements, which allows a faster execution.

11.4 Real-time requirements

Matlab Simulink is mainly designed as a simulation tool. However, with special in- and output blocks the models can be compiled with a tool called *Real-Time Workshop* and used on micro-controllers and other targets. This allow fast testing and implementations for prototypes.

The model built for the *MUTE* car has a sample time of 0.01 seconds. Running all subsystems at this speed would most certainly lead to overruns, i.e. longer calculation times than one sample. Sensor signals are read at a slower speed. Therefore, a suitable sample time has to be found for each system. These can be assigned to every subsystem marked as “atomic” as well as to external S-functions.

For the climate controller a general sample time of 0.1 second was chosen. Input values are updated at this frequency via the CAN bus. The optimiser does not need to run that often. Since the timescale of the cabin-system is in the range of several seconds (see Section 3.1.5), a sample time of two seconds was chosen. The speed for the disturbance estimator is also set independently. Here, one second was chosen in order to run slower than the rest but include all new values that are coming from the multiplexer every 0.8 seconds. To connect these systems running at different speeds, rate transition blocks are needed. They assure the data transfer by providing zero-order-hold or a delay functionality depending on the sample time difference.

12 Controller evaluation

Even though the *MUTE* car prototype will not be ready before autumn 2011, some testing was done with the help of simulations. In this way, the functioning of the controller in combination with the available hardware is shown.

12.1 Hardware-in-the-loop test

The leading institute for the *MUTE* development, the *Lehrstuhl für Fahrzeugtechnik München* has built up a hardware-in-the-loop test rig. A special computer simulates the car and some sensors. This simulation is communicating over CAN-busses[1] with the MicroAutoBox car computer (described in Section 10.7). The actuator and sensor hardware is directly connected to this box. With this configuration, the interaction of electrics, hardware control software and the (simulated) car can already be tested. A schematic drawing of the test rig (showing only the relevant hardware components for the climatisation) is found in Figure 12.1.

In this way, tests of the HVAC-unit and first parameterisations were done. One very important result is the execution time of the optimiser algorithm. Its turnaround time was measured to be 0.0018 seconds (in the automatic mode). This equals a processor load of 0.09% with the sample time of two seconds. The disturbance estimator also showed a very short turnaround time of 0.00030 seconds. The remaining control parts are included in a "0.1 s"-task because have the same sample time as other blocks in the MUTE software and can therefore not be regarded separately. This task showed a turnaround time of 0.00028 seconds. As the turnaround times are very low, they showed to be dependent on the overall system sample time. This is set to 10 milliseconds.

[1]Controller-area-network, a standard bus in vehicles.

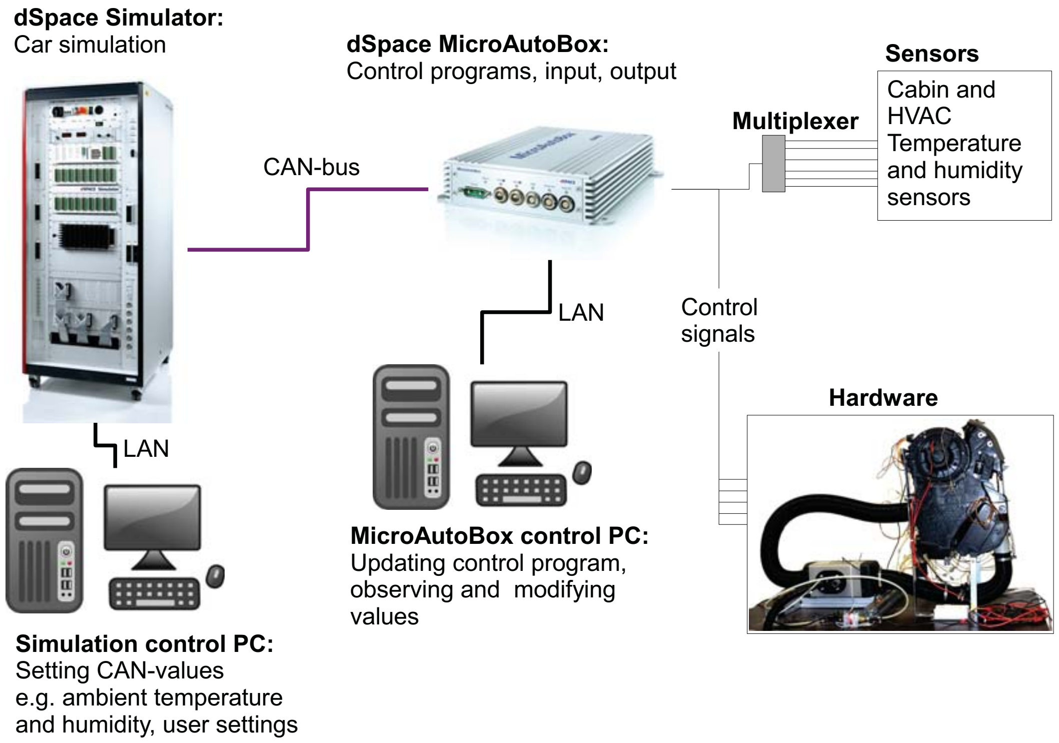
dSpace Simulator:
Car simulation
dSpace MicroAutoBox:
Control programs, input, output
Sensors
Cabin and HVAC Temperature and humidity sensors
Multiplexer
CAN-bus
LAN
LAN
Control signals
Hardware
MicroAutoBox control PC:
Updating control program, observing and modifying values
Simulation control PC:
Setting CAN-values
e.g. ambient temperature and humidity, user settings

Figure 12.1: Overview of the hardware-in-the-loop test rig for the climatisation.

All required and planned software as driving dynamics calculations are not implemented so far. Therefore, no information about the overall load of the computer can be given. However, he results show that the developed control algorithm is fast enough and suitable for the computational power that is available in a car.

12.2 Optimiser performance evaluation

It is important for the optimiser algorithm to find good solutions fast enough to be able to compensate for changes that occur in the temperature or other measurement values. This can be tested in a simulation.

A static example is created where all temperatures and other inputs are constant. Now, the optimiser results of each sample are compared to the true optimum. In this way it is seen, if the optimisation process is fast enough. To compare the solutions, their fitness is used. This is calculated by the weighted sum of the objective results. A small fitness difference does not necessarily mean that the solutions are close, but it is usually a good indication for it.

The sensor inputs and other settings are taken from the *Heat-Up* simulation test case, presented later in this chapter in Section 12.4. All estimated values are set to zero. The optimum has been found by a long-time simulation[2]. After 100 seconds, the ambient temperature is lowered by 5 degrees to show how the optimiser reacts a (sudden) change.

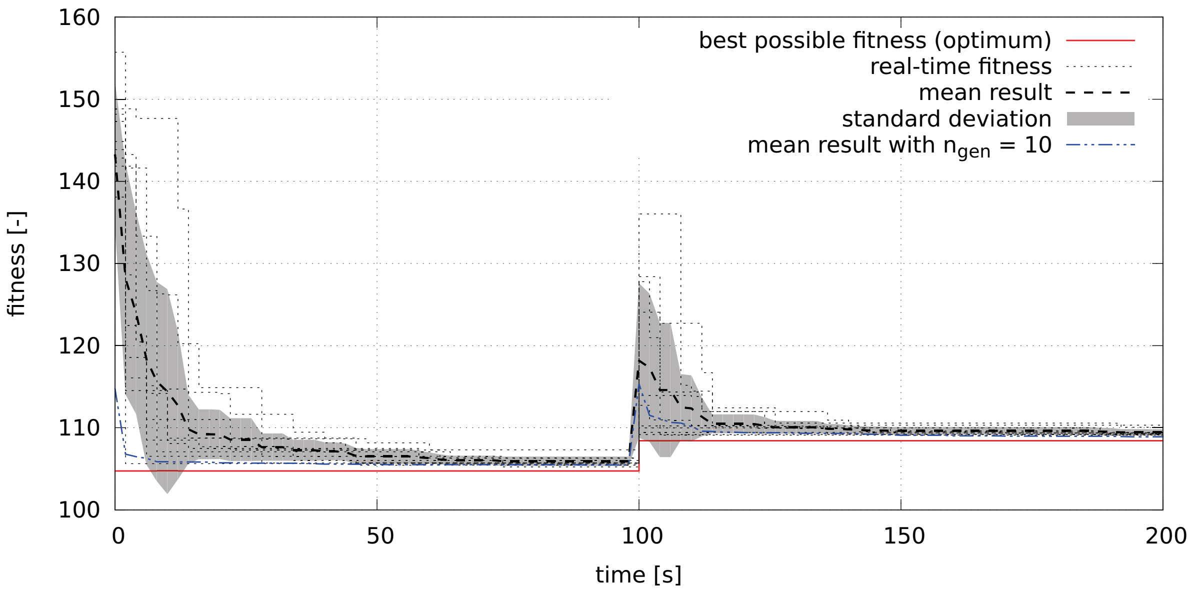

Figure 12.2: Convergence plot of optimisation runs with a static problem.

The result of 10 test-runs is shown in Figure 12.2. The stochastic nature of the evolutionary algorithm is seen by the fact that all solutions are different. Therefore, the mean value and the standard deviation are introduced to show the average algorithm results. The fitness of the best possible solution changes with the environment as it can be observed at the change of the ambient temperature.

The optimum is not reached by any of the lines, but all of the results converge to it. This happens quite fast in the beginning. After 10 seconds (5 optimiser runs) the mean only is 10 points away from the best possible fitness. This equals approximately 4% of the worst possible score $\phi_{max} = 255$.

After the sudden change at $t = 100\,\text{s}$, the peak is even smaller and 10 seconds later the mean only is 4 points away from the optimum. This small difference will usually not

[2]The optimiser will always converge to the optimum, if one can be found, after an infinite time due to its heuristic nature.

be noticed by the passenger.

The results show that the optimiser algorithm is able to come close to the optimum in 10-20 seconds in the beginning. Even a sudden and comparable big change of 5 degrees Celsius is tracked quite fast. Other conditions (different temperatures and settings) showed comparable results. This proofs that the developed algorithm is suitable for the car climate control task.

The population size was set to 10, the number of children was 20 and 2 generations were simulated per run, which has a sample time of 2 seconds. A faster convergence can be achieved with higher values, but it requires more resources. The effect of an evaluation of 10 generations is also shown in Figure 12.2. However, these better results are only obtained with a more than five times higher computational effort (cf. Section 8.6.2).

One has to keep in mind that the results above have been obtained without any parameter optimisation. The adaptive concept, which includes the base population and the random immigrants, is a trade-off between the ability to track a changing environment and convergence speed which can be adjusted, for example by changing the number of elite individuals. Even faster reactions may be achieved by adapting the number of generations, children and the population size to fully use the available computing power.

12.3 Simulation test layout

The ability of the complete controller to reach the objectives that it was designed for is examined in a computer based simulation using Matlab Simulink. Four models are used for this purpose. The first is the controller, presented in Chapter 11. The same program as in the car is used, which is possible through its design in Matlab Simulink. It is the big yellow block on the left side in the simulation model shown in Figure 12.3.

The input values to the control block are filtered by a sensor simulation (orange, to the left of the controller). Here, the approximated characteristics from the data sheet are implemented for each sensor. The temperature sensors are quite slowly reacting and have a noise in the magnitude up to one degree Celsius. The humidity sensors are faster and also have lower noise.

The outputs of the controller are fed into a model of the HVAC-unit electrics and hardware, which is seen in the cyan block in the middle of Figure 12.3. It simulates the heating, ventilation and air distribution in a simplified way. The equations and relationships are found in Sections 3.2 and 10.2. In addition, rate limitations and slow systems are introduced to model the inertia of the components. The heater model does not fully cover the complex heater behaviour. Heating and especially the temperature control will most likely differ from the simulation results.

To close the control loop, a car interior model of the *MUTE* car, made by Manuel Lorenz and based on the simplified geometry seen in Section 10.1, is taken. It simulates the air properties in the car cabin with influences of solar radiation, vehicle movement, passengers, ambient temperatures and humidity, and, of course, the HVAC-system input. The effect of direct (defrost) air flow on the windscreen is not included in the model.

Finally, a passenger simulation (magenta, on the right side) generates the comfort figures for the cabin climate. The human emission data to the cabin air are generated here as well. Additional blocks (in grey) that are found in the upper left corner of Figure 12.3 contain the "settings". The small green model below the HVAC-hardware simulation is the power estimation block, which gives information about the power consumption to the low-voltage control.

12.4 The test cases

Four test cases were defined to show the performance of the controller. The situations represent extreme conditions for a car climate control in central Europe. They are designed to be as realistic as possible. The chosen values are based on climate data for Munich shown in Figure 12.4.

An extreme winter scenario is taken for a heat-up test. In this case the heating performance can be tested and the use of 20 minutes preconditioning shown. A comparison to a result without the use of recirculation will be done as well.

A cool-down situation is tested to demonstrate the cooling ability. Here, the car was standing in the sun on a summer day. Only a comparison to the same situation with preconditioning is made, since the cooling ability of the HVAC-unit is limited to blowing in ambient air. In this case two persons enter the (preconditioned) car after twenty minutes.

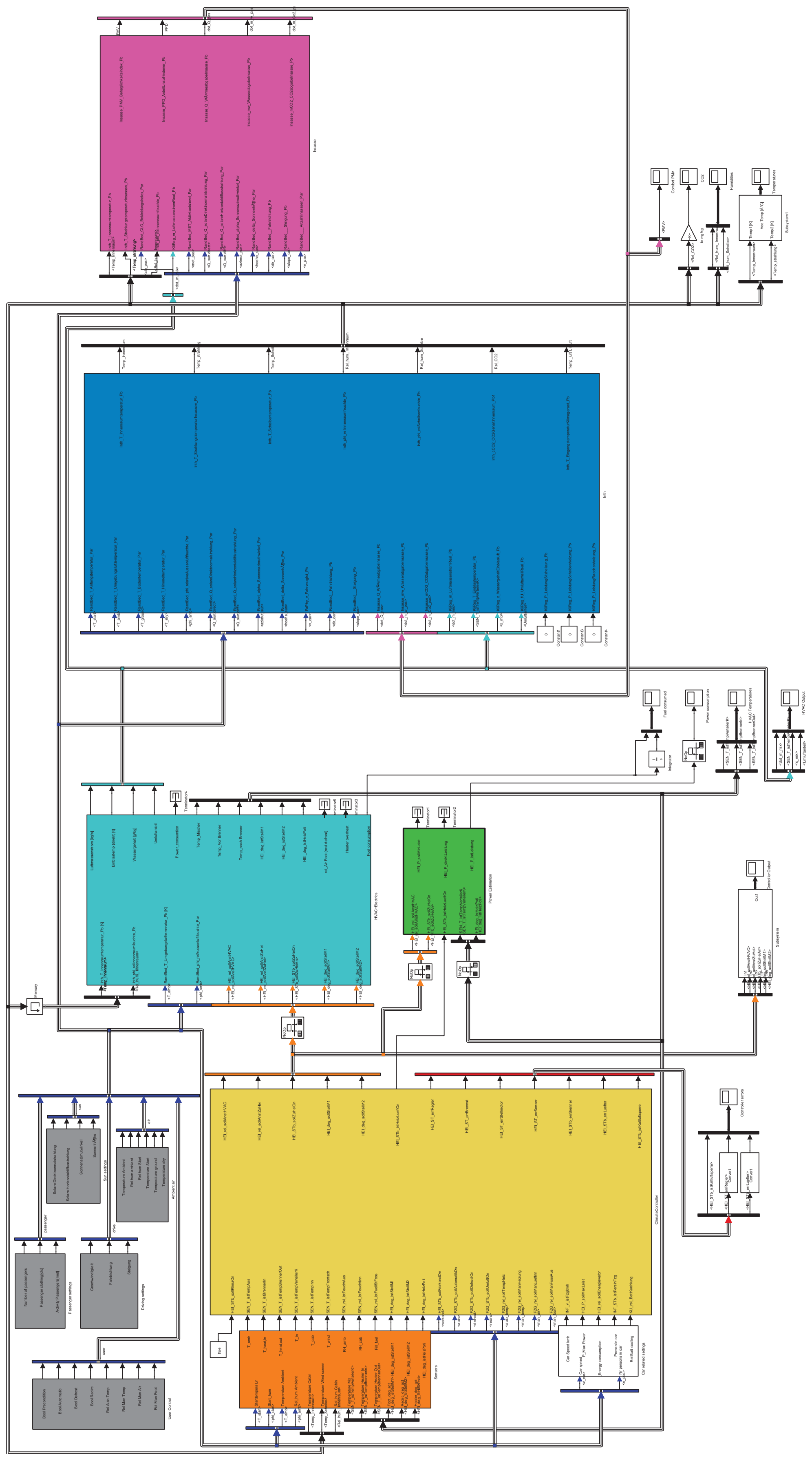

Figure 12.3: The Simulink model for the controller test.

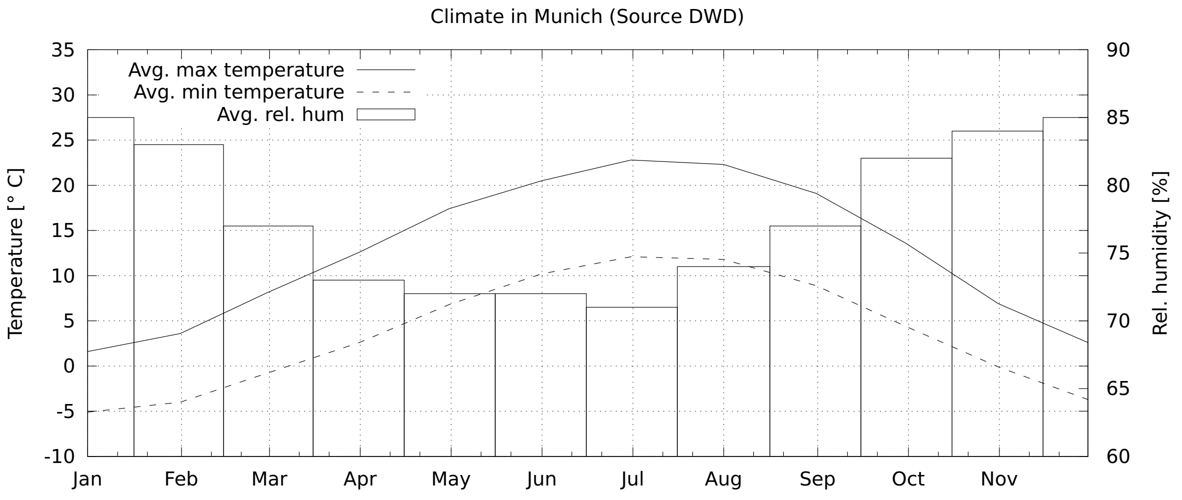

Figure 12.4: Climate data for Munich. (Data source: www.dwd.de)

This will of course not include effects as for example opened doors.

In addition, two more situations are chosen to demonstrate and test controller abilities. One is the fogging prevention. This feature is especially important when the ambient air humidity is high for example when it rains. One problem in this situation is that no means of dehumidification is available. The fourth test case was made for testing the heater management, when the temperature is on the limit to requiring heating. This, however, will probably not produce very reliable results as the heater internal control behaviour could only be approximated. An overview of the ambient air settings and the starting values are found in Table 12.1. A detailed list of all used settings is given in Appendix C.5.

The other conditions for the simulation are chosen as follows: The standard pressure is taken for relative to absolute air humidity conversion. Two (standard) passengers are sitting in the car; only in the precondition mode no person is in the cabin. Their activity level is in all cases 1.2 met, which equals light sedentary work [7]. The clothing is adapted to the season, but less than defined in the controller settings in Section 8.1.2 in order to see the effects of this option. A time span of 45 minutes is simulated.

Table 12.1: The conditions and starting values for the simulation test cases.

	Heat-up	Cool-down	Rainy autumn	Transition period
Test goal	Heating performance, energy savings	Cooling performance	Fogging prevention	Heating management
T_{amb}	-10 ℃	30 ℃	10 ℃	15 ℃
φ_{amb}	80%	70% (18.7 $\frac{\text{g}}{\text{kg}}$)	100%	80%
$T_{cab}(t=0)$	-10 ℃	50 ℃	20 ℃	15 ℃
$T_{ws}(t=0)$	-10 ℃	50 ℃	20 ℃	15 ℃
$x_{w,cab}(t=0)$	$x_{w,amb}$	$x_{w,amb}$	$x_{w,amb}$	$x_{w,amb}$
$x_{CO_2,cab}(t=0)$	$x_{CO_2,amb}$	$x_{CO_2,amb}$	$x_{CO_2,amb}$	$x_{CO_2,amb}$
v_{car}	0 $\frac{\text{km}}{\text{h}}$	0 $\frac{\text{km}}{\text{h}}$	50 $\frac{\text{km}}{\text{h}}$	50 $\frac{\text{km}}{\text{h}}$
r_{cl}	1.2 clo	0.75 clo	1 clo	1 clo
$\dot{q}_{sun,global}$	50 $\frac{\text{W}}{\text{m}^2}$	900 $\frac{\text{W}}{\text{m}^2}$	100 $\frac{\text{W}}{\text{m}^2}$	500 $\frac{\text{W}}{\text{m}^2}$

12.5 Simulation results

In the heat-up test case the functioning of the controller in extremely cold conditions is tested. The results in Figure 12.5 show that the control is able to keep the safety relevant values in a very good range.

The carbon dioxide concentration is always kept at an acceptable level. The windscreen humidity is also - once defogged - at a very good value of around 30 % which presents no fogging risk. The comfort is mainly driven by the temperature which is slightly cool with around 17 ℃. One cause for this is the difference in clothing (assumed by the controller and actual). Another one could be an error in the parameters used in the calculation of the mean radiant temperature (cf. Section 8.1.2) and the car body heat transfer (Section 10.1). Finally, the compromise between fuel consumption, air quality and comfort leads to a slightly lower temperature than the most comfortable one. It is worth mentioning that personal adaptions can be made to improve this (within the heater capabilities). This is done in another simulation, where the user temperature setting was changed to 75. There, a raise of around 3 ℃ of the cabin temperature is observed. The detailed results can be seen in Appendix D.1.2.

The potential of car preconditioning is shown in Figure 12.5 as well. When the

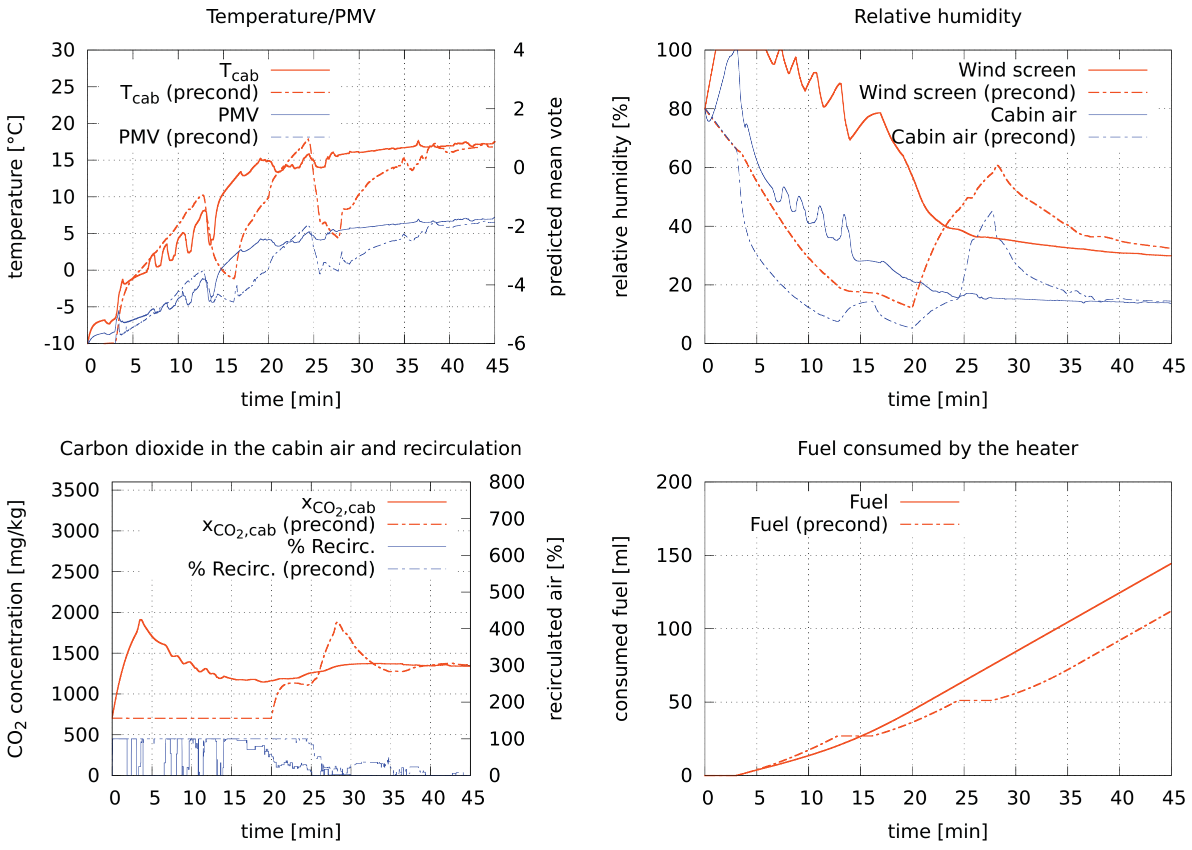

Figure 12.5: Results of the heat-up simulation with and without preconditioning.

passengers enter the car, the cabin is already heated up to around 17 °C. The overall fuel consumption is 32 ml or 22.4 % less due to the recirculation mode used in the first 20 minutes. However, the 20 minutes longer heating during the trip has to be subtracted from this saving. Therefore, this feature is mainly increasing comfort.

The fuel saving of the standard control was obtained by a comparison with a simulation with blocked recirculation. With this limitation 7.5 % or 11 ml more fuel were consumed with the resulting comfort and safety related figures being comparable in the end. The detailed simulation result of this “no-recirculation”-case is found in Appendix D.1.1.

In the results the effects of the slow starting fuel heater are seen. The first 3 minutes not much happens since the heater has not started, yet. In the precondition mode, the heater is shut down twice and requires time to start again (at $t \approx 12$ min and $t \approx 23$ min) because the cabin heats up fast and the heater has a minimum heating power.

In the summer case, fuel saving is no matter. The interesting points here are the achieved comfort and if the precondition mode is useful.

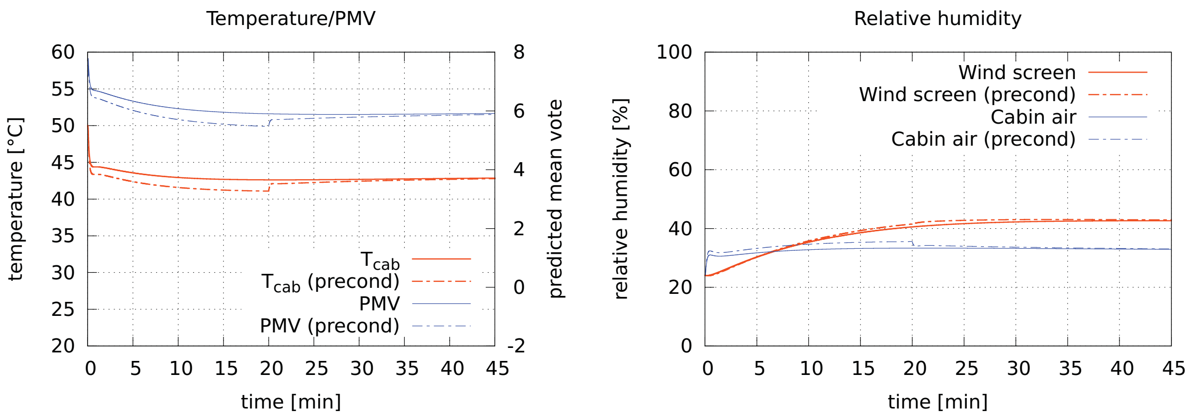

Figure 12.6: Results of the cool-down simulation with and without preconditioning.

The temperature cannot be kept below 43 °C due to the high sun radiation, as seen in Figure 12.6. The car is standing and the cabin has a quite big window share, which leads to this extreme condition. Preconditioning lowers the extreme temperature in the car before the persons enter it and is therefore recommendable. Nevertheless, the attained comfort level is not acceptable, but can, due to the hardware limitations, only be faced by opening the windows. The full results of this simulation are found in Appendix D.2.

A more comfortable functioning of the control can be shown in the case of fogging prevention. This is tested in the case of an ambient humidity at the saturation level, for example when it is raining, and comparable high temperatures.

The controller still keeps the humidity on the windshield at a high, but acceptable level of around 80 – 90 % as seen in Figure 12.7. The comfort would be judged as quite good. The stopping and the starting of the heater can be seen in this simulation twice as well.

The final test case shows the handling of a problematic case for the employed fuel heater and the control. The ambient temperatures are only some degrees Celsius away from a comfortable sensation and therefore the heater, which has a minimum heating power of 1000 Watt, is only required from time to time.

This behaviour of switching can is visible in the results in Figure 12.8. As seen in the fuel consumption chart, the heater is only active the first 21 minutes. After that only

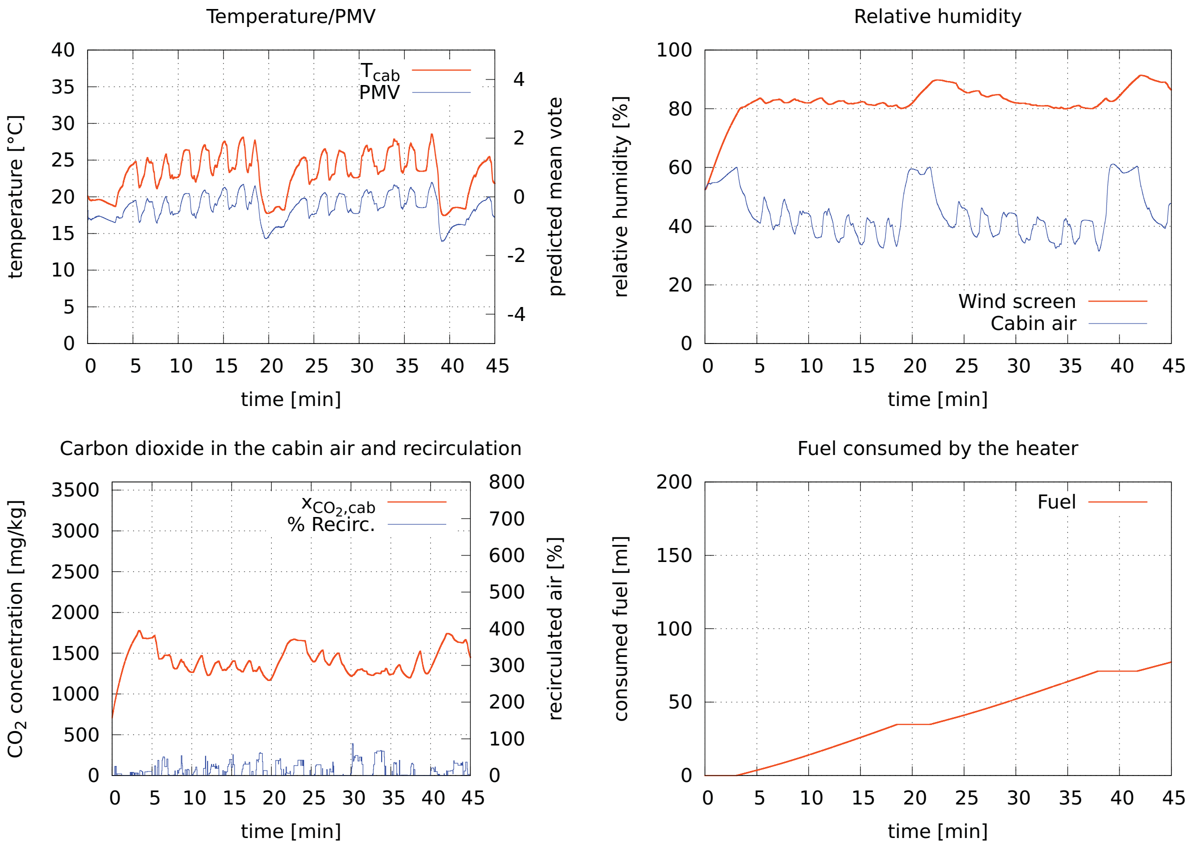

Figure 12.7: Results of the climate control simulation with high ambient air humidity.

little and partially recirculated air is blown into the cabin.

12.6 Stability and robustness

As the controller has its built-in boundaries it gives by definition a bounded output on a bounded input signals (BIBO stability). This reduces the possible instabilities to oscillations.

In the first 15 minutes of the heat-up results four temperature drops can be seen. They are related to windscreen fogging *panics* making the optimiser switch to a replacement output. Only fresh air is heated and blown into the cabin, but does not reach the temperature that is possible with recirculated air.

Slight oscillations are also found in the simulation results for the “rainy autumn” case (Figure 12.7). They are of a quite constant amplitude of 4 °C, which could be acceptable, but is not nice. This is caused by the different speeds of the system actuators.

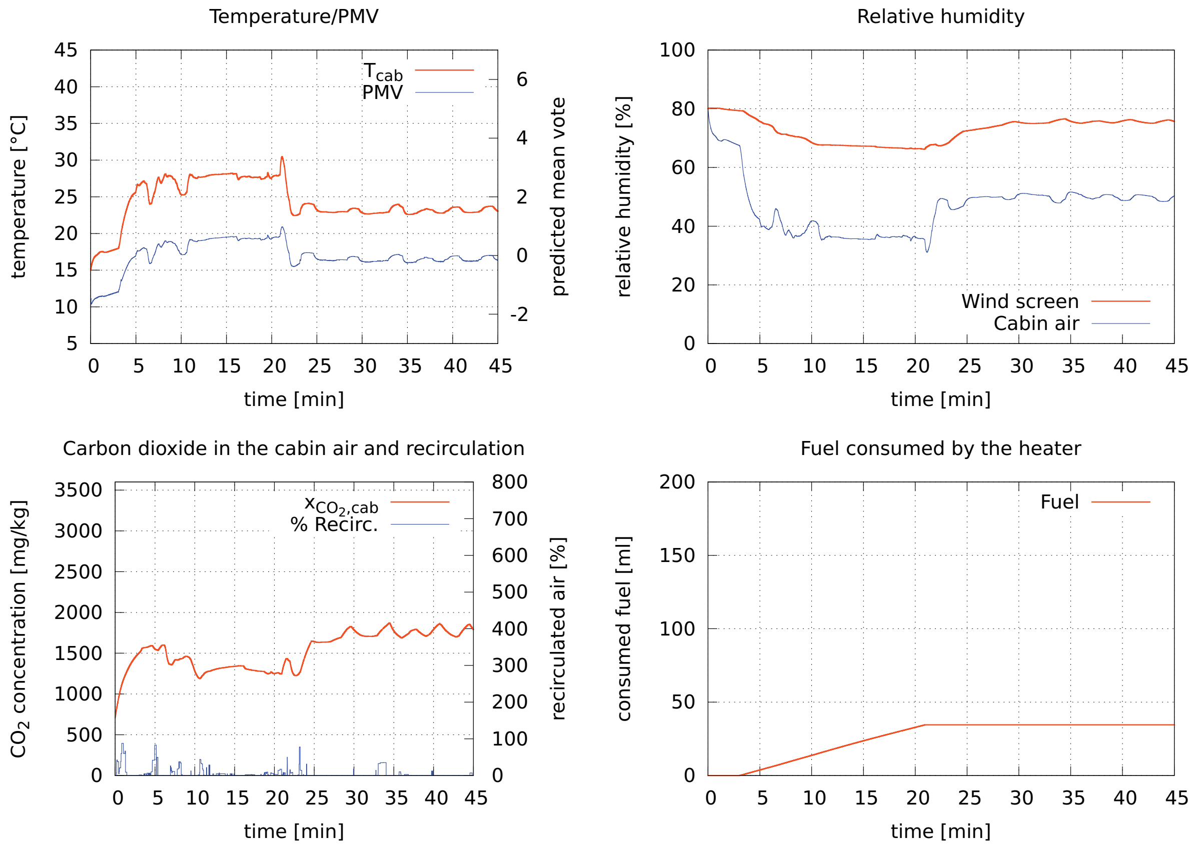

Figure 12.8: Results of the climatisation simulation when only little heating is required.

The recirculation flap position can be changed much faster than the heating power, which is quite slow. How a temperature change relates to an increased recirculation can also be seen in the results of the heat-up test case with adapted temperature in Appendix D.1.2. It is to be seen, if these effects occur in the prototype in the same magnitude and if better parameterisation has an influence. A countermeasure could be to implement the heating inertia in a model in the HVAC-system controller and adapt the amount of recirculated air to the slower heater reaction.

The robustness of the controller is demonstrated by the fact that the results have been achieved with many simplifications and parameter estimations made. User setting or mode changes produce no oscillations as seen in the test cases with precondition (Figures 12.5 and 12.6). A full study of influences of parameter variations still needs to be done.

13 Conclusion

The hardware control is working in the HIL-test rig. The control program showed its suitability for an online application by very short execution times. The evolutionary optimiser algorithm proofed its efficiency and its ability to adapt to changes in a test on a static problem with one switched parameter.

In the simulations the control design has proven that it is able to meet the demands. Energy savings are achieved through (partial) recirculation in a normal usage. Fogging can be prevented, and in extreme conditions the control - limited by the hardware - reacts to the situation. The oscillations that occur in certain situations are always limited.

It can therefore be stated that a viable automatic control for a prototype car has been created.

13.1 Extension for full car air conditioning

In order to add full car air conditioning capability to the implemented controller the air humidity design variable $x_{w,in}$ has to be integrated like in the general description in Chapter 4. All related settings, like the boundaries or the *panic handlers*, need to be extended. In addition, objectives may be required for certain system like the heat pump (see Sections 8.1.7 and 8.2). A power consumption model for the cooling system needs to be integrated into the controller-internal simulation.

Finally, a control mechanism adapted the cooling system has to be included in the HVAC-system control. The result is better control over the cabin air humidity and an increased comfort in hot weather compared to the results in Figure 12.6.

13.2 Possible improvements

At large, more or better information allows better control. Better system models can increase the control accuracy. Inclusion of the interior thermal masses temperature as a separate state could improve the disturbance estimation, but would require an additional sensor. Air leakage could be integrated - if known - into the model, too. In general, a validation of the models will be required to some extent to assure good control in the real car. Not only the system, but also the objective models can be improved, most importantly the thermal comfort model. For example, the effect of air jets with temperatures different from the cabin air temperature could be included.

On the hardware side a better temperature and comfort estimation could be obtained with a solar sensor, especially when it is coupled with an adapted comfort model. For better carbon dioxide concentration values a sensor could be added. With more accurate values, more use of recirculation could be made, resulting in savings of heating energy. In particular this applies if water in the cabin (from shoes or clothes) causes the CO_2 simulation to give too high values.

For the HVAC-system, better control over the air flow is required. Influences like the car speed, flaps or recirculation can be taken into account by different means. One way is to measure the effects and to implement a model to compensate for them. Another way are additional sensors capturing the pressure drop and allowing closed-loop control. Finally, the hardware can be adapted to reduce some effects. This is possible for the recirculation with the help of a so-called *ram door* (cf. Section 3.2.1).

The HVAC-unit in the *MUTE* project is taken from a “normal” car which will probably cause minor problems in the way it is used. The openings and the flap are not designed for partial recirculation. This can lead to direct air inflow through the recirculation path at higher car speeds. An adapted design would also reduce the pressure drop, the acoustics, the size, and it could improve the controllability.

13.3 Outlook

The designed and implemented controller includes a means of using recirculated air to reduce energy consumption. Simultaneous it takes into account comfort and windscreen fogging. Altogether it meets the requirements of a modern climate control: providing comfort and safety in an energy efficient way.

The design is modular and model-based. Different car, comfort or completely new models can easily be integrated and adapted. Complicated interfaces as the energy consumption bias can also be realised. Thus it is attuned to the developments in car climate control for the electric cars which are going to take place in the next years.

Bibliography

[1] Holger Großmann. *Pkw-Klimatisierung: Physikalische Grundlagen und technische Umsetzung*. Springer, Berlin, 1st edition, September 2010. ISBN 3642054943.

[2] Alexander Kolb. Lecture notes of the course Kfz-Klimatisierung. Lehrstuhl für Thermodynamik, TU München, 2010.

[3] M. Arndt, M. Sauer, and M. Wolz. Verbrauchssenkung durch verbesserte Klimaanlagen-Regelung. *ATZ-Automobiltechnische Zeitschrift*, 109(5):404.

[4] D. Nagel and R. Trapp. Komfort in der Fahrzeugklimatisierung-Der intelligente Solarsensor. *ATZ-Automobiltechnische Zeitschrift*, 109(05):404–410, 2007. ISSN 0001-2785.

[5] Toyota Motor Corporation. *TOYOTA Technical Training - Toyota Hybrid System Diagnosis - Course 072*.

[6] C. Gühmann and J. Pahlke. Prediction of Water Vapor Condensation on Automobile Windscreens. *tm Technisches Messen*, 68(10/2001):473–480, 2001. ISSN 0171-8096.

[7] DIN EN ISO 7730. Ergonomics of the thermal environment - Analytical determination and interpretation of thermal comfort using calculation of the PMV and PPD indices and local thermal comfort criteria, May 2006.

[8] B.W. Olesen. Thermal Comfort. *Technical Review*, (2), 1982. ISSN 0007-2621.

[9] DIN EN ISO 14505-2. Ergonomics of the thermal environment - Evaluation of thermal environments in vehicles - Part 2: Determination of equivalent temperature, April 2007.

[10] Arbeitsbedingungen SECO – Direktion für Arbeit. Wegleitung zu den Verordnungen 3 und 4 zum Arbeitsgesetz - Arbeit und Gesundheit, 1995. 5th revision 2007/2008.

[11] DIN 1946-3. Ventilation systems - Part 3: Airconditioning of passenger cars and commercial vehicles, June 2006.

[12] FP. Leusden and H. Freymark. Darstellung der Raumbehaglichkeit für den einfachen, praktischen Gebrauch. *Ges.-Ing.*, 72:271–273, 1951.

[13] Umweltbundesamt. Gesundheitliche Bewertung von Kohlendioxid in der Innenraumluft. *Bundesgesundheitsbl - Gesundheitsforsch - Gesundheitsschutz*, 51:1358–1369, 2008.

[14] European Collaborative Action Indoor Air Quality and its Impact on Man (ECA). Guidelines for Ventilation Requirements in Buildings. Technical Report 11, 1992. Report No. 11 (EUR 14449 EN).

[15] Modine Europe GmbH. The Modine-Europe Climatic Wind Tunnel, 2005.

[16] N. Rajaratnam. *Turbulent Jets*, volume 5 of *Series in Developments in Water Science*. Elsevier Science Ltd, 1976. ISBN 0444413723.

[17] T. Sattelmayer and W. Polifke. Arbeitsunterlagen zu den Vorlesungen Wärmetransportphännomene, Wärme- und Stoffübertragung. Lehrstuhl für Thermodynamik, TU München, 2010.

[18] T. Sattelmayer and R. Kathan. Skriptum zur Vorlesung Thermodynamik II. Lehrstuhl für Thermodynamik, TU München, 2007.

[19] L. Hörth. Wärmepumpentechnik in Elektrofahrzeugen. Lehrstuhl für Thermodynamik, TU München, April 2011.

[20] H. Sandner, M. Kröner, M. Pöschl, and C. Heinz. Begleitendes Lehrbuch zur Vorlesung Thermodynamik I. Lehrstuhl für Thermodynamik, TU München, November 2006.

[21] Bohman, Fischer, Jeck, and Lorenz. Item Definition für die Funktion "Thermomanagement". ePerformance-Projekt, March 2011.

[22] M. Wang, T.M. Urbank, and K.V. Sangwan. Clear Vision Automatic Windshield Defogging System. *Developments in Automotive Climate Control Technology (SP-1859)*, pages 69–78, 2004.

[23] Seunggyoon Jung, Changwon Lee, and Kilyong Jang. Automatisches Windschutzscheiben - Antibeschlagsystem im Hyundai Genesis. *ATZ-Automobiltechnische Zeitschrift*, 111(03):196–201, 2009. ISSN 0001-2785.

[24] M. Wang, J.L. Pawlak, and C.A. Archibald. Development of Next Generation Automatic Climate Control. *Thermal Systems & Management Systems (SP-2132)*, 2007.

[25] LI Davis Jr, TF Sieja, RW Matteson, GA Dage, and R. Ames. Fuzzy Logic for Vehicle Climate Control. In *Fuzzy Systems, 1994. IEEE World Congress on Computational Intelligence., Proceedings of the Third IEEE Conference on*, pages 530–534. IEEE, 1994. ISBN 078031896X.

[26] Y. Farzaneh and A.A. Tootoonchi. Intelligent Control of Thermal Comfort in Automobile. In *Cybernetics and Intelligent Systems, 2008 IEEE Conference on*, pages 510–514. IEEE, 2008.

[27] R.Z. Freire, G.H.C. Oliveira, and N. Mendes. Predictive Controllers for Thermal Comfort Optimization and Energy Savings. *Energy and buildings*, 40(7):1353–1365, 2008. ISSN 0378-7788.

[28] N. Nassif, S. Kajl, and R. Sabourin. Optimization of HVAC Control System Strategy using Two-Objective Genetic Algorithm. *HVAC&R Research*, 11(3):459–86, 2005.

[29] Anders Robertsson. Lecture slides of the course Nonlinear Control. Department of Automatic Control, Lunds tekniska högskola, 2008.

[30] Michael Buhl. Moderne Methoden der Regelungstechnik III Teil: Ljapunow-basierte Regelungen. Lehrstuhl für Regelungstechnik, TU München, 2009.

[31] Horst Baier, Ögmundur Petersson, Erich Wehrle, and Eunjung Yoo. Lecture Notes Multidisciplinary Design Optimization. Institute of Lightweight Structures, TU München, April 2010.

[32] P.J. Fleming and R.C. Purshouse. Evolutionary Algorithms in Control Systems Engineering: a Survey. *Control engineering practice*, 10(11):1223–1241, 2002. ISSN 0967-0661.

[33] Q. Wang, P. Spronck, and R. Tracht. An Overview of Genetic Algorithms Applied to Control Engineering Problems. In *Machine Learning and Cybernetics, 2003 International Conference on*, volume 3, pages 1651–1656. IEEE, 2003. ISBN 0780381319.

[34] Harald Langer. *Extended Evolutionary Algorithms for Multiobjective and Discrete Design Optimization of Structures.* PhD thesis, Technische Universität München, 2005.

[35] Helen G. Cobb and John J. Grefenstette. Genetic Algorithms for Tracking Changing Environments. In Stephanie Forrest, editor, *ICGA*, pages 523–530. Kaufmann, Morgan, 1993. ISBN 1-55860-299-2.

[36] Steven Daly. *Automotive Air Conditioning and Climate Control Systems.* Butterworth-Heinemann, 1 edition, October 2006. ISBN 978-0750669559.

[37] G. A. Spinas and U. Heitz. Ernährung- und Energiestoffwechsel. Projekt MEGRU - MEdizinische GRUndlagen, 2004.

[38] Lehrstuhl für Fahrzeugtechnik, TU München. TUM Electric Mobility Homepage. http://www.mute-automobile.de/, 2011. [Online; as May 18th 2011].

[39] Webasto AG. Webasto Caravan - Heating - AirTop 2000 ST product information. http://motorhome.webasto.co.uk/, 2011. [Online; as May 18th 2011].

[40] Meteorologisches Institut der Universität München. Meteowiki Messwerte München. http://www.meteo.physik.uni-muenchen.de/dokuwiki/doku.php?id=wetter:stadt, 2011. [Online; as May 18th 2011].

Appendices

A Constants and material properties

A.1 Tabular material constants

Material	T	ρ	c, c_p	k	η	ν	a	Pr	Source
	°C	$\frac{\mathrm{kg}}{\mathrm{m}^3}$	$\frac{\mathrm{kJ}}{\mathrm{kg \cdot K}}$	$\frac{\mathrm{W}}{\mathrm{m \cdot K}}$	$\frac{\mathrm{Ns}}{\mathrm{km}^2}$	$\frac{\mathrm{m}^2}{10^6 \cdot \mathrm{s}}$	$\frac{\mathrm{m}^2}{10^6 \cdot \mathrm{s}}$	-	
Air (1013 hPa)	20	1.2045	1.005	0.0257	18.2	15.11	21.19	0.713	[17]
Carbon dioxide	50	1.648	0.875	0.0178	16.2	9.8	12.6	0.80	[17]
Window glass	20	2480	0.7-0.93	1.163					[17]

A.2 Miscellaneous material constants

Symbol	Value	Unit	Description	Source
Δh_v	2502	$\frac{\mathrm{kJ}}{\mathrm{kg}}$	Enthalpy of water vaporisation	[18]
$c_{p,v}$	1.86	$\frac{\mathrm{kJ}}{\mathrm{kg \cdot K}}$	Heat capacity of water vapour	[18]
$c_{V,air}$	0.719	$\frac{\mathrm{kJ}}{\mathrm{kg \cdot K}}$	Specific heat capacity of air at constant volume	[18]

B In- and outputs

The interface between the car-system and the climate controller block are listed in the following two tables. The signal names are the names used car-wide and are therefore in German. They are separated into inputs and outputs (from the controller's point of view).

ts

Signal	Unit	Range	Type	Comment
Ambient air temperature	°C	-30...95	uint	Replacement-value: heater inlet temperature
Heater inlet temperature	°C	-30...95	uint	Replacement-value: ambient temperature
Heater outlet temperature	°C	-30...120	uint	
Mixing chamber temperature	°C	-30...95	uint	
Windscreen temperature	°C	-30...95	uint	Replace-value : ambient temperature
Cabin temperature	°C	-30...95	uint	
Relative ambient air humiditiy	%	0...100	uint	
Relative cabin air humiditiy	%	0...100	uint	
Heater fuel fill level	%	0...100	uint	
Position recirculation flap	°	0...180	uint	
Position foot outlet flap	°	0...180	uint	
Position heater control servo	°	0...340	uint	
Car speed	km/h	0...150	uint	
Status: person in car	-	1: person in car 0: no person in car	bool	
Main battery cooling PWM	%	0...100	uint	Fans take air from the cabin
Allowed power consumption	W	0...200	uint	Given by the low-voltage supply management
Power consumption manipulation	%	0...100	uint	<50 consume less, >50 consume more

Continued on the next page

Signal	Unit	Range	Type	Comment
Status: climate control	-	1: climate control on 0: off-mode	bool	
Status: precondition mode	-	1: precondition mode 0: normal operation	bool	
Status: automatic mode	-	1: automatic mode 0: manual mode	bool	Set by passenger
Desired temperature	%	0...100	uint	<50 cooler 50 neutral >50 warmer; only used in automatic mode
Status: defrost mode	-	1: defrost mode 0: normal operation	bool	Set by passenger; only used in automatic mode
Status: force recirculation	-	1: air recirculation 0: fresh air/automatic	bool	Set by passenger
Fan intensity	%	0...100	uint	Set by passenger; only used in manual mode
Inlet temperature	%	0...100	uint	Set by passenger; only used in manual mode
Air flow to the foot-outlet	%	0...100	uint	Set by passenger; only used in manual mode

puts

ignal	Unit	Range	Type	Comment
an motor	%	0...100	uint	Percent of 5V going to fan PWM
leater set-temperature	°	0...340	uint	Rotation of heater potentiometer
tatus: heater	-	1: heater on 0: heater off	bool	
et position recirculation flap	°	0...180	uint	
et position foot-outlet flap	°	0...180	uint	
Iinimal power requirement	W	0...200	uint	
stimated power consumption	W	0...200	uint	
tatus: heater fan	-	1: heater fan spins 0: heater fan off	bool	Ensure proper heater cooling after shut-down
leater error	-	1: heater failure 0: no error	bool	
ervo error	-	1-7: servo fail 0: no error	uint	Servo number binary coded
an error	-	1: fan failure 0: no error	bool	
ensor error	-	1-255: sensor failure 0: no error	uint	Sensor number binary coded
uel error	-	2: fuel empty 1: fuel short 0: no error	uint	
limate controller error	-	$\neq 0$: controller error 0: no error	uint	Error code
tatus: cold air prevention	-	1: active 0: inactive	bool	

B.3 Error codes

The error codes for the three coded outputs. X means “value does not matter”.

HEI_ST_errStellmotor

Binary error	**Error/warning description**
XX1	Servo 1 (recirculation flap, HEI_deg_istStellM1) is not reacting as expected
X1X	Servo 2 (foot/defrost flap, HEI_deg_istStellM2) is not reacting as expected
1XX	Servo 3 (heater potentiometer, HEI_deg_istHeizPoti) is not reacting as expected

HEI_ST_errSensor

Binary error	**Error/warning description**
XXXXXXX1	Sensor 1 out of range (SEN_T_istTempAus)
XXXXXX1X	Sensor 2 out of range (SEN_T_istTempBrennerIn)
XXXXX1XX	Sensor 3 out of range (SEN_T_istTempBrennerOut)
XXXX1XXX	Sensor 4 out of range (SEN_T_istTempVerteilerK)
XXX1XXXX	Sensor 5 out of range (SEN_T_istTempInn)
XX1XXXXX	Sensor 6 out of range (SEN_T_istTempFrontsch)
X1XXXXXX	Sensor 7 out of range (SEN_rel_istFeuchtAus)
1XXXXXXX	Sensor 8 out of range (SEN_rel_istFeuchtInn)

HEI_ST_errRegler

Binary error	**Error/warning description**
XXXX1	Warning: CO_2 simulation has reached the lower bound
XX1XX	Warning: disturbance estimations have reached a limit
1XXXX	Warning: the optimiser has not found a suitable control output, a *panic handler is taken*
>1XXXXXX	Error: the optimiser could not allocate the required memory

C Simulation parameters

The parameters for the controller used in the simulation in Chapter 12 are found in this appendix. Partly, they are already mentioned in the hardware description in Chapter 10. Some might already be good enough for the use in the *MUTE* car, while others need further measurements or adjustments. The *Source* column indicates where this value has been obtained from and gives an idea about the reliability of the data. The column *Used in* gives the section number to show in which context this parameter is used in this work and the controller.

and system parameters

	Value	Unit	Used in	Source
O_2 concentration	700	$\frac{mg_{CO_2}}{kg_{air}}$	3.1.3, 5.2, 8.1.5	[14]
e *MUTE* cabin	2.4	kg	3.1.1, 3.1.2, 3.1.3	CAD-measurements
of the car interior parts	100 (37500)	$\frac{J}{K}$	3.1.1	Estimation
f the car body	52	$\frac{W}{K}$	3.1.1	Estimation based on [1]
coefficient of the CFRP-parts	5.14	$\frac{W}{m^2 \cdot K}$	8.1.2	5mm air gap, see 10.1
or of the car body parts	0.365	-	8.1.2	CAD-measurements
or of the windows	0.274	-	8.1.2	CAD-measurements
or of the interior parts	0.361	-	8.1.2	CAD-measurements
essure coefficient	0.75	-	3.1.4	Estimation, [15]
ickness	3.85	mm	3.1.4	Product data
ight	0.735	m	3.1.4	CAD-measurements
ea	0.84	m^2	3.1.4	CAD-measurements
rost outlets	96.0	cm^2	3.1.4, v_{air} in 2.2.1	CAD-measurements
rost outlets to side windows	33.6	cm^2	3.1.4, v_{air} in 2.2.1	CAD-measurements
nozzle size	15.6	mm	3.1.4	CAD-measurements
air speed reaching the passenger	0.3	-	v_{air} in 2.2.1	Estimation
ing power	1000	W	8.1.6, 8.2	Fuel heater data sheet

Continued on the next page

Table C.1: Hardware data used for the simulation

	Value	Unit	Used in	Source
lable heating power	2000	W	8.1.6, 8.2	Fuel heater data sheet
electric power consumption	29	W	8.1.6	Fuel heater data sheet
er consumption, glow plug active	100	W	8.1.6	Measurements
time	180	s	8.1.6	Measurements
tinuation after stop	180	s	8.1.6	Measurements
ug duration at start	160	s	8.1.6	Measurements
ug duration at stop	40	s	8.1.6	Measurements
mass flow limit	7	$\frac{kg}{h}$	8.2	Measurements
mass flow limit	300	$\frac{kg}{h}$	8.2	Measurements
water emission	50	$\frac{g}{h}$/pers	3.1.2	[14]
carbon dioxide emission	31.3	$\frac{g}{h}$/pers	3.1.3	[14]

C.2 Controller settings

C.2.1 Design variable related settings

Property	$\boldsymbol{T_{in}}$ [°C]	$\boldsymbol{\dot{m}_{air,in}}$ $[\frac{\text{kg}}{\text{h}}]$	$\boldsymbol{\mu_{recirc}}$ [-]	$\boldsymbol{\mu_{foot}}$ [-]
Base lower bounds	5	$\dot{m}_{air,min}$	0.0	0.0
Base upper bounds	55	$\dot{m}_{air,max}$	1.0	1.0
Defrost lower bounds	5	$\dot{m}_{air,max}/2$	0.0	0.0
Defrost upper bounds	55	$\dot{m}_{air,max}$	0.5	0.0
Starting output	30-T_{amb}	$\dot{m}_{air,min}$	1.0	0.0

C.2.2 Objective related settings

Objective	**Priority**	**Standard weight**	**Precond. weight**	**Limit**
Fogging affinity	3	3.0	3.0	230
Thermal comfort	1	2.0	4.0	254
Humidity comfort	1	1.0	1.0	255
Air quality	2	2.0	0.0	250
Power consumption (electric)	1	1.0	1.0	255
Power consumption (fuel)	1	0.2	0.2	255
Battery air flow (constr.)	2	0.0	0.0	0
Min. inlet temperature (constr.)	4	0.0	0.0	0
Max. inlet temperature (constr.)	4	0.0	0.0	0
Max. electric power (constr.)	4	0.0	0.0	0
Cold air prevention limit (constr.)	4	0.0	0.0	0

Symbol	**Parameter**	**Value**	**Used in objective**
ϕ_{max}	Maximum weight	255	All
$x_{CO_2,min}$	Lowest carbon dioxide concentration	$x_{CO_2,amb}$	Air quality
$x_{CO_2,max}$	Highest carbon dioxide concentration ($AQF = \phi_{max}$)	3600 $\frac{\mathrm{mg_{CO_2}}}{\mathrm{kg_{air}}}$	Air quality
P_{max}	Maximum energy consumption	200 W	Power consumption (el.)
κ_{max}	Maximum fogging “distance”	5 K	Fogging affinity
$a_{p_{sat}}$	Pressure scaling factor	83 $\frac{\mathrm{Pa}}{\mathrm{K}}$	Fogging affinity
$\varphi_{pas,max}$	Maximum humidity user bias	30 % rH	Humidity comfort
φ_{max}	Maximum comfortable humidity	70 % rH	Humidity comfort
φ_{min}	Minimum comfortable humidity	30 % rH	Humidity comfort
$M_{pas,max}$	Maximum for the user adjustable metabolism	2.25 met	Thermal comfort
$M_{pas,min}$	Minimum for the user adjustable metabolism	0.75 met	Thermal comfort
$T_{cl,min}$	Minimum temperature for the clothing adaption	-5.0 ℃	Thermal comfort
$T_{cl,max}$	Maximum temperature for the clothing adaption	25.0 ℃	Thermal comfort
$I_{cl,min}$	Minimum clothing insulation	0.3 clo	Thermal comfort
$I_{cl,max}$	Maximum clothing insulation	1.5 clo	Thermal comfort
$T_{in,low}$	Lower limit for the cold air prevention	8 ℃	Cold air prevention limit
$T_{in,high}$	Upper limit for the cold air prevention	18 ℃	Cold air prevention limit

Panic handler for	$\boldsymbol{T_{in}}$	$\boldsymbol{\dot{m}_{air,in}}$	$\boldsymbol{\mu_{recirc}}$	$\boldsymbol{\mu_{foot}}$	**Comment**
Fogging affinity	$T_{amb}+22$	ub_2	lb_3	lb_4	
Thermal comfort	$30 - T_{amb}$	ub_2	$\frac{lb_3+ub_3}{2}$ 1	lb_4	
Humidity comfort	$30 - T_{amb}$	ub_2	lb_3	lb_4	Not reachable
Air quality	$30 - T_{amb}$	ub_2	lb_3	lb_4	
Power consumption (electric)	lb_1	lb_2	ub_3	ub_4	Not reachable
Power consumption (fuel)	lb_1	ub_2	ub_3	ub_4	Not reachable
Battery air flow (constr.)	$30 - T_{amb}$	ub_2	lb_3	ub_4	Constraint
Min. inlet temperature	lb_1	lb_2	lb_3	lb_4	Constraint
Max. inlet temperature	lb_1	lb_2	ub_3	lb_4	Constraint
Max. electric power	lb_1	lb_2	ub_3	ub_4	Constraint
Cold air prevention limit	lb_1	lb_2	lb_3	ub_4	Constraint

Exceeded constraint limits should normally not occur. *Not reachable* designates objectives with an unreachable limit, meaning this its "panic" does never happen.

C.3 Disturbance estimator settings

Symbol	**Parameter**	**Value**
$t_{sample,est}$	Sample time for the disturbance estimator	1.0 s
n	Values to use for derivative estimation	40
$\dot{Q}_{cab,dist,max}$	Cabin heat disturbance limit	2000 W
$\dot{m}_{w,dist,max}$	Humidity disturbance limit	$3 \cdot \dot{m}_{w,pas}$
$\dot{Q}_{ws,dist,max}$	Windscreen temperature disturbance limit	500 W

[1]This value is replaced depending on the ambient temperature. Below 15 ℃ the upper bound is taken, above 28 ℃ the lower bound.

C.4 Optimiser settings

Symbol	Parameter	Value
$t_{sample,opt}$	Sample time for the optimiser	2.0 s
n_{pop}	Population size	10
n_c	Number of children	20
n_{elite}	Number of elite individuals	3
n_{gen}	Number of generations	2
$s_{x,max}$	Maximum exploring factor	0.6
$s_{x,min}$	Minimum exploring factor	0.1
δ_{s_x}	Exploring factor adaption increment	0.05
$w_{pow,max}$	Maximum power weight bias	1.0
$t_{horizon}$	Prediction horizon	30.0 s
δt	System prediction sample time	10.0 s
ϵ_{thr}	Diversity threshold	0.02

Base population

T_{in}	$\dot{m}_{in}$	μ_{recirc}	μ_{foot}	Comment
T_{amb}	lb_2	lb_3	lb_4	Little fresh air
$T_{cab}+22$	ub_2	ub_3	$\frac{lb_4+ub_4}{2}$	Fast warm up
$T_{amb}+22$	ub_2	lb_3	lb_4	Defrost/defogg
22	$\frac{lb_2+ub_2}{2}$	$\frac{lb_3+ub_3}{2}$	$\frac{lb_4+ub_4}{2}$	Steady state mode
T_{amb}	ub_2	lb_3	lb_4	Maximum cooling

22 ℃ is the maximum possible temperature increase possible with the available heating power at full air mass flow.

C.5 Test case parameters

	Heat-up	**Cool-down**	**Rainy autumn**	**Transition period**
T_{amb}	-10 ℃	30 ℃	10 ℃	15 ℃
T_{sky}, T_{ground}	T_{amb}	T_{amb}	T_{amb}	T_{amb}
φ_{amb} $(x_{w,amb})$	80% $(1.3\,\frac{g}{kg})$	70% $(18.7\,\frac{g}{kg})$	100% $(7.6\,\frac{g}{kg})$	80% $(8.5\,\frac{g}{kg})$
$T_{cab}(t=0)$	-10 ℃	50 ℃	20 ℃	15 ℃
$T_{ws}(t=0)$	-10 ℃	50 ℃	20 ℃	15 ℃
$x_{w,cab}(t=0)$	$x_{w,amb}$	$x_{w,amb}$	$x_{w,amb}$	$x_{w,amb}$
$x_{CO_2,cab}(t=0)$	$x_{CO_2,amb}$	$x_{CO_2,amb}$	$x_{CO_2,amb}$	$x_{CO_2,amb}$
$\dot{q}_{sun,direct}$	$0\,\frac{W}{m^2}$	$800\,\frac{W}{m^2}$	$0\,\frac{W}{m^2}$	$400\,\frac{W}{m^2}$
$\dot{q}_{sun,diffuse}$	$50\,\frac{W}{m^2}$	$100\,\frac{W}{m^2}$	$100\,\frac{W}{m^2}$	$100\,\frac{W}{m^2}$
$\alpha_{sun,azimuth}$	π rad (South)	π rad (South)	π rad (South)	π rad (South)
$\alpha_{sun,altitude}$	$\frac{\pi}{4}$ rad	$\frac{\pi}{3}$ rad	$\frac{\pi}{4}$ rad	$\frac{\pi}{4}$ rad
v_{car}	$0\,\frac{km}{h}$	$0\,\frac{km}{h}$	$50\,\frac{km}{h}$	$50\,\frac{km}{h}$
Driving direction	0 rad	0 rad	0 rad	0 rad
Slope	0 rad	0 rad	0 rad	0 rad
n_{pas}	2/0	2/0	2	2
r_{cl}	1.2 clo	0.75 clo	1 clo	1 clo
M_{pas}	1.2 met	1.2 met	1.2 met	1.2 met
Precondition	Off/On	Off/On	Off	Off

Automatic mode was enabled in all cases. The defrost or recirculation mode was not active. The temperature control was set to 50%. No limits regarding the battery cooling air (cf. section 10.5) or energy consumption were made in these tests. The energy management influence was set to 50 %. The values for the sun radiation were taken from measurements [40] made by the *Meteorologisches Institut der Universität München* on the following dates: 30/01/2011, 03/07/2010,03/06/2010, 14/09/2010.

The simulations were run with a fixed sample time of 0.1 seconds. As solver the “ode3 (Bogacki-Shampine)” algorithm was used. For all test cases 2700 seconds (45 minutes) were simulated.

D Additional simulation results

In the following figures the test results mentioned in Section 12.5 are shown in detail. *Precond* indicates that for a period of 20 minutes the precondition mode was activated and no passengers were in the car at the start of the simulation. After that time two persons are in the car and the automatic mode is active.

D.1 Heat-up test case

D.1.1 No recirculation

The recirculation flap was forced to stay into the “fresh air” position.

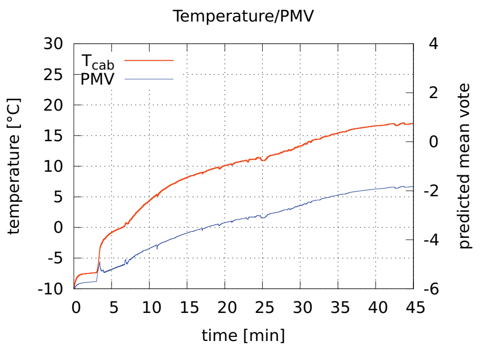

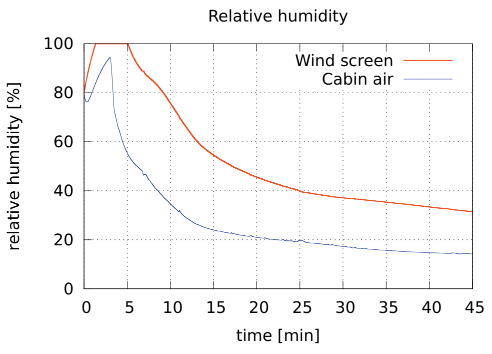

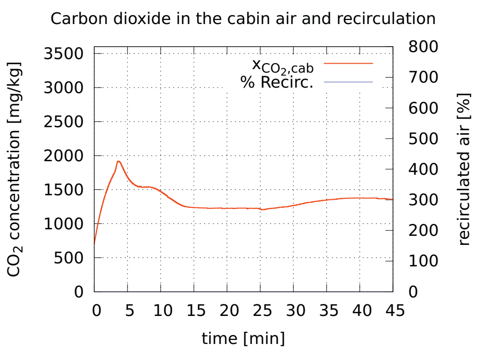

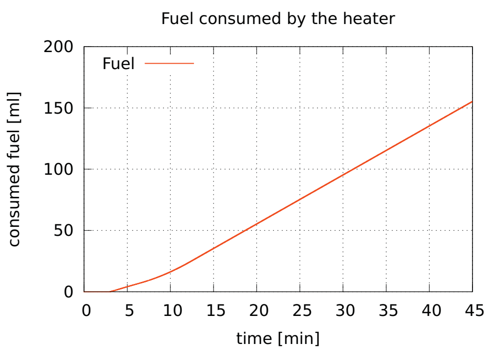

D.1.2 Changed user settings

The user temperature setting was changed from 50 to 75.

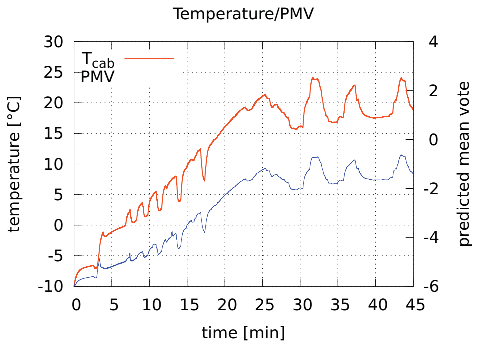

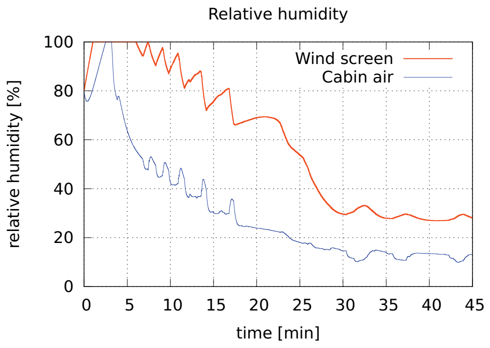

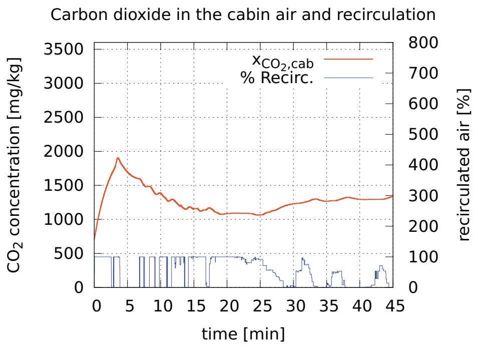

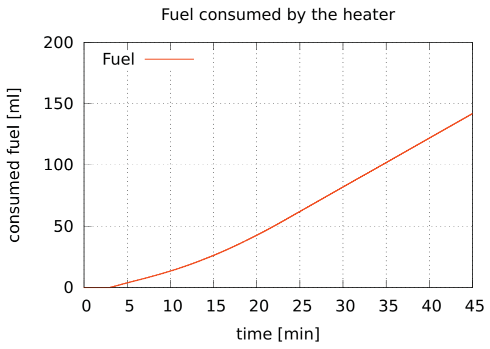

D.2 Cool-down test case

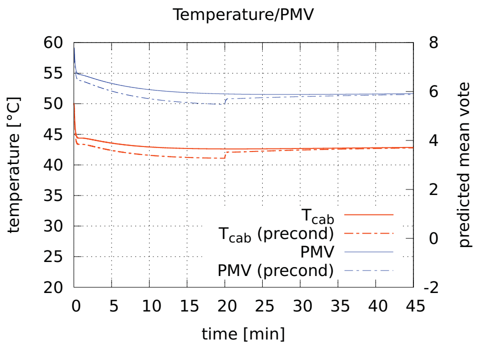

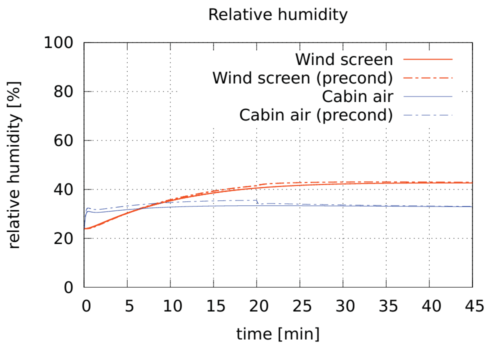

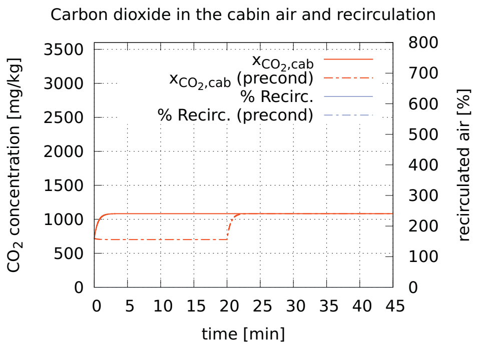

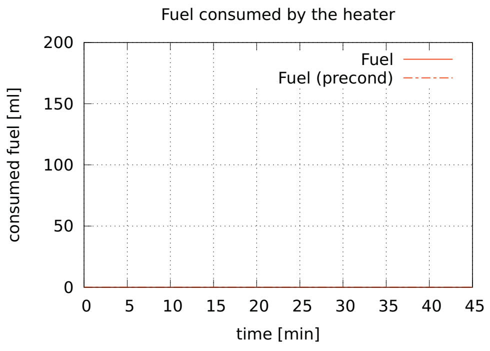

E Optimiser code

Listing E.1: Structures for the use with the IMEA algorithm

```c
/* Function pointer type definitions */
typedef real_T (*objFunc)(real_T*, real_T*,real_T*);                              /* Objective
    functions */
typedef void (*sysFunc)(real_T*, real_T*, real_T*,real_T*, real_T, real_T); /* System
    function */

/* Structure of one individual */
struct individual {
  real_T *DV;            /* Array of the lenght numDV */
  real_T *ObjResults; /* Array of the lenght numObj */
  real_T weightedSum;
  int_T  ranking;
};
/* Structure of the system related values */
struct system {
   /* Pointer to a system function in the form of
      f(*DesignVariables, *EstimatedSystemStates, *SystemParameters, Timestep,
          Simulation_Horizon)
   */
    sysFunc systemFunction;
    real_T  *SYS_States;    /* Values to be modified through the control (and predicted)
       */
    real_T  *SYS_Param;     /* Values assumed to be constant during one timestep */
    int_T   numSysStates;   /* Number if system states */
};
/* Structure of values related to the objectives */
struct objectives {
   /* Array of pointers to objective functions in the form of
      f(*DesignVariables, *EstimatedSystemStates, *SystemParameters)
   */
    objFunc *objectiveFctArray;
    int_T   *priorities;    /* Array of objective priorities */
    real_T  *weights;       /* Array of objective weights */
    real_T  *limits;        /* Array of objective limits */
    real_T  *panic_order;   /* Array of objective panic order */
    real_T  *panic_instructions; /* Array of panic instructions, size:numObj*numDV */
    int_T   numObj;          /* Number of objectives */
};
/* Structure of values related to the design variables */
struct designVariables {
    real_T  *lb;    /* Array of the lower boundaries */
    real_T  *ub;    /* Array of the upper boundaries */
    int_T   numDV;  /* Number of design variables */
};
/* Structure holding the settings for the IMEA algorithm */
struct IMEAoptions {
    int_T  popSize;      /* Population size */
    int_T  numChild;     /* Number of children */
    int_T  numElite;     /* Number of elite individuals */
    real_T *basePop;     /* Array holding the base population, size: numBase*numDV */
    int_T  numBase;      /* Size of the base population */
    real_T simHorizon;   /* Simulation/predicition horizon in seconds */
    real_T simSampleT;   /* Simulation/predicition sample time in seconds */
    real_T adapMutFractionMin; /* s_x minimum value */
    real_T adapMutFractionMax; /* s_x maximum value */
    real_T adapMutFractIncr;    /* Step siez for s_x adaption*/
    int_T  numGen;         /* Number of generations */
    real_T conDivThresh;  /* Diversity threshold */
};
/* Structure of variables bein exchanged with the main loop and saved for the next run */
struct ExchValues {
    real_T *elitePop;   /* Elite population, size: numElite*numDV */
    real_T *u_out;      /* Control output */
    real_T *fit;        /* Fitness of control individual */
    real_T *fit_last;   /* Fitness of last control individual */
    real_T *explFactor;/* Actual exploration factor */
};
```

Listing E.2: C implementation of the IMEA algorithm

```
/*********************************************************************
 * CC_IMEA.c
 * The optimisation algorithm is based on an evolutionary strategy.
 * Structure loosly based on the MDO excercise by the Insititute of
 * lightweight structures by Prof. Baier (SS2010)
 * Some ideas taken from GAME (Harald Langer, 2005)
 * Programmed by Matthias Busl 2011
 *********************************************************************/

#include "CC_IMEA.h"

/* function prototypes */
```

```
static void IMEA_initPop(struct individual*,real_T*, real_T*, int_T, int_T, int_T, int_T,
      real_T*, real_T*);
static void IMEA_evaluateObjectives(struct individual*, struct system, objFunc*, real_T*,
      real_T, real_T, int_T, int_T, int_T);
static void IMEA_priorisedWeighting(struct individual*, struct objectives, int_T*, int_T,
      int_T);
static void IMEA_breeding(struct individual*, struct designVariables, real_T*, int_T*,
    int_T, int_T, real_T);
static void IMEA_sortTruncate(struct individual*, int_T, int_T);
static int_T IMEA_selectControl(struct individual*, struct designVariables, struct
    objectives, real_T*, real_T, int_T);
static void IMEA_selectElite(struct individual*, struct designVariables, real_T*, real_T
    *, int_T, int_T, int_T, int_T, real_T);
/* Debug functions */
static void DEBUG_print_pop(struct individual*, int_T, int_T, int_T);

int_T IMEA_Main(struct designVariables DV, struct system Sys, struct objectives Obj,
    struct IMEAoptions Opt, struct ExchValues ExVal)
{
    struct individual *pop;
    real_T              *Estim_SYS_States;
    int_T               *ordPrio;
    real_T              *fitness;
    int_T               *parents;
    real_T              max_change    = 0.8;
    int_T               selected_ind = 0;
    int_T  i = 0;

    /* allocate memory for the population */
    /* population, +1 for result */
    pop = (struct individual*)malloc((Opt.popSize+Opt.numChild+1)*sizeof(struct
        individual));
    if(pop == NULL)
        return 10;

    for(i=0;i<Opt.popSize+Opt.numChild+1;i++)
    {
        pop[i].DV            = (real_T*)malloc(DV.numDV*sizeof(real_T));
        if(pop[i].DV == NULL)
            return 10;
        pop[i].ObjResults = (real_T*)malloc(Obj.numObj*sizeof(real_T));
        if(pop[i].ObjResults == NULL)
            return 10;
    }

    Estim_SYS_States = (real_T*)malloc(Sys.numSysStates*sizeof(real_T));
    if(Estim_SYS_States == NULL)
```

```
        return 10;

    ordPrio           = (int_T*)malloc((Obj.numObj+1)*Obj.numObj*sizeof(int_T));
    if(ordPrio == NULL)
        return 10;

    fitness           = (real_T*)malloc(Opt.popSize*sizeof(real_T));
    if(fitness == NULL)
        return 10;

    parents           = (int_T*)malloc(2*Opt.numChild*sizeof(int_T));
    if(parents == NULL)
        return 10;

    /* initialise RNG */
    /*PlantSeeds(time(NULL)); needs to be done once outside this function*/

    /* Calculate maximum canges based on the change of the fitness (hypermutation) */
    if(ExVal.fit[0] == ERROR_FITNESS) /* Start or limit exceeded */
        max_change      = Opt.adapMutFractionMax;
    else if((ExVal.fit[0]<ExVal.fit_last[0])
          && ExVal.explFactor[0] > Opt.adapMutFractionMin) /* always allow minimal change
              */
        max_change      =  ExVal.explFactor[0]-Opt.adapMutFractIncr;
    else if((ExVal.fit[0]>ExVal.fit_last[0])
          && ExVal.explFactor[0] < Opt.adapMutFractionMax) /* Never allow more than
              maximum */
        max_change      =  ExVal.explFactor[0]+Opt.adapMutFractIncr;
    else
        max_change = ExVal.explFactor[0];
    #if DEBUG_IMEA >= 2
    printf("==last= %f ===old= %f===\n",ExVal.fit[0],ExVal.fit_last[0]);
    #endif
    /* Initialise population */

    /* create initial population */
    IMEA_initPop(pop, Opt.basePop, ExVal.elitePop, Opt.popSize, Opt.numElite, Opt.numBase
        , DV.numDV,DV.lb, DV.ub);
    /* Evaluate the fitness of the initial population */
    IMEA_evaluateObjectives(pop, Sys, Obj.objectiveFctArray, Estim_SYS_States, Opt.
        simHorizon, Opt.simSampleT, Opt.popSize, DV.numDV, Obj.numObj);
    IMEA_priorisedWeighting(pop, Obj, ordPrio, Opt.popSize, DV.numDV);

    /* Main loop */
    for(i=0; i<Opt.numGen; i++)
    {
        /* select parents, create offspring */
        IMEA_breeding(pop, DV, fitness, parents, Opt.popSize, Opt.numChild, max_change);
        /* evaluate children */
        IMEA_evaluateObjectives(&pop[Opt.popSize], Sys, Obj.objectiveFctArray,
            Estim_SYS_States, Opt.simHorizon, Opt.simSampleT, Opt.numChild, DV.numDV, Obj
            .numObj);
        /* rank parents & children */
        IMEA_priorisedWeighting(pop, Obj, ordPrio, Opt.popSize+Opt.numChild, DV.numDV);
        #if DEBUG_IMEA >= 3
        DEBUG_print_pop(pop, Opt.popSize+Opt.numChild, DV.numDV, Obj.numObj);
        #endif
        /* sort best to the first places */
        IMEA_sortTruncate(pop, Opt.popSize, Opt.numChild);
    }
    #if DEBUG_IMEA >= 2
        DEBUG_print_pop(pop, Opt.popSize, DV.numDV, Obj.numObj);
    #endif
    /* Output determination   */
    /* select and store output */
    selected_ind = IMEA_selectControl(pop, DV, Obj, ExVal.u_out , max_change, Opt.popSize
        );
    /* select and store elite */
    IMEA_selectElite(pop, DV, Opt.basePop, ExVal.elitePop, Opt.popSize, Opt.numBase, Opt.
        numElite, selected_ind, Opt.conDivThresh);
    #if DEBUG_IMEA >= 1
        DEBUG_print_pop(&pop[selected_ind], 1, DV.numDV, Obj.numObj);
    #endif

    #if DEBUG_IMEA >= 2
        printf(">>>>> %d <<<< %f >>>>>>\n", selected_ind, max_change);
    #endif
    /* Save values */
    ExVal.explFactor[0] = max_change;
    ExVal.fit_last[0]   = ExVal.fit[0];
    ExVal.fit[0]        = pop[selected_ind].weightedSum;

    /* free memory */
    for(i=0;i<Opt.popSize+Opt.numChild+1;i++)
    {
        free(pop[i].DV);
        free(pop[i].ObjResults);
    }
    free(pop);
    free(Estim_SYS_States);
    free(ordPrio);
    free(fitness);
    free(parents);
    /* return */
    if(ExVal.fit[0]==ERROR_FITNESS)
        return 1;
    else
        return 0;
}

static void IMEA_initPop(struct individual *pop, real_T *basePop, real_T *elitePop,
                         int_T popSize, int_T numElite, int_T numBase, int_T numDV,
                         real_T *lb, real_T *ub)
/* ==========================================================================
 * IMEA_initPop creates an initial population with 'popsize' individuals
 * using a base population, the elite from ast run and fills the remaining with
 * random induviduals  within the lower and upper bounds lb and ub.
 * ==========================================================================
 */
{
    int_T i,j;
    int_T ind = 0;

    /* insert base population */
    for(i=0; i<numBase; i++)
    {
        for(j=0; j<numDV;j++)
        {
            pop[ind].DV[j] = basePop[i*numDV+j];
            if(pop[ind].DV[j] < lb[j])
                pop[ind].DV[j] = lb[j];
            else if (pop[ind].DV[j] > ub[j])
                pop[ind].DV[j] = ub[j];
        }
        ind++;
    }

    /* insert elite and move back into design space if needed */
    for(i=0; i<numElite-1; i++)
    {
        for(j=0; j<numDV;j++)
        {
            pop[ind].DV[j] = elitePop[i*numDV+j];
            if(pop[ind].DV[j] < lb[j])
                pop[ind].DV[j] = lb[j];
            else if (pop[ind].DV[j] > ub[j])
                pop[ind].DV[j] = ub[j];
        }
        ind++;
    }
    /* Create remaining idividuals randomly */
    for (;ind < popSize;ind++)
    {
        for(j=0; j<numDV;j++)
        {
            pop[ind].DV[j] = randu(lb[j],ub[j]);
        }
    }
}

static void IMEA_evaluateObjectives(struct individual *pop, struct system Sys,
                                    objFunc *objectiveFctArray, real_T *Estim_SYS_States,
                                    real_T SET_s_Horizon, real_T SET_s_Timestep,
                                    int_T evalSize, int_T numDV, int_T numObj)
{
/* ================================================================================
 * IMEA_evaluateObjectives calculates the objective function values for the population
     matrix pop
 * ================================================================================
 */
    int_T i,j;

    for (i=0;i<evalSize;i++)
    {
        /* Predict states for a control output */
        Sys.systemFunction(Estim_SYS_States, pop[i].DV , Sys.SYS_States, Sys.SYS_Param,
            SET_s_Timestep, SET_s_Horizon);
        for (j=0;j<numObj;j++)
        {
            /* Evaluate objectives for the predicted situation */
            pop[i].ObjResults[j] = objectiveFctArray[j](pop[i].DV,Estim_SYS_States,Sys.
                SYS_Param);
        }
    }
}

static void IMEA_priorisedWeighting(struct individual *pop, struct objectives Obj,
                                    int_T *ordPrio, int_T evalSize, int_T numDV)
{
/* ================================================================================
 *IMEA_priorisedWeighting ranks the population by a limits and
 *priorities approach
 *   First the individues are compared with respect to fullfilled limits.
 *   If they stay below the given limits in the same number of objectives
 *   for the highest priority this is tested for a lower one.
 *   at the lowest priority the final preference is decided by weighting
 * ===========================================================================
 */
    int_T       i,j,k;
    int_T       limi, limj, prio;
    real_T      sumWeights = 0;
    boolean_T done = 0;

    /* order priorities */
    for(i=0;i<Obj.numObj;i++)
        for(j=0;j<Obj.numObj;j++)
            ordPrio[i*Obj.numObj+j]=-1;

    for(i=0;i<Obj.numObj;i++)
    {
        if(Obj.priorities[i] > 0 && Obj.priorities[i] <= Obj.numObj)
        {
        j=0;
        while(ordPrio[(Obj.priorities[i]-1)*Obj.numObj+j] != -1)
            j++;
        ordPrio[(Obj.priorities[i]-1)*Obj.numObj+j]=i;
        }
        sumWeights += Obj.weights[i];
    }

    /* reset ranking */
    for  (i=0; i<evalSize;i++)
    {
        pop[i].ranking = 0;
    }

    /* Calculate weighted sum */
    for(i=0;i<evalSize;i++)
    {
        pop[i].weightedSum = 0;
        for(j=0;j<Obj.numObj;j++)
        {
            pop[i].weightedSum+=pop[i].ObjResults[j]*Obj.weights[j]/sumWeights;
        }
    }

    /* Ranking loop, compare ind. i and ind. j */
    for(i=0;i<evalSize;i++)
    {
        for(j=i+1;j<evalSize;j++)
        {
            done = 0;
            prio = Obj.numObj-1;

            while(!done)
            {
                k    = 0;
                limj = 0;
                limi = 0;
                /* check if more limits broken by one than by the other individual */
                while(ordPrio[prio*Obj.numObj+k] != -1)
                {
                    if(pop[i].ObjResults[ordPrio[prio*Obj.numObj+k]] > Obj.limits[ordPrio
                        [prio*Obj.numObj+k]])
                        limi++;
                    if(pop[j].ObjResults[ordPrio[prio*Obj.numObj+k]] > Obj.limits[ordPrio
                        [prio*Obj.numObj+k]])
                        limj++;
                    k++;
                }
                if(limj > limi)
                {
                    pop[j].ranking++;
                    done = 1;
                }
                else if (limj < limi)
                {
                    pop[i].ranking++;
                    done = 1;
                }
                /* if no preference found through limits, compare weighting */
                if(prio==0 && !done)
                {
                    done = 1;
                    if(pop[i].weightedSum < pop[j].weightedSum)
                        pop[j].ranking++;
                    else if (pop[i].weightedSum > pop[j].weightedSum)
                        pop[i].ranking++;
                }
                prio--;
            }
        }
    }
}

static void IMEA_breeding(struct individual *pop, struct designVariables DV,
                          real_T *fitness, int_T *parents, int_T popSize,
                          int_T numChild, real_T max_change)
{
/* ==================================================================
* IMEA_breeding selects 'numChild'*2 parents via global stochastic remainder
* selection and creates the children by recombining the parents and mutating
* ==========================================================================
*/
    real_T fitSum = 0.0;
    real_T tmpSum = 0.0;
    real_T randNr = 0.0;
    int_T  rankMax = 0;
    int_T  rankMin = 0;

    int_T  i,j,cnt_parent;


    /* determine max and min ranking */
    for(i=0;i<popSize;i++)
    {
        if(pop[i].ranking < rankMin)
            rankMin = pop[i].ranking;
        else if(pop[i].ranking > rankMax)
            rankMax = pop[i].ranking;
    }
    /* assign selection probability */
    if(rankMin == rankMax)
    {
        /*avoid problems if all equal */
        for(i=0;i<popSize;i++)
        {
            fitness[i] = 1;
            fitSum     += fitness[i];
        }
    }
    else
    {
        for(i=0;i<popSize;i++)
        {
            fitness[i] = (real_T)(rankMax-pop[i].ranking)/(real_T)(rankMax-rankMin);
            fitSum     += fitness[i];
        }
    }
    for(i=0;i<popSize;i++)
    {
        fitness[i] = fitness[i]/fitSum;
    }

    cnt_parent = 0;
    /* fill parent array */
    for(i=0;i<popSize;i++)
    {
        for(j=0;j<(int_T)floor(fitness[i]*2.0*numChild);j++)
        {
            parents[cnt_parent] = i;
            cnt_parent++;
        }
    }
    for(i=cnt_parent;i<2*numChild;i++)
    {
        /* fill with random individuals */
        tmpSum = 0;
        j      = 0;
        randNr = Random();
        parents[i] = 0;
        while(parents[i] == 0)
        {
            if(tmpSum < randNr && j < popSize-1)
            {
                tmpSum += fitness[j];
                j++;
            }
            else
            {
               parents[i] = j;
            }
        }

    }
    shuffle_array(parents,2*numChild); /*shuffle array*/


    /* Recombination & mutation - generate offspring */
    for(i=0; i<numChild;i++)
    {
        for(j=0;j<DV.numDV;j++)
        {
            /*recombination */
            pop[popSize+i].DV[j]  = Random()*(pop[parents[2*i]].DV[j] - pop[parents[2*i
                +1]].DV[j])+pop[parents[2*i+1]].DV[j];
            /* Mutation */
            pop[popSize+i].DV[j] = randn(pop[popSize+i].DV[j],max_change*(DV.ub[j]-DV.lb[
                j]));
            /* Repair mechanism */
            if(pop[popSize+i].DV[j] < DV.lb[j])
                pop[popSize+i].DV[j] = DV.lb[j];
            else if(pop[popSize+i].DV[j] > DV.ub[j])
                pop[popSize+i].DV[j] = DV.ub[j];
        }
    }
}

static void IMEA_sortTruncate(struct individual *pop, int_T popSize, int_T numChild)
/* ==========================================================================
 * IMEA_sortTruncate sorts the population in order to use the best for the
 * next generation.
 * ==========================================================================
 */
{
    int_T i;
    int_T rank      = 0;
    int_T pop_count = 0;
    struct individual tmpInd;

    while(pop_count < popSize)
    {
        for(i=0; i<popSize+numChild; i++)
        {
            if(pop[i].ranking == rank)
            {
                tmpInd = pop[pop_count];
                pop[pop_count] = pop[i];
                pop[i] = tmpInd;
                pop_count++;
            }
        }
        rank++;
    }
}

static int_T IMEA_selectControl(struct individual *sortedPop, struct designVariables DV,
                                struct objectives Obj, real_T *x_old, real_T
                                    allowed_change,
                                int_T popSize)
/* ==========================================================================
 * CC_Opt_IMEA_selectControl selects a suited individuum for control
 * return: index of the chosen individual
 * ==========================================================================
 */
{
    boolean_T done = 0;
    boolean_T check = 1;
    int_T     i = 0;
    int_T     ind = 0;
    int_T     panic = -1;
    int_T        panic_weight = 0;

    while (!done)
    {
        check = 1;
       /* calculate difference to old values to avoid jumps */
        for(i = 0; i<DV.numDV; i++)
        {
             check &=(fabs(sortedPop[ind].DV[i] - x_old[i])<allowed_change*(DV.ub[i]-DV.
                 lb[i]));
        }

       /* result found! take it! */
       if(check)
           done = 1;
       else
           ind++;

       /* no result found in population */
       if(ind == popSize-1)
       {
           done = 1;
           ind  = 0;
       }
    }

    /* Detection if a limit is reached */
    for(i=0; i< Obj.numObj; i++)
    {
        if(sortedPop[ind].ObjResults[i]>Obj.limits[i])
        {
            if(panic_weight < Obj.panic_order[i])
            {
                panic = i;
                panic_weight = Obj.panic_order[i];
            }
        }
    }
    if(panic >= 0)
    {
      #if DEBUG_IMEA >= 1
        printf("Panic in objective: %d !!!\n", panic+1);
      #endif
        /* use panic handler */
        for(i=0; i<DV.numDV; i++)
        {
            sortedPop[popSize].DV[i]         = Obj.panic_instructions[panic*DV.numDV+i];
            if (sortedPop[popSize].DV[i] < DV.lb[i])
                sortedPop[popSize].DV[i] = DV.lb[i];
            else if (sortedPop[popSize].DV[i] > DV.ub[i])
                sortedPop[popSize].DV[i] = DV.ub[i];
            sortedPop[popSize].weightedSum = ERROR_FITNESS;
            ind = popSize;
        }
    }

    for(i=0; i<DV.numDV; i++)
    {
        x_old[i] = sortedPop[ind].DV[i];
    }

    return ind;
}

static void IMEA_selectElite(struct individual *sortedPop, struct designVariables DV,
                             real_T *basePop, real_T *elitePop,
                             int_T popSize, int_T numBase, int_T numElite,
                             int_T selected_ind, real_T conDivThresh)
/* ==========================================================================
 * IMEA_selectElite selects the elite to be transferred to  the new run.
 * It will be selected from the population ordered by their fitness and
 * depending if they are close to the base pop (which will be added in the
 * beginning of each run). In every case the chosen control output will be
 * stored.
 * ==========================================================================
 */
{
    int_T i,j,k;
    int_T elite_count;
    boolean_T check = 0;

    /* ensure chosen individuum in the next run */
    for(i=0;i<DV.numDV;i++ )
    {
        elitePop[i] = sortedPop[selected_ind].DV[i];
    }

    /* find individues close to the base population */
    for(i=0; i< popSize; i++)
    {
        sortedPop[i].ranking = 0;
        for(j=0;j<numBase;j++)
        {
            check = 1;
```

```
                for(k=0; k<DV.numDV; k++)
                {
                    check &= sortedPop[i].DV[k] < (basePop[j*DV.numDV+k]+conDivThresh*(DV.ub[
                        k]-DV.lb[k]));
                    check &= sortedPop[i].DV[k] > (basePop[j*DV.numDV+k]-conDivThresh*(DV.ub[
                        k]-DV.lb[k]));
                }
                if(check)
                    sortedPop[i].ranking++;
            }
            check = 1;
             /* find individuals close to chosen control output*/
            for(k=0; k<DV.numDV; k++)
            {
                check &= sortedPop[i].DV[k] < (elitePop[k]+conDivThresh*(DV.ub[k]-DV.lb[k]));
                check &= sortedPop[i].DV[k] > (elitePop[k]-conDivThresh*(DV.ub[k]-DV.lb[k]));
            }
            if(check)
                sortedPop[i].ranking++;
        }

        /* store individuals with lowest neighbours in the storage for next run */
        elite_count = 1;
        k = 0;
        while(elite_count < numElite)
        {
            for(i=0;i<popSize; i++) /* look in population for individuals with lowest
                neighbours */
            {
                if((sortedPop[i].ranking == k) && (elite_count < numElite))
                {
                    for(j=0;j<DV.numDV;j++) /* copy into elite storage */
                    {
                        elitePop[elite_count*DV.numDV+j] = sortedPop[i].DV[j];
                    }
                   elite_count++;
                }
            }
            k++;
        }
}


static void DEBUG_print_pop(struct individual *pop, int_T nrToPrint, int_T numDV,
                            int_T numObj)
{
/* ==================================================================
 * Printout a population for debugging
 * ============================================================
 */
    int_T i,j;

    printf("----------------------------------------------------\n");
    for (i=0; i<nrToPrint;i++)
    {
        for (j=0; j<numDV;j++)
        {
            printf("% 7.2f | ", pop[i].DV[j]);
        }
        printf("| ");

        for (j=0; j<numObj;j++)
        {
            printf("% 7.2f | ", pop[i].ObjResults[j]);
        }
        printf("| % 7.2f | ", pop[i].weightedSum);
        printf("| %d | ", pop[i].ranking);
        printf("\n");
    }
    printf("----------------------------------------------------\n");
}

void shuffle_array(int_T *array, int_T n)
{
/* ============================================================
 * Arrange the N elements of ARRAY in random order.
 * Idea taken from Ben Pfaff, 2004.
 * http://benpfaff.org/writings/clc/shuffle.html
 * ============================================================
 */
    int_T i, j;
    int_T tmp;

    if (n > 1) {
        for (i = 0; i < n; i++) {
          j = (int_T)floor(randu(0,n))%n;
         /* j = i + Random()*(n - i) + 1;*/
          tmp = array[j];
          array[j] = array[i];
          array[i] = tmp;
        }
    }
}

```

```
real_T randn(real_T m,real_T s)
/* ========================================================================
 * Returns a normal (Gaussian) distributed real number.
 * NOTE: use s > 0.0
 *
 * Taken from
 * Name              : rvgs.c  (Random Variate GeneratorS)
 * Author            : Steve Park & Dave Geyer
 * Language          : ANSI C
 * Latest Revision   : 10-28-98
 * http://www.cs.wm.edu/~va/software/park/
 *
 * Uses a very accurate approximation of the normal idf due to Odeh & Evans,
 * J. Applied Statistics, 1974, vol 23, pp 96-97.
 * ========================================================================
 */
{
  const real_T p0 = 0.322232431088;      const real_T q0 = 0.099348462606;
  const real_T p1 = 1.0;                 const real_T q1 = 0.588581570495;
  const real_T p2 = 0.342242088547;      const real_T q2 = 0.531103462366;
  const real_T p3 = 0.204231210245e-1;   const real_T q3 = 0.103537752850;
  const real_T p4 = 0.453642210148e-4;   const real_T q4 = 0.385607006340e-2;
  real_T u, t, p, q, z;

  u   = Random();
  if (u < 0.5)
    t = sqrt(-2.0 * log(u));
  else
    t = sqrt(-2.0 * log(1.0 - u));
  p   = p0 + t * (p1 + t * (p2 + t * (p3 + t * p4)));
  q   = q0 + t * (q1 + t * (q2 + t * (q3 + t * q4)));
  if (u < 0.5)
    z = (p / q) - t;
  else
    z = t - (p / q);
  return (m + s * z);
}

real_T randu(real_T a, real_T b)
/* ===============================================================
 * Returns a uniformly distributed real number between a and b.
 * NOTE: use a < b
 *
 * Taken from
 * Name              : rvgs.c  (Random Variate GeneratorS)
 * Author            : Steve Park & Dave Geyer
 * Language          : ANSI C
 * Latest Revision    : 10-28-98
 * http://www.cs.wm.edu/~va/software/park/
 *
 * ==============================================================
 */
{
  return (a + (b - a) * Random());
}


real_T Random(void) {
/* ==============================================================
 * Returns random value between 0 and 1.0.
 * Uses internal rand() generator
 * ==============================================================
 */
    return (real_T) rand()/RAND_MAX;
}

void PlantSeeds(int_T x)
/* ------------------------------------------------------------------------
 * Use this function to initialise the random number generator
 * ------------------------------------------------------------------------
 */
{
  srand((unsigned)x);
}
```